

University of Nevada, Reno

Melting Temperature Variation and Electrochemical Study of  
Lanthanide Elements in LiCl-KCl Eutectic Molten Salt

A THESIS SUBMITTED IN PARTIAL FULFILLMENT OF THE  
REQUIREMENTS FOR THE DEGREE OF MASTER OF SCIENCE IN

**Materials Science and Engineering**

By

Sudhir Baral

Dr. Manoranjan Misra / Thesis Advisor

August 2010



University of Nevada, Reno  
Statewide • Worldwide

THE GRADUATE SCHOOL

We recommend that the thesis  
prepared under our supervision by

**SUDHIR BARAL**

entitled

**Melting Temperature Variation and Electrochemical Study of Lanthanide  
Elements in LiCl-KCl Eutectic Molten Salt**

be accepted in partial fulfillment of the  
requirements for the degree of

**MASTER OF SCIENCE**

Dr. Manoranjan Misra, Advisor

Dr. Krishnan S. Raja, Committee Member

Dr. Carl Nesbitt, Graduate School Representative

Marsha H. Read, Ph. D., Associate Dean, Graduate School

August, 2010

## ***Acknowledgements***

I would like to take this chance to thank Dr. Misra for giving me the opportunity to work on this project as well as financially supporting me while I attended at University of Nevada Reno (UNR). I am equally very grateful to Dr. Raja for his advice and constant guidance throughout my work. Without his advice and guidance this thesis would not have been completed. I would also like to thank Dr. Alonso for his instructions and regular suggestions which helped me a lot to complete this work. I would also like to thank Dr. Carl Nesbitt for being a member of my committee.

I am very thankful to all the members of the Department of Chemical and Metallurgical Engineering for their help. I am very grateful to my colleagues for their support and friendship which made my life easier during my stay here at UNR.

I would also like to express my kind love to my parents, brother, sister and all of my family members and friends for their support. Without their effort I would not be where I am today. At last but not least I would like to thank Sohana Khanal for her constant support and encouragement.

Finally, financial support of US DOE through Office of Waste Processing, grant no. DE-FG30-08 CC000f0 is gratefully acknowledged.

## ***Abstract***

The core objective of this project was to provide the supportive information for the pyrochemical reprocessing of spent nuclear fuels. The specific goals were to determine the thermodynamic and electrochemical data base of lanthanide elements in LiCl-KCl eutectic molten salts which is required for the better process control of pyrometallurgical reprocessing of spent fuels. In this thesis, two different scopes related to reprocessing of spent fuels were studied. The first study was to determine the melting temperature variation of LiCl-KCl eutectic mixture in presence of lanthanide elements and the second was study of the reduction behavior of lanthanide elements mixed with LiCl-KCl eutectic. The first study was performed by thermal analysis in order to determine the temperature variations of LiCl-KCl eutectic mixture in the presence of lanthanide elements. The result of single, as well as multi-component lanthanide elements below 5 mol% contain in LiCl-KCl eutectic mixture is presented. The results showed that the lanthanide elements below 5 mol% do not vary the melting temperature significantly. The mixture temperatures are well below the melting temperature of LiCl-KCl eutectic melting temperature. For the second case cyclic voltammetry studies were carried out to determine the changes occurring in reduction potentials when multi-components lanthanide elements are present in molten salt containing LiCl-KCl eutectic mixture. The result of mixtures containing binary, ternary and quaternary systems showed that the initiation of cathodic waves occur at lower cathodic potential than the standard redox potential of the component presents in the system. The cathodic wave potentials are shifted to less negative values, and in some cases closer to  $-1.7\text{ V Ag/AgCl}$  at  $500\text{ }^{\circ}\text{C}$ . This reduction potential is closer to the redox potential

of Pu(III)/Pu system. These results indicate that presence of multiple fission products in the LiCl+KCl eutectic could affect the separation kinetics of the actinides.

## ***Table of Contents***

| <b>Section</b>   | <b>Page Number</b> |
|--|--------------------|
| <i>Acknowledgements</i>                                  | <i>i</i>           |
| <i>Abstract</i>  | <i>ii</i>          |
| <i>Table of Contents</i>                                 | <i>iv</i>          |
| <i>List of Tables</i>                                    | <i>viii</i>        |
| <i>List of Figures</i>                                   | <i>x</i>           |
| 1. Introduction  | 1                  |
| 2. Background  | 2                  |
| 2.1. Nuclear Energy                                      | 2                  |
| 2.2. Nuclear Power Plants                                | 4                  |
| 2.2.1. Classification of Nuclear Reactors                | 5                  |
| 2.2.2. Current Nuclear Power plant in use                | 7                  |
| 2.2.2.1. Pressurized Water Reactor (PWR)                 | 7                  |
| 2.2.2.2. Boiling Water Reactor (BWR)                     | 8                  |
| 2.2.2.3. Pressurized Heavy Water Reactor (PHWR or CANDU) | 9                  |
| 2.2.2.4. Advanced Gas-cooled Reactor (AGR)               | 10                 |
| 2.2.2.5. Light water graphite moderated reactor (RBMK)   | 11                 |

|  |    |
|--|----|
| 2.2.3. Future and developing reactors                | 12 |
| 2.2.3.1. Advanced Reactors                           | 12 |
| 2.2.3.2. Future technologies: Generation IV reactors | 13 |
| 2.3. Spent Nuclear Fuels                             | 15 |
| 2.3.1. Oxide based fuels                             | 16 |
| 2.3.2. Metal Fuel                                    | 16 |
| 2.3.3. Nitride Fuel                                  | 17 |
| 2.3.4. Carbide Fuel                                  | 17 |
| 2.4. Reprocessing of Spent Nuclear Fuels             | 18 |
| 2.4.1. History of Reprocessing                       | 18 |
| 2.4.2. Reprocessing countries                        | 19 |
| 2.4.3. Reprocessing options                          | 21 |
| 2.4.4. Reprocessing processes                        | 22 |
| 2.4.4.1. Aqueous Process: PUREX                      | 22 |
| 2.4.4.1.1. Modifications of PUREX                    | 24 |
| 2.4.4.2. Non Aqueous: Pyrochemical Process           | 26 |
| 2.4.4.2.1. Molten Salt                               | 29 |
| 2.4.4.2.2. LiCl-KCl System                           | 29 |

|  |    |
|--|----|
| 2.4.5. Issues on Spent Fuel Reprocessing   | 30 |
| 2.5. Scope and Objective   | 32 |
| 3. Project Description   | 33 |
| 3.1. Temperature Variations of eutectic LiCl-KCl by additions of lanthanide trichlorides | 33 |
| 3.2. Electrochemical Separation of Lanthanides from LiCl-KCl                             | 33 |
| 4. Experimental Methods  | 36 |
| 4.1. Temperature Variations of eutectic LiCl-KCl by additions of lanthanide trichlorides | 36 |
| 4.2. Electrochemical Separation of Lanthanides from LiCl-KCl                             | 44 |
| 5. Results and Discussions   | 49 |
| 5.1. Temperature Variations of eutectic LiCl-KCl by additions of lanthanide trichlorides | 49 |
| 5.2. Electrochemical Separation of Lanthanides from LiCl-KCl                             | 62 |
| 6. Conclusion  | 85 |
| 6.1. Temperature Variations of eutectic LiCl-KCl by additions of lanthanide trichlorides | 85 |
| 6.2. Electrochemical Separation of Lanthanides from LiCl-KCl                             | 85 |
| 7. References  | 87 |
| Appendix-1   | 92 |

|            |    |
|------------|----|
| Appendix-2 | 95 |
|------------|----|

### **List of Tables**

| <b>Table Name</b>   | <b>Page Number</b> |
|---|--------------------|
| 1. Major Current Commercial Light Water Spent Fuel Reprocessing Capacity  | 21                 |
| 2. Standard potential vs Ag/AgCl at 450 °C in LiCl-KCl  | 35                 |
| 3. Eutectic concentration and melting temperature   | 37                 |
| 4. Change in Melting Temperature after LaCl <sub>3</sub> addition in (LiCl-KCl) <sub>Eutectic</sub>   | 51                 |
| 5. Change in Melting Temperature after CeCl <sub>3</sub> addition in (LiCl-KCl) <sub>Eutectic</sub>   | 52                 |
| 6. Change in Melting Temperature after PrCl <sub>3</sub> addition in (LiCl-KCl) <sub>Eutectic</sub>   | 53                 |
| 7. Change in Melting Temperature after GdCl <sub>3</sub> addition in (LiCl-KCl) <sub>Eutectic</sub>   | 54                 |
| 8. Change in Melting Temperature after GdCl <sub>3</sub> addition in (LiCl-KCl) <sub>Eutectic</sub>   | 55                 |
| 9. Change in Melting Temperature after NdCl <sub>3</sub> addition in (LiCl-KCl) <sub>Eutectic</sub>   | 56                 |
| 10. Change in temperature 5 wt% lanthanides in ternary system (LiCl+KCl) <sub>Eutectic</sub> +5%CeCl <sub>3</sub> +5%LaCl <sub>3</sub>                            | 59                 |
| 11. Change in temperature of 5 wt% lanthanides in quaternary system (LiCl+KCl) <sub>Eutectic</sub> +5%CeCl <sub>3</sub> +5%LaCl <sub>3</sub> +5%GdCl <sub>3</sub> | 59                 |

|   |    |
|---|----|
| 12. Change in temperature of 5 wt% lanthanides in quinary system (LiCl-KCl)<br>$\text{Eutectic}+5\%\text{CeCl}_3+5\%\text{LaCl}_3+5\%\text{GdCl}_3+5\%\text{PrCl}_3-5\%\text{DyCl}_3$ | 59 |
| 13. Change in temperature of 10 wt% lanthanides in ternary system (LiCl+KCl) $\text{Eutectic}+10\%\text{CeCl}_3+10\%\text{DyCl}_3$  | 59 |
| 14. Change in temperature of 10 wt% lanthanides in ternary system (LiCl+KCl) $\text{Eutectic}+10\%\text{CeCl}_3+10\%\text{GdCl}_3$  | 60 |
| 15. Change in temperature of 10 wt% lanthanides in ternary system (LiCl+KCl) $\text{Eutectic}+10\%\text{CeCl}_3+10\%\text{PrCl}_3$  | 60 |
| 16. Change in temperature of in ternary system with (LiCl+KCl)<br>$\text{Eutectic}+10\%\text{CeCl}_3+20\%\text{PrCl}_3$   | 60 |
| 17. Change in temperature of 20 wt% lanthanides in ternary system with LiCl-KCl-20% $\text{CeCl}_3$ -20% $\text{PrCl}_3$  | 60 |
| 18. Obtained reduction potential in comparison with literature values   | 69 |
| 19. Obtained reduction potential for multi-component system   | 82 |

### ***List of Figures***

| <b>Figures Name</b>                              | <b>Page Number</b> |
|--|--------------------|
| 1. History and projected energy use              | 3                  |
| 2. Nuclear fission                               | 4                  |
| 3. Schematic of Nuclear reactors in general      | 5                  |
| 4. Generations of Nuclear energy system          | 7                  |
| 5. Pressurized Water Reactor                     | 8                  |
| 6. Boling Water Reactor                          | 9                  |
| 7. CANDU reactor                                 | 10                 |
| 8. Advanced Gas-Cooled Reactor                   | 11                 |
| 9. Light water graphite moderated reactor (RMBK) | 12                 |
| 10. Generation IV nuclear reactors               | 14                 |
| 11. Regular and Spent fuels                      | 15                 |
| 12. Purex flow sheet                             | 23                 |
| 13. PUREX process                                | 23                 |
| 14. UREX flow sheet                              | 24                 |
| 15. Pyroprocessing flow sheet                    | 27                 |
| 16. Molten salt system                           | 30                 |

|   |    |
|---|----|
| 17. Potential vs Concentration showing actinides concentration reducing and lanthanide concentration increasing             | 35 |
| 18. Experimental Setup for thermal analysis   | 38 |
| 19. Setup inside glove box  | 39 |
| 20. Heating and Cooling curve obtained from the experiments   | 41 |
| 21. Heating curve showing halt point  | 41 |
| 22. Heating Curve analysis showing peak   | 42 |
| 23. Smoothened Curve  | 44 |
| 24. Experimental arrangement for electrochemical studies in molten salt   | 46 |
| 25. Eutectic Curve obtained   | 50 |
| 26. Melting temperature distribution after adding various mol % of $\text{LaCl}_3$ in $(\text{LiCl-KCl})_{\text{Eutectic}}$ | 52 |
| 27. Melting temperature distribution after adding various mol % of $\text{CeCl}_3$ in $(\text{LiCl-KCl})_{\text{Eutectic}}$ | 53 |
| 28. Melting temperature distribution after adding various mol % of $\text{PrCl}_3$ in $(\text{LiCl-KCl})_{\text{Eutectic}}$ | 54 |
| 29. Melting temperature distribution after adding various mol % of $\text{GdCl}_3$ in $(\text{LiCl-KCl})_{\text{Eutectic}}$ | 55 |
| 30. Melting temperature distribution after adding various mol % of $\text{DyCl}_3$ in $(\text{LiCl-KCl})_{\text{Eutectic}}$ | 56 |

|   |    |
|---|----|
| 31. Melting temperature distribution after adding various mol % of $\text{NdCl}_3$ in $(\text{LiCl-KCl})_{\text{Eutectic}}$   | 57 |
| 32. 3-D area plot of Temperature difference vs mol % $\text{LnCl}_3$  | 57 |
| 33. 3-D surface plot for Temperature difference vs $\text{CeCl}_3$ , $\text{PrCl}_3$  | 61 |
| 34. Cyclic voltammograms of $(\text{LiCl} + \text{KCl})_{\text{Eutectic}} + 5 \text{ wt } \% \text{ CeCl}_3$ binary system at 723 K (450 °C) using tungsten as substrate at 20 mV/s scan rate | 63 |
| 35. Cyclic voltammograms of $(\text{LiCl} + \text{KCl})_{\text{Eutectic}}$ at 773 K (500 °C) using tungsten as substrate at 10 mV/s scan rate   | 65 |
| 36. Cyclic voltammograms of $(\text{LiCl} + \text{KCl})_{\text{Eutectic}} + 5 \text{ wt } \% \text{ CeCl}_3$ binary system at 773 K (500 °C) using tungsten as substrate at 20 mV/s scan rate | 65 |
| 37. Cyclic voltammograms of $(\text{LiCl} + \text{KCl})_{\text{Eutectic}} + 5 \text{ wt } \% \text{ LaCl}_3$ binary system at 773 K (500 °C) using tungsten as substrate at 20 mV/s scan rate | 66 |
| 38. Cyclic voltammograms of $(\text{LiCl} + \text{KCl})_{\text{Eutectic}} + 5 \text{ wt } \% \text{ GdCl}_3$ binary system at 773 K (500 °C) using tungsten as substrate at 20 mV/s scan rate | 66 |
| 39. Cyclic voltammograms of $(\text{LiCl} + \text{KCl})_{\text{Eutectic}} + 5 \text{ wt } \% \text{ NdCl}_3$ binary system at 773 K (500 °C) using tungsten as substrate at 20 mV/s scan rate | 67 |
| 40. Cyclic voltammograms of $(\text{LiCl} + \text{KCl})_{\text{Eutectic}} + 5 \text{ wt } \% \text{ DyCl}_3$ binary system at 773 K (500 °C) using tungsten as substrate                      | 67 |

|   |    |
|---|----|
| at 20 mV/s scan rate  |    |
| 41. Cyclic voltammograms of (LiCl + KCl) <sub>Eutectic</sub> + 5 wt % PrCl <sub>3</sub> binary system at 773 K (500 °C) using tungsten as substrate at 20 mV/s scan rate  | 68 |
| 42. Cyclic voltammograms of (LiCl + KCl) <sub>Eutectic</sub> + 5 wt % SmCl <sub>3</sub> binary system at 773 K (500 °C) using tungsten as substrate at 20 mV/s scan rate  | 68 |
| 43. Cyclic voltammograms of (LiCl + KCl) <sub>Eutectic</sub> + 5 wt % GdCl <sub>3</sub> binary system at 773 K (500 °C) using tungsten as substrate at different scan rate  | 69 |
| 44. CV of (LiCl-KCl) <sub>Eutectic</sub> + 5wt% CeCl <sub>3</sub> and (LiCl-KCl) <sub>Eutectic</sub> + 5wt% LaCl <sub>3</sub> binary systems in comparison with ternary (LiCl-KCl) <sub>Eutectic</sub> +5wt% CeCl <sub>3</sub> + 5wt% LaCl <sub>3</sub> system at 773 K (500 °C) at 20 mV/s | 71 |
| 45. XRD pattern of the deposit of (LiCl + KCl) <sub>Eutectic</sub> + 5 wt % CeCl <sub>3</sub> + 5 wt % LaCl <sub>3</sub> ternary system at 773 K (500 °C) using tungsten as substrate at -1.7 V   | 72 |
| 46. SEM image of deposit obtained after cathodic scan of CV until -1.8 V of the ternary (LiCl+KCl) <sub>Eutectic</sub> +5 wt% CeCl <sub>3</sub> + 5 wt% LaCl <sub>3</sub> system at 773 K (500 °C) at 20 mV/s scan rate; and (b) EDX analysis of the deposit                                | 73 |
| 47. CV of (LiCl-KCl) <sub>Eutectic</sub> + 5wt% CeCl <sub>3</sub> and (LiCl-KCl) <sub>Eutectic</sub> + 5wt% NdCl <sub>3</sub> binary systems in comparison with ternary (LiCl-KCl) <sub>Eutectic</sub> +5wt% CeCl <sub>3</sub> + 5wt% NdCl <sub>3</sub> system at 773 K (500 °C) at 20 mV/s | 75 |

|   |    |
|---|----|
| <p>48. SEM image of deposit obtained after cathodic scan of CV until -1.8 V of the ternary <math>(\text{LiCl}+\text{KCl})_{\text{Eutectic}}+3 \text{ wt}\% \text{ CeCl}_3 + 3 \text{ wt}\% \text{ NdCl}_3</math> system at 773 K (500 °C) at 20 mV/s scan rate; and (b) EDX analysis of the deposit</p>   | 76 |
| <p>49. CV of <math>(\text{LiCl}-\text{KCl})_{\text{Eutectic}}+ 5\text{wt}\% \text{ CeCl}_3</math> and <math>(\text{LiCl}-\text{KCl})_{\text{Eutectic}}+ 5\text{wt}\% \text{ SmCl}_3</math> binary systems in comparison with ternary <math>(\text{LiCl}-\text{KCl})_{\text{Eutectic}} +5\text{wt}\% \text{ CeCl}_3 + 5\text{wt}\% \text{ SmCl}_3</math> system at 773 K (500 °C) at 20 mV/s</p> | 77 |
| <p>50. CV of <math>(\text{LiCl}-\text{KCl})_{\text{Eutectic}}+ 5\text{wt}\% \text{ CeCl}_3 + 5\text{wt}\% \text{ LaCl}_3</math> ternary system in comparison with quaternary <math>(\text{LiCl}-\text{KCl})_{\text{Eutectic}} +5\text{wt}\% \text{ CeCl}_3 + 5\text{wt}\% \text{ NdCl}_3</math> system at 773 K (500 °C) at 20 mV/s</p>   | 78 |
| <p>51. CV of <math>(\text{LiCl}-\text{KCl})_{\text{Eutectic}}+ 5\text{wt}\% \text{ CeCl}_3 + 5\text{wt}\% \text{ SmCl}_3</math> binary system in comparison with ternary <math>(\text{LiCl}-\text{KCl})_{\text{Eutectic}} +3\text{wt}\% \text{ CeCl}_3 + 3\text{wt}\% \text{ SmCl}_3</math> system at 773 K (500 °C) at 20 mV/s</p>   | 79 |
| <p>52. (a) SEM image of partial deposit removed from tungsten wire after deposition at -1.9 V for 60 seconds in quaternary <math>(\text{LiCl}+\text{KCl})_{\text{Eutectic}}+5 \text{ wt}\% \text{ CeCl}_3 + 5 \text{ wt}\% \text{ NdCl}_3 + 5 \text{ wt}\% \text{ SmCl}_3</math> system at 773 K (500 °C); and (b) EDX analysis of the deposit</p>  | 80 |
| <p>53. CV of <math>(\text{LiCl}-\text{KCl})_{\text{Eutectic}}+ 5\text{wt}\% \text{ CeCl}_3</math> and <math>(\text{LiCl}-\text{KCl})_{\text{Eutectic}}+ 5\text{wt}\% \text{ LaCl}_3</math> binary systems in comparison with ternary <math>(\text{LiCl}-\text{KCl})_{\text{Eutectic}} +3\text{wt}\% \text{ CeCl}_3 + 3\text{wt}\% \text{ LaCl}_3</math> system at 773 K (500 °C) at 20 mV/s</p> | 81 |
| <p>54. CV of <math>(\text{LiCl}-\text{KCl})_{\text{Eutectic}}+ 5\text{wt}\% \text{ CeCl}_3</math> and <math>(\text{LiCl}-\text{KCl})_{\text{Eutectic}}+ 5\text{wt}\%</math></p>   | 82 |

|  |  |
|--|--|
| <p>NdCl<sub>3</sub> binary systems in comparison with ternary (LiCl-KCl)<sub>Eutectic</sub> +3wt% CeCl<sub>3</sub> + 3wt% NdCl<sub>3</sub> system at 773 K (500 °C) at 20 mV/s</p> |  |
|--|--|

# Chapter 1: Introduction

---

The spent nuclear fuel (SNF) management has been considered an important issue because of the large amount of spent fuel being progressively accumulated in the world. The expected growth of nuclear energy generation in the world would further add a lot of spent nuclear fuels. Therefore the reprocessing of the used nuclear fuel will be necessary to continue nuclear power into the future. There are a multitude of possible methods to employ in a future fuel cycle. Several literature sources focus on the operation of a future fuel cycle being a combination of fast and thermal reactors, fully fast reactors and a continuation of open fuel cycle practices [1]. A necessary component for the fuel cycle requires a reprocessing technology that can satisfy all the technical, environmental, economic and political requirements [2].

Spent fuels contain a fairly large amount of useful elements that can be reprocessed in the reactors. With the reprocessing of spent fuels, useful elements can be separated, the radiotoxicity of the contents of permanent repository can be greatly reduced and plutonium is no longer present in the disposable waste which reduces the proliferation risk.

There are different methods of reprocessing spent fuels. PUREX is one of the current reprocessing processes and the pyroprocessing is the future of reprocessing process. Various developments are being done over this technique via research and developments (R&D). With the advantages of pyroprocessing over the PUREX process (discussed in chapter 2.6.4.1), significant amounts of R&D are under way in order to develop the pyroprocessing technology for the future reprocessing of spent nuclear fuels. This research focus on a pyroprocessing method and research work on molten salt electrolysis of lanthanides elements is presented.

The work was focused on determining the temperature variation of lanthanide elements on the lithium chloride- potassium chloride (LiCl-KCl) eutectic molten salt system. The paper also includes the electrochemical study of lanthanides in LiCl-KCl eutectic system at 500 °C.

## Chapter 2: Background

---

### 2.1. Nuclear Energy

Nuclear Energy is one of the sources of energy useful to reduce the energy crisis that the world is facing today. With the increasing world population the demands for energy is also increasing at a rapid pace. Figure 1 shows past energy use and projected energy demand up to 2030. The expanded demand of energy means an increase the use of fossil fuels as most of the energy today is generated from burning fossil fuel i.e. coal, oil and natural gas. These fuels are being consumed so rapidly that we are going to run out of the source. Not only the scarcity will be a problem but burning fuels increases the pollution due to carbon dioxide emissions [3].

According to the world nuclear association, each year fossil fuels add 25 billion tonnes of carbon dioxide to the atmosphere which is 70 million tonnes each day or 800 tonnes a second [4]. The huge amount of increasing carbon dioxide elevates the green house effects causing the earth to capture more solar heat and ultimately affecting the entire civilization. Therefore alternative energy is required for both energy demand and for pollution reduction.

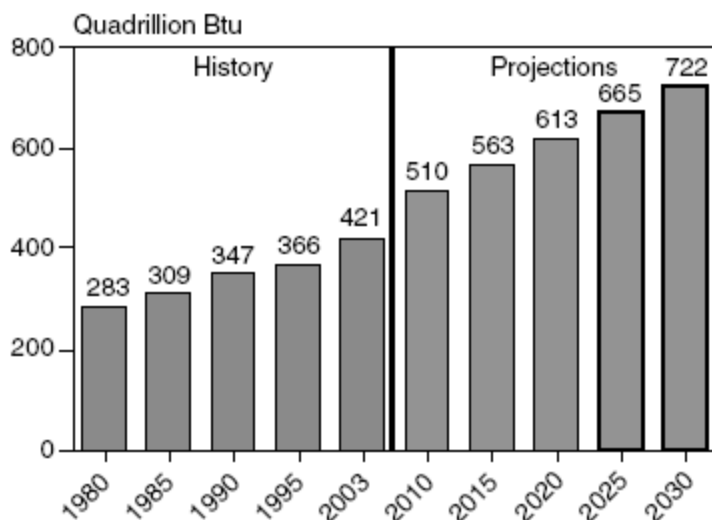


**Figure 1:** History and projected energy use [5]

There are various alternative sources of energy that have been developed. These alternative sources include wind power, solar power, geothermal, tides, biofuels, hydroelectric and nuclear[6]. However nuclear energy is already implemented extensively and currently in use compare to other sources which are still in hindrance for energy production due to the cost and limited technology development. Therefore with nuclear energy, it is only a matter of improving the efficiency and reduction of waste.

Nuclear energy is the advanced technology that produces electricity via nuclear fission reactions. This technique consists of tapping of the energy stored in the nuclei of atoms. “When unstable atoms such as uranium isotope, a primary fuel for nuclear power reactors, are bombarded with neutrons, they split and released their encased energy, which can be redistributed throughout the electrical grid” [3], as in Figure 2. Although the atoms are tiny, a large amount of energy holds their nuclei together, as they split this energy is released in the

form of heat. The splitting behavior is called fission and the energy released can be used to generate electricity in power plants [3]. As of today there are more than 400 nuclear power plants (NPP) in the world, which produce about 17% of the world's electricity [7].

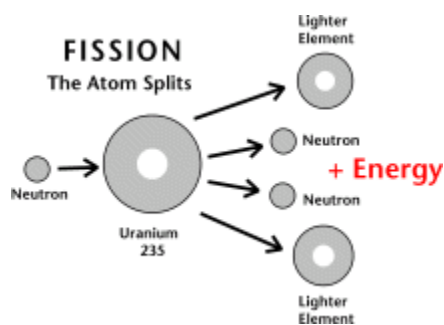


**Figure 2:** Nuclear fission [8]

## 2.2. Nuclear power plants

Nuclear power plants or nuclear power reactors produce and control the heat release from the splitting the atoms of certain elements which is used to make steam to generate electricity [7].

A nuclear reactor consists of different parts (as shown in Fig. 3). The heart of every reactor is an active core where the fission chain reaction is sustained. The core consists of control rods which hold fissile fuel, a moderator to slow down the fission neutrons, coolant to remove the extra heat generated by the fissions and structural materials which maintains the physical integrity of the core. The core is surrounded by reflectors whose main purpose is to reflect back scattered neutrons to towards the main core. And for the protection the core and the reflector are in turn surrounded by the shield which is generally called reactor vessel. The power plants have a turbine to generate electricity and a heat exchanger, also called condenser, to convert steam in to liquid [9]. Nuclear reactors are classified in different categories.

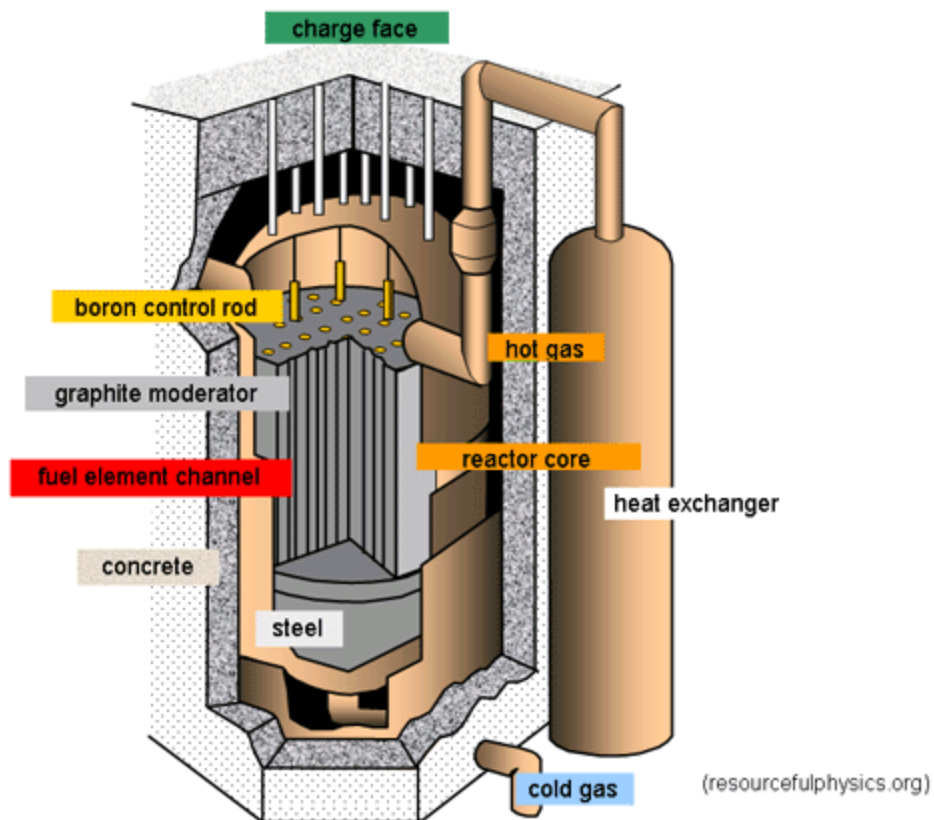


**Figure 3:** Schematic of Nuclear reactors in general [10]

### 2.2.1. Classification of Nuclear reactors

Generally the nuclear reactors are classified depending upon the type of reaction, the coolant, moderator, fuels and use. But the most important classification is by generations because it provides the advancement of the technology since inception and includes all the possible reactor systems.

Classification by generations incorporate all the classification types and divide the nuclear reactors into four different generation categories with regard to the developments made in the reactors. The nomenclature for the reactor designs by “Generations” was proposed by the US Department of Energy. The Generation I was considered the earliest reactor type. They were

mainly used for research purposes in early 1950's to mid 1960's. Later Generation II was introduced. These reactors were used for electricity generation and they referred to the class of commercial reactors built up to the 1990's. All the reactors in use today are of generation II reactor which include Boiling Water Reactors (BWR), Pressurized Water Reactors (PWR), Canadian reactors (CANDU), Advanced Gas Cooled Reactors (AGR) etc. Generation III is the advancement of generation II nuclear reactor design which include improved fuel technology, thermal efficiency, safety systems and standardized design for reduced maintenance and capital costs. Generation IV reactors are the future generation reactors. They are still being researched stage and not expected to be in use until the 2030s. These reactors are predicted to be very economical, with higher safety features, lightweight and capable for producing minimal waste [11].

**Generation IV:** Nuclear Energy Systems Deployable no later than 2030 and offering significant advances in sustainability, safety and reliability, and economics

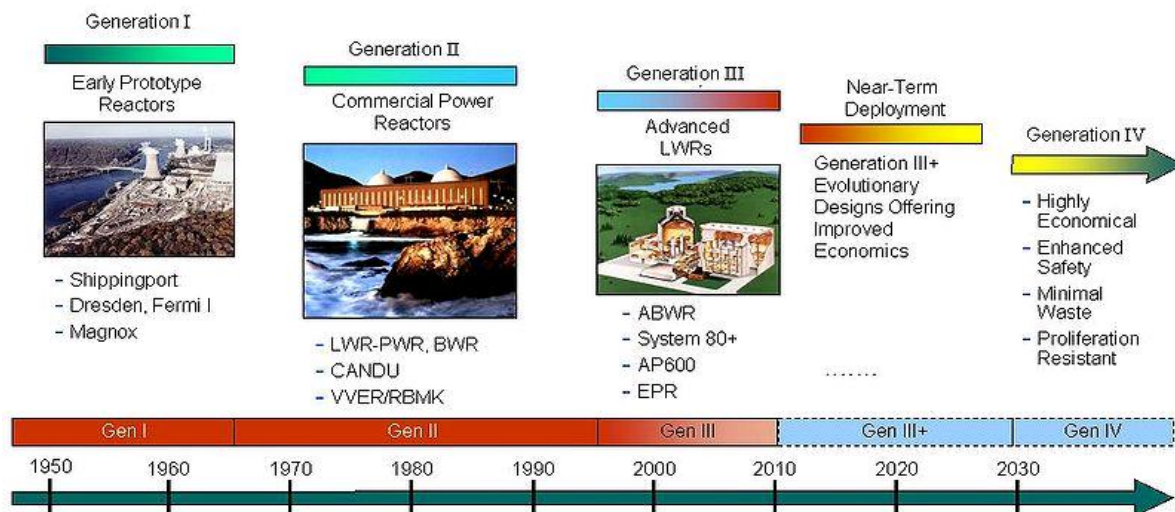


**Figure 4:** Generations of Nuclear energy system [12]

## **2.3. Current Nuclear Power plant in use**

### **2.3.1. Pressurized Water Reactors (PWR)**

PWRs are the most common type of reactors with more than 230 in use for power generation and naval propulsion in US. These reactors use the pressure vessel to contain the nuclear fuel, control rods, moderator and coolant. They use ordinary water for both coolant and moderator. These reactors have primary cooling circuit which flows through the core of the reactor under very high pressure and a secondary circuit in which steam is generated to drive the turbine. The secondary circuit is under lower pressure and the water boils in the heat exchangers thus generating steam. The schematic is shown in Figure 5. The main advantage of this reactor is that the fuel leak in the core does not pass any radioactive contaminants to the turbine and condenser. Another advantage is they provide a higher Carnot efficiency because they operate at higher pressure and temperature unlike other reactors. The disadvantage of PWR is that these reactors are more complicated and costly to construct. [13-15].

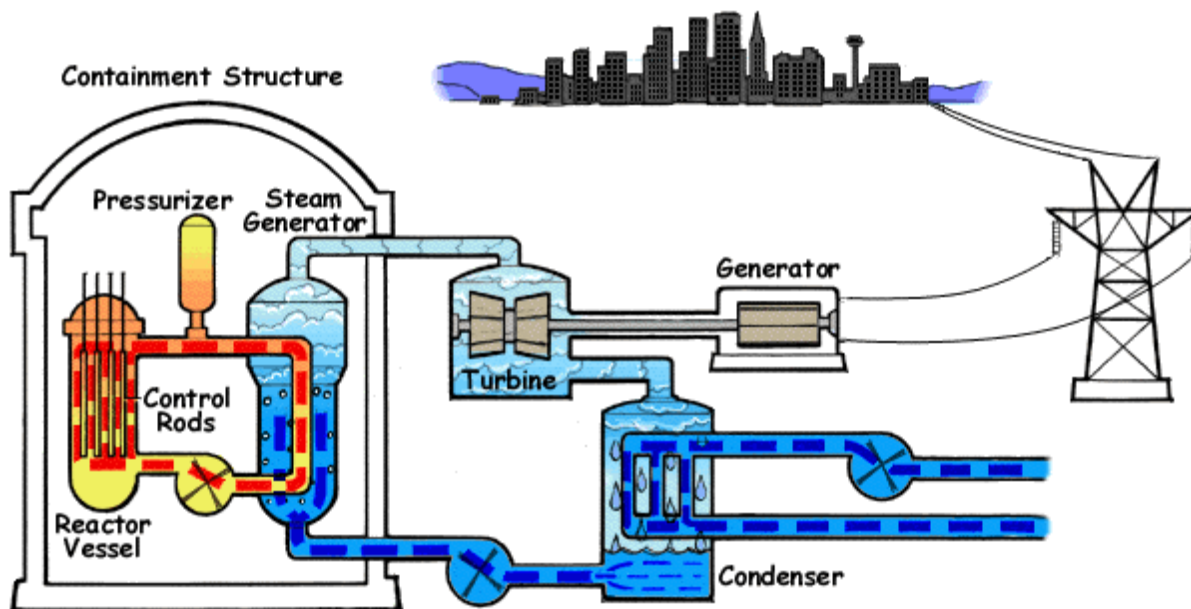
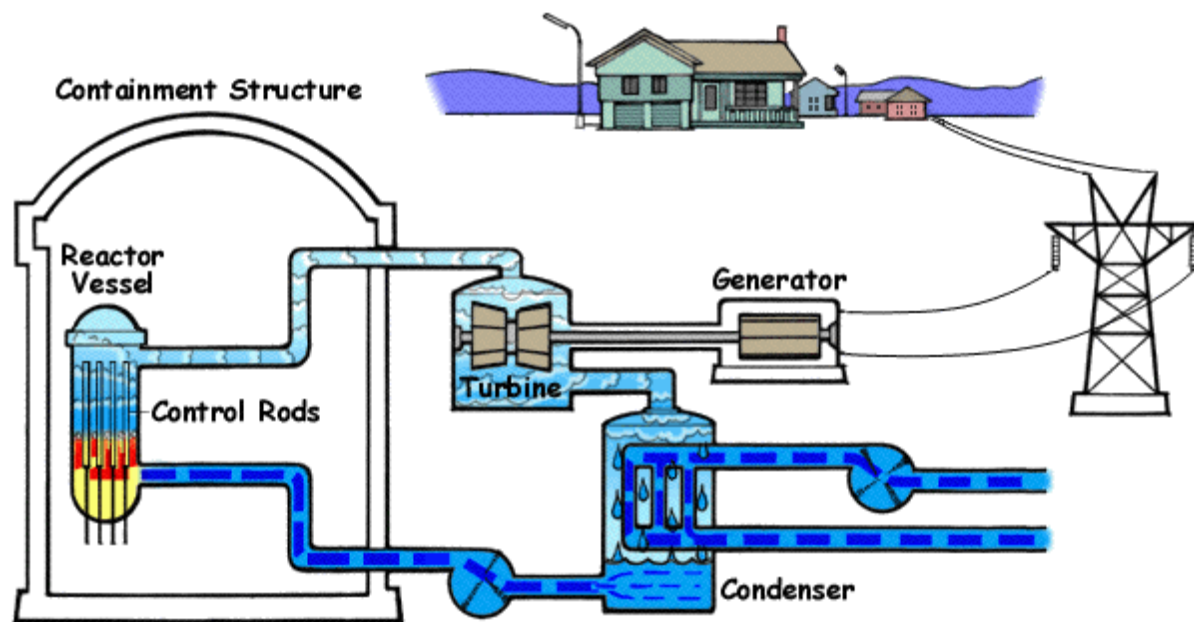


Figure 5: Pressurized Water Reactor [16]

### 2.3.2. Boiling Water Reactor (BWR)

BWRs are the second most common type of electricity generating nuclear reactors after PWR.

The design of the reactor is similar to a PWR but has only one channel reactor (as shown in Figure 6) in which the water is at low pressure and boils in the core at about  $285^{\circ}\text{C}$ . In BWRs, the water which passes over the reactor core act as the moderator and the coolant is also the steam source for the turbine. The steam passes through drier plates above the core and then directly to the turbines. Then the steam is cooled in a condenser back to liquid water. The water is then returned to the reactor core, completing the loop. The disadvantage of BWR is that the water around the core reactor is always contaminated with traces of radionuclides which are fed to the turbine and rest of the loop so the turbine must be shielded. Also the typical operating pressure of BWR is only about 70 atmospheres so the efficiency is lower than PWR. [14, 17].



**Figure 6:** Boiling Water Reactor [16]

### 2.3.3. Pressurized Heavy Water Reactor (PHWR or CANDU)

The PHWR reactor design was developed in the 1950s in Canada. Today other countries like India, Argentina, China, Pakistan, Romania and South Korea have also adapted CANDU reactor technology. This reactor uses the natural uranium oxide as fuel requiring the use of an efficient moderator such as heavy water ( $D_2O$ ) to act as coolant. Unlike PWR, the fuel is contained in hundreds of pressure tubes and can be refueled while at full power which make them very efficient in their use of uranium. A CANDU assembly consists of a bundle of 37 half meter long fuel rods with supportive structure and 12 bundles lying end to end in a fuel channel. They are operated at about  $290^\circ C$ . As in PWR, the primary coolant generates steam in a secondary circuit to drive the turbines. [18-19].

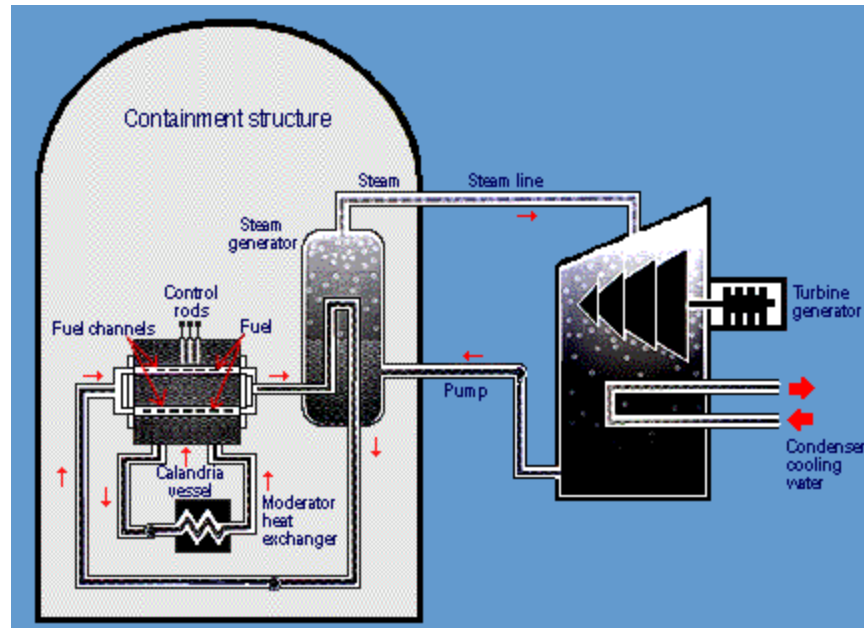
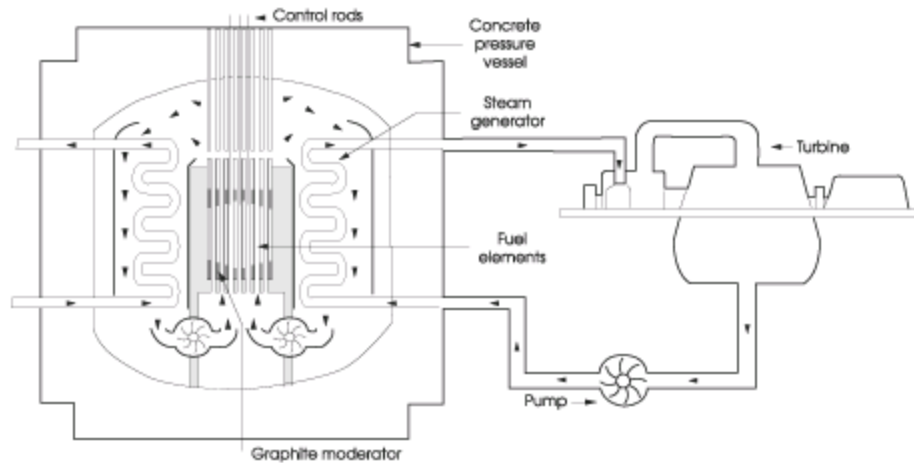


Figure 7: CANDU reactor [19]

#### 2.3.4. Advanced Gas-cooled Reactor (AGR)

These are the second generation of British gas-cooled reactors. They are generally graphite moderated and  $\text{CO}_2$  cooled. The fuel is uranium oxide pellets, enriched to 2.5-3.5%, in stainless steel tubes. These reactors have high thermal efficiency compared to PWRs due to the higher operating temperature of  $650^\circ\text{C}$ . The AGR was developed from Magnox (cladding materials) reactor during the late 1950s, both reactor types are still in use in the UK [20].



**Figure 8:** Advanced Gas-Cooled Reactor [19, 21]

### 2.3.5. Light water graphite moderated reactor (RBMK)

RBMK is a Soviet designed reactor, developed from plutonium production reactors. It employs 7 meter vertical pressure tubes running through graphite moderator (shown in Figure 9) and is cooled by water which is allowed to boil in the core at 290°C as in BWR. They use the low-enriched uranium oxide fuel made up into 3.5 meter long fuel assemblies. They are considered very dangerous because of positive feedback which can arise from the excess boiling that reduces the cooling and neutron absorption without inhibiting the fission reaction. That is the reason for these reactors not being built outside the Soviet Union [22-23].

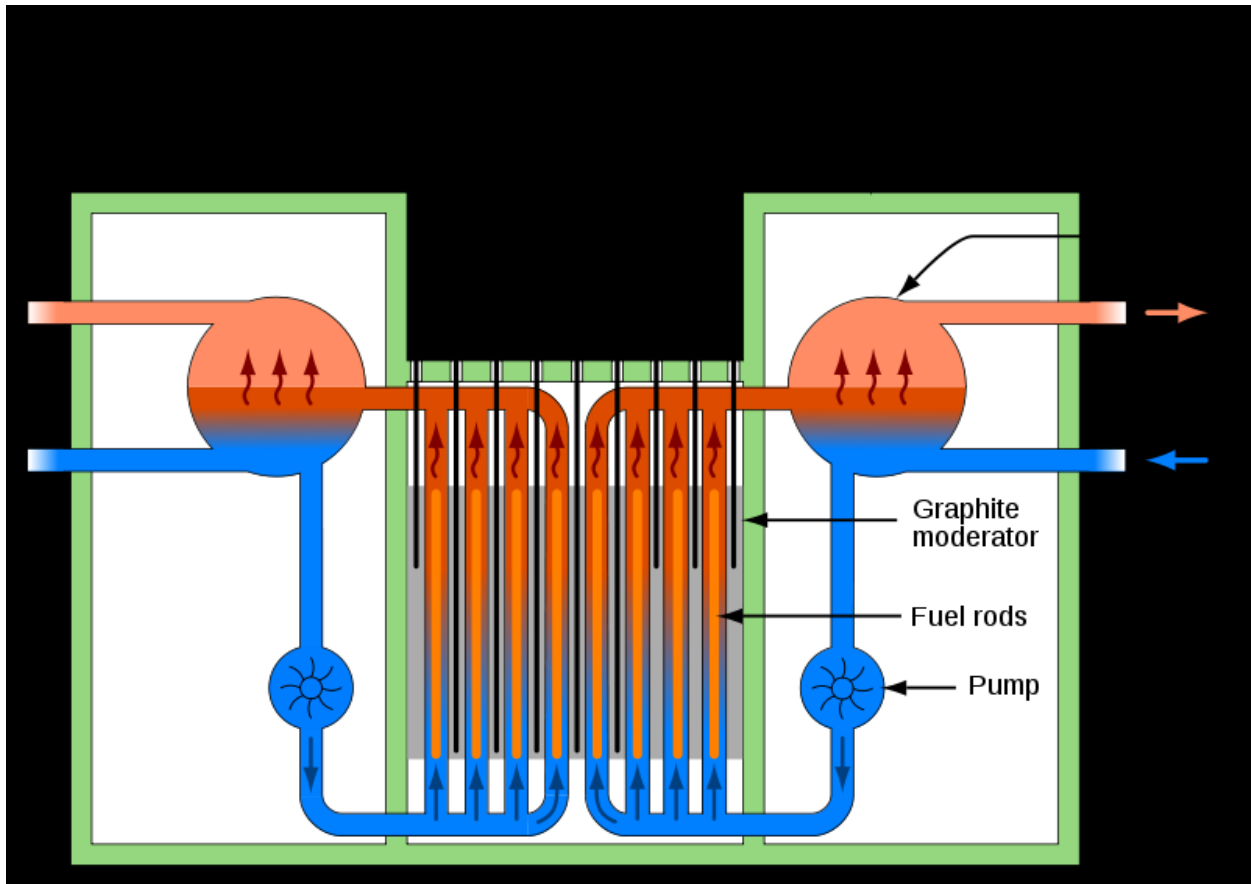


**Figure 9:** Light water graphite moderated reactor (RMBK) [23]

## 2.4. Future and developing reactors

### 2.4.1. Advanced Reactors

Generation III reactors are more advanced reactors. Advanced reactors are already in operation in Japan and others being constructed. Most of the advanced reactors are based on PWR, BWR and CANDU designs. The advanced light water reactors use a high efficiency fuel instead of conventional solid cylindrical fuel. Advanced heavy water reactors are being built which use thorium in its fuel core. This is now being developed at Bhabha Atomic Research Center (BARC), Mumbai, India. The fast neutron reactor is also considered an advanced reactor. They do not have the moderator and utilize fast neutrons, generating power from plutonium via the U-238

isotope in or around the fuel. They get more than 60 times more energy compared to normal reactors [22].

#### **2.4.2. Future technologies: Generation IV reactors**

Generation IV are the theoretical nuclear reactor designs currently being researched and expected to be available for construction before 2030. According to the World Nuclear Association, research in these reactors was officially started by the Generation IV International Forum (GIF). The GIF includes the group of 13 countries: USA, Argentina, Brazil, Canada, China, France, Japan, Russia, South Korea, South Africa, Switzerland and UK along with EU (Euratom) [24]. This forum is developing about six of these reactors. All of these reactors operate at higher temperatures than those being operated today. Most of the six systems employ a closed fuel cycle to maximize the resources and minimize the waste. Three of the six are the fast neutrons reactors (FNR); one can be described as epithermal, and only two operate with the slow neutrons like today's reactors. They all have different coolants: one is cooled by light water, two by helium and others have lead-bismuth, sodium or fluoride salt as coolant. They operate at the temperature range from 510°C to 1000°C and also four of them can be used for hydrogen production. Their sizes range from 150 to 1500 MWe with one exception being lead cooled which only produces about 50-150 MWe [25].

According to the GIF, the main goals for generation IV reactors are sustainability, economics, safety and reliability, proliferation resistance and physical protection [2]. Sustainability is the ability to meet the needs of the present generation while enhancing the ability of future generations to meet society's need indefinitely into the future by extending the fuel supply with recycling the used fuel to recover its energy content and reducing the polluting energy.

Safety is the most important goal for the future generation which would be obtained by increasing the use of inherent safety features, robust designs and transparent safety features that can be understood by general people. Proliferation resistance and physical protection are the means for controlling and securing nuclear material and nuclear facilities by providing effective explosion resistance of nuclear energy systems through improved design features and increasing the robustness of new facilities. With these four effects in prospective including general missions of electricity generation, heat and hydrogen production, and cost effectiveness; they envision following six reactors for the future. These six reactors consist of in built facilities for reprocessing of spent nuclear fuels and recycle all the useful elements.

| <b>Generation IV System</b>               | <b>Acronym</b> |
|---|----------------|
| Gas-Cooled Fast Reactor System            | GFR            |
| Lead-Cooled Fast Reactor System           | LFR            |
| Molten Salt Reactor System                | MSR            |
| Sodium-Cooled Fast Reactor System         | SFR            |
| Supercritical-Water-Cooled Reactor System | SCWR           |
| Very-High-Temperature Reactor System      | VHTR           |

**Figure 10:** Generation IV nuclear reactors [26]

## 2.5. Spent nuclear fuels

Spent nuclear fuel is nuclear fuel that has been irradiated in a nuclear reactor to the point where it is no longer useful in sustaining a nuclear reaction. Spent fuels typically contains 93% uranium (mostly <sup>238</sup>U), 1% plutonium, 0.1% minor actinides (Neptunium, Curium and Americium) and 5.4% fission products [27].

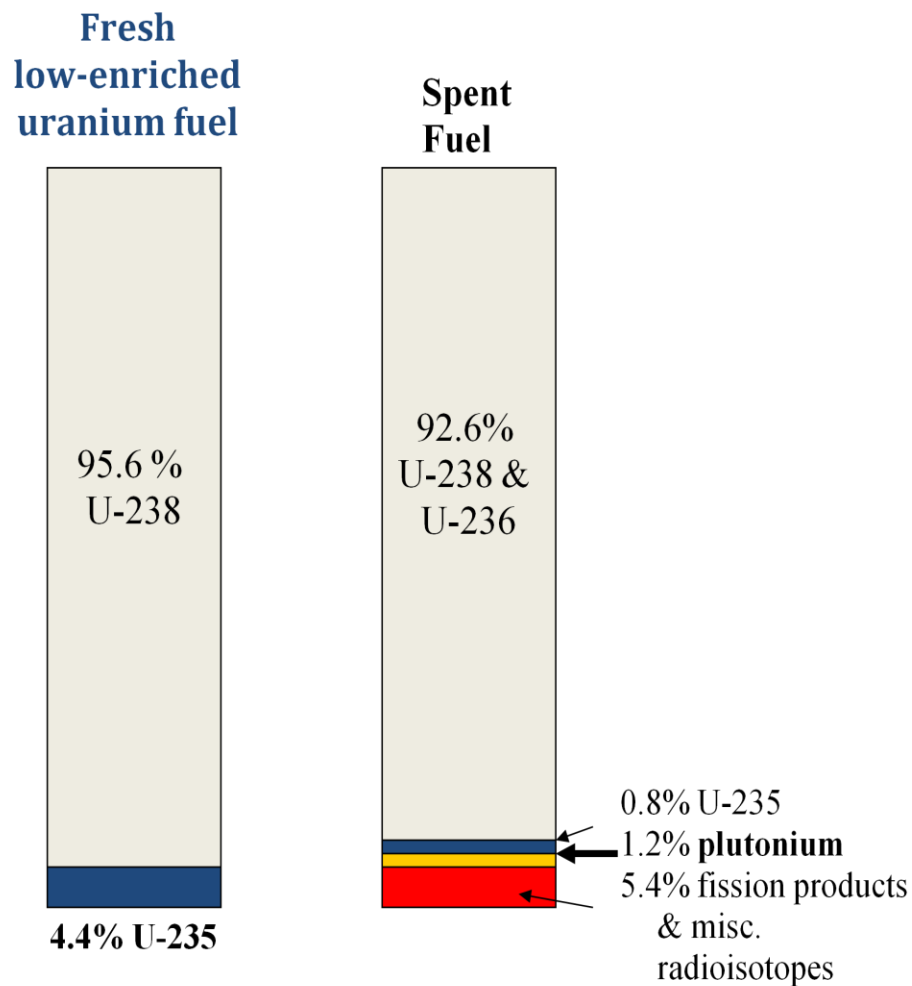


Figure 11: Regular and Spent fuels [28]

Nuclear fuels can come in a variety of different forms. The fuel forms that are currently being used are oxide, nitride, metal and carbide fuels.

### **2.5.1. Oxide based fuels**

The oxide fuels are mainly of two types, Uranium dioxide and mixed oxide fuel. The vast majority of nuclear fuel used in the reactors is Uranium dioxide which is mostly used in light water reactors. The thermal conductivity of uranium dioxide is low that it is affected by burn-up results of fission products dissolved in the lattice, precipitation and formation of gas bubbles like Xenon and Krypton. The mixed oxide is a blend of plutonium and natural uranium which behaves similarly to the enriched uranium fuel and is an alternative to the low enriched uranium fuel used in light water reactors. This fuel itself has concern of disposing the surplus plutonium. The status of the research for oxide fuels is still in its early stages. Some pellets and rodlets containing Pu, Am and Np have been irradiated in the SuperFact experiment in Phenix (France). Oxide TRU fuel compositions are also being prepared for irradiation in JOYO (Japan) [29].

### **2.5.2. Metal fuel**

Metal fuel has the higher advantage than the oxide fuel in terms of thermal conductivity but they cannot keep up with the high temperature. These fuels generally contain the metal composition U/Pu/Zr and are from EBR-II. According to the General Nuclear Energy Partnership (GNEP), the status of the research for metal fuels is at its early stages. The conceptual design for large scale fabrication has been developed, but not yet tested. The limited range of composition (Pu, Np and Am. Zr with and without U) investigated so far show good quality metallurgical properties with high melting eutectics and burn-ups up to 10% shows good

behavior in the fuel [30]. So far no fabrication experience exists with prototypic materials from separation processes.

### **2.5.3. Nitride fuel**

These fuels are based on Uranium nitride and are the choice for reactor designs that NASA produces. The advantage of this fuel is that they have better thermal conductivity than uranium oxide but they have a higher risk than oxide fuels and metal fuels. Because of the higher conductivity this fuel type is the primary candidate for lead-alloy cooled breeder reactors considered under the GEN-IV program [31].

### **2.5.4. Carbide fuel**

They consist of uranium carbide in the form of pin-type elements for liquid metal fast breeder reactors. They have high thermal conductivity and a high melting point. The carbide fuels are mainly dispersion fuels. The fabrication of the fuel is very difficult. But researches on these fuels are continuing because they are the suitable candidate for high temperature reactors applications for Generation IV reactors [26].

## 2.6. Reprocessing of Spent Nuclear Fuels

Reprocessing of spent fuels refers to the chemical separation of fissionable uranium and plutonium and other radioactive elements. Early days of reprocessing was originally conducted to build the atomic bomb but now the reprocessing is important because of a perceived scarcity of uranium as well as reduction of radioactive waste rather than proliferation. Since the uses of uranium increasing from the last few years because of the increasing amount of power plants, the idea of reprocessing would serve better in the near future. Reprocessing is performed to recover elements include uranium, plutonium, minor actinides and fission products which are the result from the splitting or fissioning atoms of U-235. The uranium recovered from the reprocessing is about 0.6% of U-235 and 99.4% of U-238. The plutonium recovered can be mixed with uranium and other actinides to make mixed oxide fuel (MOX) and used in a nuclear reactor which reduces the risk of proliferation. So the reprocessing helps in reducing the radioactive waste and the recovered elements can be further recycled in the power plants as a fuel.

### 2.6.1. History of Reprocessing

Reprocessing began in the 1940s which was originally for military purposes to recover plutonium for weapons [32]. In 1944 Oak Ridge National Laboratory developed the bismuth phosphate process which required several stages including dissolution of the cladding materials and precipitate formation along with centrifuge steps [33]. But due to the disadvantages of not separating uranium and large amounts of waste and chemicals, a new process was developed at Argonne National Laboratory (ANL) which used reduction and oxidation (REDOX) process. This aqueous process involved aluminum nitrate in the aqueous phase with hexane as the

solvent for extraction which created less waste and more complete extraction, but had drawback of large amounts of aluminum nitrate being used [34].

Lately, the scientists at Oak Ridge National Laboratory developed the plutonium and Uranium extraction (PUREX) process which is implemented throughout the world today. All commercial reprocessing plants in operation today use this technology. This process involves a bath of nitric acid and solvent extraction of uranium and plutonium with tributyl phosphate (TBP) in hydrocarbon diluents [34]. Also with modifications to the PUREX process, it is possible to selectively extract uranium, minor actinides and fission products which will be discussed in the later part of this chapter.

Another reprocessing technology known as pyroprocessing was developed by US Department of Energy. Initial research in pyroprocessing was carried out by the Department of Energy (DOE) for treatment of spent fuel from the experimental breeder reactor II (EBR-II). A melt refining process was developed which recovered actinides while removing volatile fission products from this metal fuel [35]. This process only offered partial separation of actinides and was not able to separate plutonium which was desirable at that time but this is yet to be adopted [36].

### **2.6.2. Reprocessing countries**

Commercial nuclear reactors in the United States began operating since 1957. Nuclear power now constitutes about 20% of the electricity generated in the US and there are more than 104 nuclear reactors currently operating which produces the huge amount of waste. The U.S produces more than 2000 metric tons of spent nuclear fuel every year and there will be more than 60,000 metric tons accumulated by the end of 2010 [37]. The sheer volume of spent fuel

produced in the United States demonstrates the need for the reprocessing. Now the repository constructed in YUCCA Mountain has no longer been considered suitable for waste storage, the need of reprocessing is even more important. In the U.S there are no civil reprocessing plants that are operating currently. Three civil reprocessing plants had been built. The first one, a 300 tonne/year plant at West Valley, NY which was operated successfully from 1966-72 was shut down due to high cost for the modification requirements. The second one was also a 300 tonne/year plant built at Morris, Illinois; incorporating new technology failed to work successfully in production and was shut down in 1974. A third for 1500 tonne/year plant built at Barnwell, South Carolina was ruled out because of a change in policy by the government [37].

Current nuclear waste reprocessing capacities are shown in Table 1. Countries like the UK reprocessed metal fuel from the Magnox generation gas cooled reactors at Sellafield for 50 years to ensure safety, hygiene and other regulatory standards. Oxide fuels were also reprocessed from 1969 to 1973. In France a 400 tonne/year reprocessing plant was operated for metal fuels from gas-cooled reactors at Marcoule until 1997. Oxide fuel reprocessing has been done since 1976 and also other two operating plants of 800 tonne/year are operating now. The provision to store the reprocessed uranium for up to 250 years as a strategic reserve has also been set-up. The reprocessed plutonium is immediately recycled as mixed oxide (MOX) fuels. The reprocessing output in France is coordinated with a MOX plant input to avoid any build up of plutonium[38-39]. A reprocessing plant is running in Tarapur, India for 100 tonne/year oxide fuel plant. Japan is also starting up a major plant of 800 tonne/year at Rokkasho, but has been in use to reprocess and also most of their fuels are reprocessed in Europe. Russia owns the oxide fuel reprocessing plant at Ozersk [34, 38, 40].

**Table 1:** Major Current Commercial Light Water Spent Fuel Reprocessing Capacity [38]

| <b><u>Commercial Plant</u></b>   | <b><u>Nominal Capacity, tonnes Heavy Metal/year</u></b> |
|----------------------------------|---|
| France, LaHague                  | 1700  |
| UK, Sellafield (THORP)           | 900   |
| Russia, Mayak                    | 400   |
| Japan<br>Tokai<br>Rokkasho       | ~100<br>800   |
| <b>Approximate Sub-Total</b>     | ~3900   |
| <b>Other</b>                     |   |
| UK                               | 1500  |
| India                            | 275   |
| Approximate Sub-Total            | 1775  |
| <b>Total Commercial Capacity</b> | 5675  |
| (U.S. commercial capacity)       | (0)   |

### 2.6.3. Reprocessing options

Reprocessing can be accomplished via several courses. Reprocessing includes options such as separating U and Pu; separating U and mixed U+Pu; separating U, Pu and minor actinides; separating U, Pu+Np and Am+Cm; separating U+Pu only, separating U, Pu+ actinides and certain fission products, but these options have two perceived problems [37]. The separated plutonium is a potential proliferation risk and the minor actinides remain in the waste has longer radioactivity than the fission products alone. So the focus is to remove the actinides from the final waste and burn them with the recycled uranium and plutonium in the fast reactors. The combination of reprocessing and recycling should be an interim phase of nuclear development [41].

## 2.6.4. Reprocessing processes

There are many reprocessing techniques. Spent fuels in the past were reprocessed with several processes like Purex, Bismuth, Butex, Thorex and aqueous waste processing. But this paper discusses only two of those processes: Aqueous process including Purex and its modifications and non aqueous processes called pyrochemical processing especially molten salt system.

### 2.6.4.1. Aqueous Process: PUREX

To date the most dominant aqueous reprocessing process is PUREX. PUREX (Plutonium and Uranium Recovery by Extraction) is one of the main aqueous processes which have been used all over the world. The success of the PUREX has led to the replacement of various other reprocessing processes like Redox, Butex, Thorex process etc.

In this process the spent fuel is dissolved in nitric acid where uranium and plutonium are extracted and remaining constituents of fission products and minor actinides are left as wastes. Uranium and plutonium are transferred to an organic phase by intensive mixing with an organic solvent tributyl phosphate (TBP) in kerosene and fission products remain in the aqueous nitric phase as shown in Figure 13 [42]. PUREX was the primary reprocessing used in U.S before federal government halted the reprocessing of used nuclear fuel. Today it is used actively in countries like Britain, France, Japan and Russia for reprocessing. The biggest problem of the PUREX process is plutonium. The reprocessing results in pure plutonium which is the concern for proliferation of nuclear weapons.

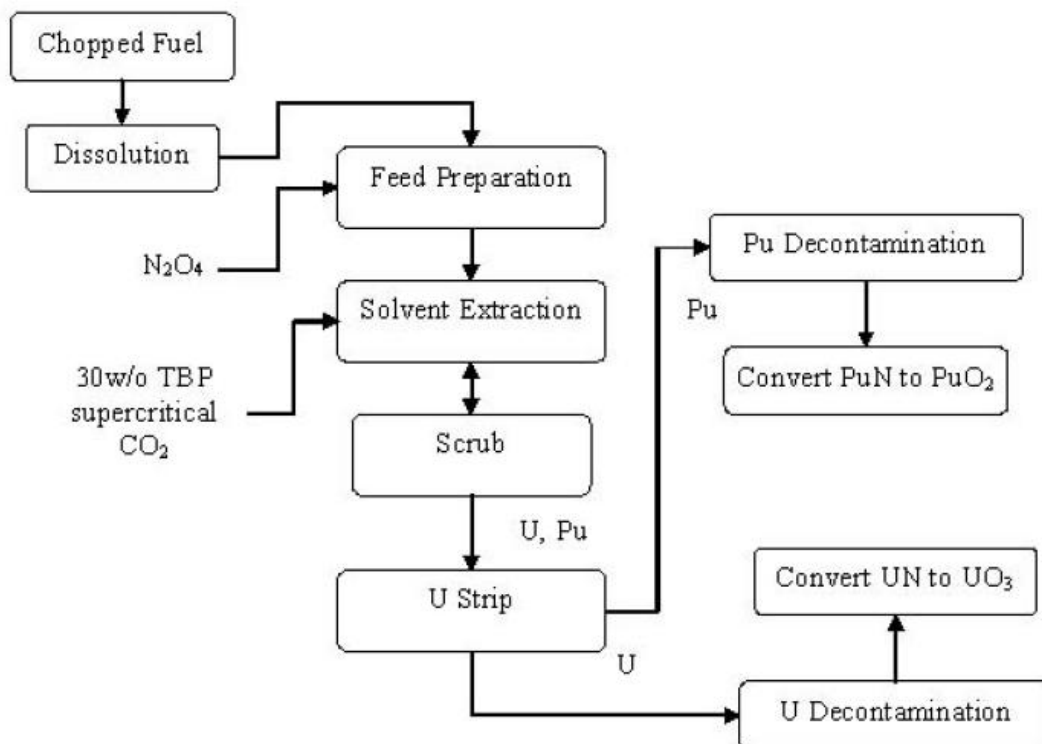


Figure 12: Purex flow sheet [43-44]

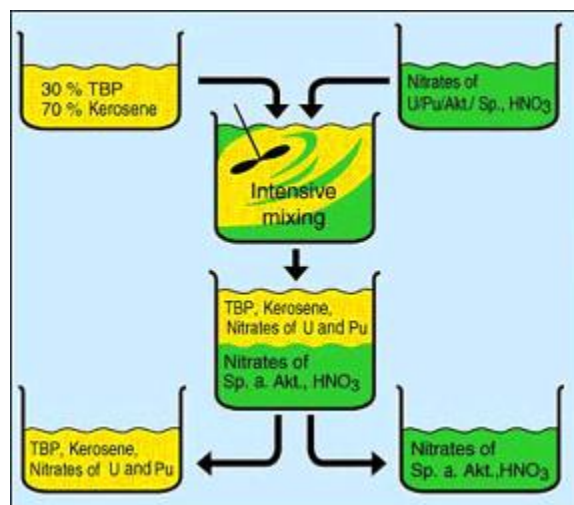
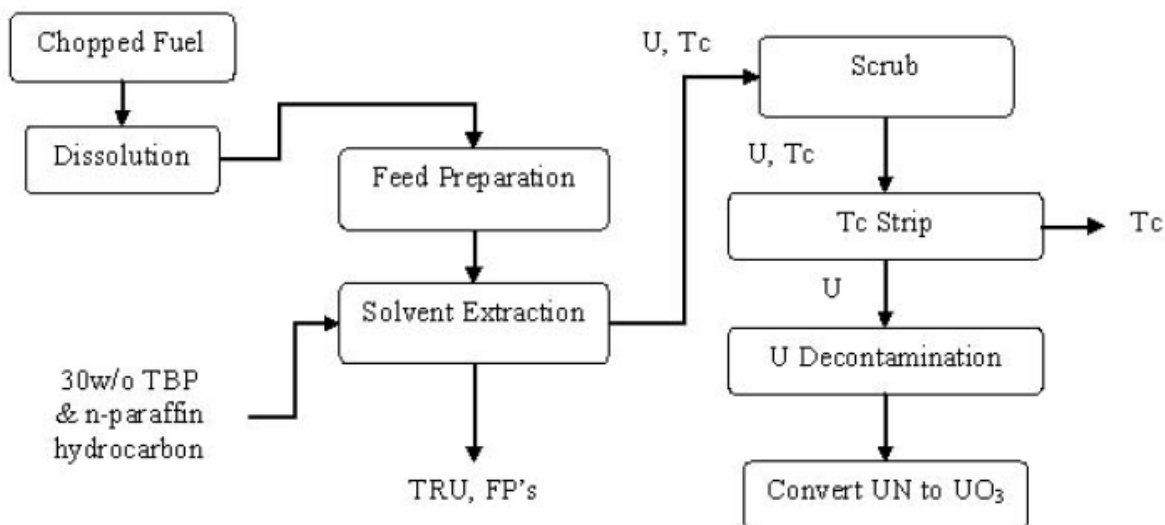


Figure 13: PUREX process [42]

### 2.6.4.1.1. UREX

The UREX (Uranium Extraction) process is the modified version of the PUREX process. The UREX flow sheet is shown in Figure 14. This process does not involve the isolation of the plutonium providing better proliferation resistance than the PUREX process. In this process the plutonium remains mixed with the fission products and minor actinides. It can also be supplemented to recover fission product iodine by volatilization and technetium by electrolysis. In the UREX process 99.9% of uranium and 95% of technetium are separated individually from each other; and from other fission products and actinides. In this process acetohydroxamic acid (AHA) is added which greatly diminishes the extractability of plutonium and neptunium.



**Figure 14:** UREX [45]

#### *2.6.4.1.2. Other modifications of PUREX process*

##### **Transuranic Extraction (TRUEX)**

TRUEX is the extraction process for the transuranic elements by the addition of another extraction agent octyl(phenyl)-N, N-dibutyl carbamoylmethyl phosphine oxide (CMPO) in the traditional PUREX process. It was developed in the US by Argonne National Laboratory (ANL) to remove transuranic metals, like americium and cerium from the waste.

##### **Diamide Extraction (DIAMEX)**

This process is the alternative of TRUEX using malondiamide which selectively separates long-lived radionuclides from short-lived fission products. The DIAMEX has the advantage of avoiding the formation of organic waste which contains elements other than carbon, hydrogen, nitrogen and oxygen.

##### **Selective Separation of Actinides (SANEX)**

SANEX involves the separation of actinides. Managing actinides, either used in industrial sources or as fuel, is necessary for the lanthanides to be extract from the PUREX raffinate. Since lanthanides have large neutron cross sections there is the possibility for the contaminating the nuclear reaction. The process has not been developed yet but the researchers are working towards its development.

##### **Universal extraction (UNEX)**

UNEX was developed in Russia and the Czech Republic. It is designed to completely remove the most troublesome radioisotopes (Sr, Cs and minor actinides) from the raffinate remaining after the extraction of U and Pu.

#### 2.6.4.2. Non-Aqueous Process

Nonaqueous processes have been used in reprocessing plants to separate materials for nuclear weapons and for reprocessing spent reactor fuels. A detail description of non-aqueous process can be found in International Atomic Energy Agency [46] and World Nuclear Association [47] websites.

##### 2.6.4.2.1. Pyrochemical process

The pyrochemical reprocessing method uses high temperature oxidation-reduction medium in non-aqueous media to separate the actinides, U and Pu from the fission products (as shown in Figure 15). This method makes use of the differences in the volatilities or thermodynamic stabilities of the compounds of actinides and fission products to achieve the separation. It can be achieved by using electrochemical method instead of chemical equilibration. The generic principles consist of dissolving the elements in a bath of molten salts at high temperature, then separating the desired species electrochemically. The pyroprocessing involves several stages including volatilization, liquid-liquid extraction, using immiscible metal-metal phases or metal-salt phases, electrolytic separation in molten salt and functional crystallization. The technique is generally based on the use of either fused salts such as chlorides or fluorides (eg:  $\text{LiCl}+\text{KCl}$  or  $\text{LiF} + \text{CaF}_2$ ) or fused metals such as cadmium, bismuth or aluminum.

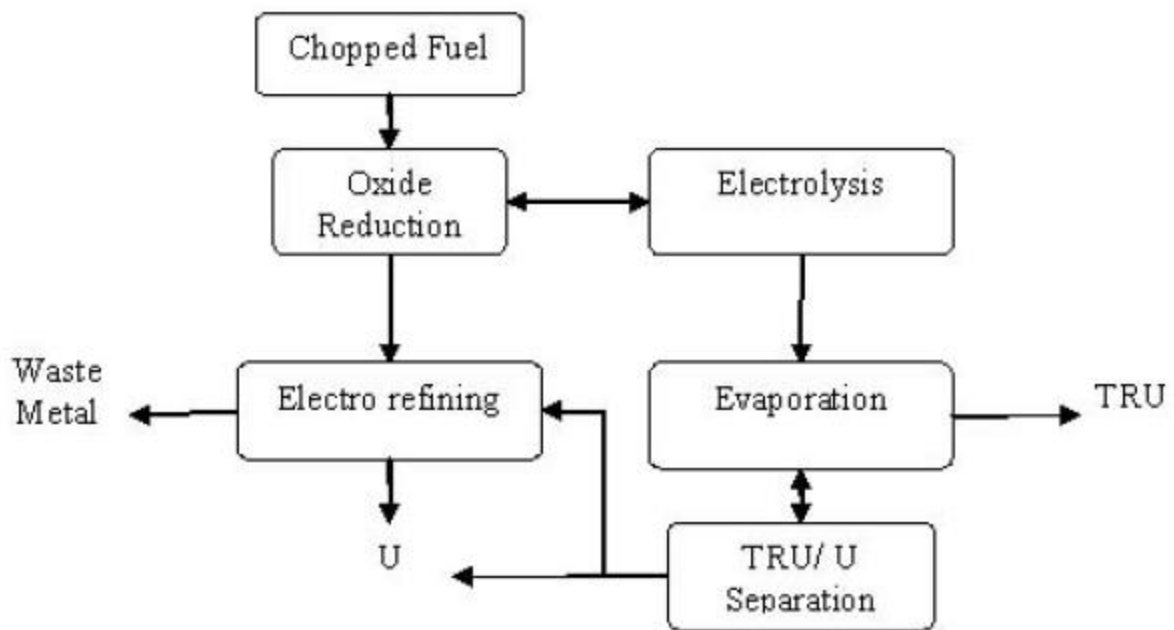


**Figure 15:** Pyroprocessing [48]

The interest in pyrochemical processing is mainly due to its advantages over aqueous methods.

The main advantages are [46]:

- Ability to accommodate short cooled and high burn-up fuels due to the higher radiation stabilities of non-aqueous reagents
- Low process volume and compact equipment due to the higher solubility of the actinides in molten salts than in aqueous solutions
- Wide temperature range is available to amplify the differences in the thermodynamic stabilities that control the separation factors
- Small volume of waste in the solid form makes easier waste treatment
- Less criticality problems because no water is present
- The process is very suitable for advanced fuels. The PUREX process is very problematic and costly in the case of metallic alloy fuels. As the irradiated fuel has to be brought from metallic state to an aqueous and again to metal. This process requires numerous steps for reconversion while in pyroprocessing method the fuel directly yields in metal products
- Highly suitable for nitride fuels

Due to the significance of this process, the techniques to separate nuclides from the radioactive waste stream has been under development in the US Department of Energy, Argonne National laboratory (ANL); Korea Atomic Energy Research Institute (KAERI) and Russian Institute of Atomic Reactors (RIAR)[49].

### 2.6.5. Molten salt system

Molten salt are often used as reaction media in extractive metallurgy and as electrolytes for electrochemical refining. They are more attractive because of the low viscosity and high thermal conductivity. There are two basic types of molten salt system used in pyroprocessing of spent nuclear fuels: (1) the mixed fluoride salt fluid system, used as coolant and a homogeneous fuel and blanket system in the reactor experiments, and (2) the simple chloride salts, used as an ionic solvent in pyrochemical spent fuel reprocessing systems that are intended for use with highly irradiated metallic reactor fuels [50]. In the molten salt reactor experiment application, the fluoride salt consists of  $\text{BeF}_2$ ,  $\text{LiF}$ ,  $\text{ThF}_4$  and  $\text{UF}_4$  as the working fluid. Molten salt provide a fertile thorium blanket, a neutron multiplier, the fissile fuel, the reactor coolant and the reprocessing solvent. The main features of using ionic molten inorganic salts are that they are resistant to radiation damage effects. The chloride system with  $\text{LiCl-KCl}$  as an electrolyte is the main focal point of this project.

#### 2.6.5.1. $\text{LiCl-KCl}$ System

The electrorefining process using  $\text{LiCl-KCl}$  molten system has various advantages. It exhausts considerable amounts of salt wastes containing some metal chlorides such as rare earth chlorides which can be separated easily. It provides very low electric conduction unlike the fluoride system which saves energy. It also has high thermal conductivity. The  $\text{LiCl-KCl}$  has a lower eutectic melting point than fluoride systems [51]. And they are also not suitable for production of high quality uranium and plutonium for the manufacture of fuel. So the chloride system seems to be a preferred choice. So far only one pyroprocessing technique using  $\text{LiCl-KCl}$  molten salt has been licensed for the use in integral fast reactor (IFR). This is the electrolytic process developed by the ANL and used for pyroprocessing of the used fuel from experimental

breeder reactor II (EBR-II) which operated from 1963-1994. The process is shown in Figure 16. Details were discussed in a status report from World Nuclear Association and Nuclear Energy Agency published in 2004 [37, 52].

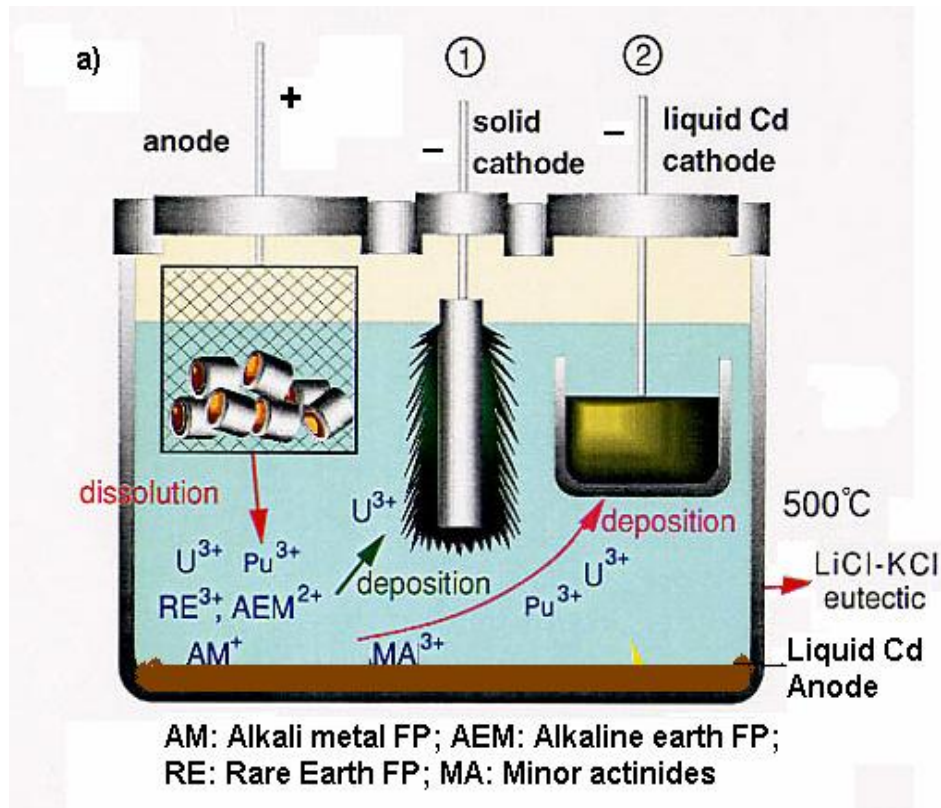


Figure 16: Molten salt system [46, 53]

### 2.6.6. Issues on spent fuel reprocessing

There are numerous issues regarding the spent nuclear fuel reprocessing including but not limited to technical, national legal and regulatory framework, political, economics, and environmental protection. Earlier reprocessing was done for missile materials recycling but due to the concern of proliferation and unfavorable economics some countries chose to store spent fuel rather than recycle. Presently about 30% of the spent fuel has been reprocessed with the remaining being stored temporarily which are yet to be disposed or reprocessed. The consequence

has been a continuing increase in spent fuel inventory in various modes of interim storage. As a result reprocessing technology is now expected to play an increasing role as a major option for optimizing the management of spent nuclear fuels.

Conventional reprocessing technology is expected to continue to play an important role in the medium term until the future reprocessing technology completely established. There are still challenges for future reprocessing which includes economics competitiveness, national and international standards and regulations, proliferation risk, environmental protection and higher reactor fuel performance [54].

In summary, current civil reprocessing of spent nuclear fuel utilizing the Purex process has been successfully practiced on a commercial scale for over 40 years without occurrences of diversion of special nuclear materials. These operations have been for the purpose of spent fuel management and for recovery of uranium and plutonium for recycle as UOX and MOX fuel for light water and fast reactors. Such a combination of spent nuclear fuel reprocessing and recycling is leading to benefits in ultimate waste disposal but due to some other disadvantages and issues like discussed above cannot fully fulfilled by Purex process. Even though Purex process fulfills the current needs of reprocessing, it will be insufficient for future reprocessing. The futures Gen IV reactors will be operating at high temperature are designed to have on site reprocessing facilities attached to it. So the Purex process which is low temperature process is inadequate. Hence high temperature reprocessing technology is needed and pyroprocessing which is a high temperature processing would be the ultimate choice.

## 2.7. Objective and Scope

The main objectives of the current R&D on spent fuel reprocessing are to develop a separations system that can be effectively deployed to serve next generation spent fuel reprocessing plants.

The goal of next generation fuel is to use pyroprocessing process as a reprocessing system so it is important to develop the pyrochemical concepts. Currently pyroprocessing methods are being developed for on-site use and expected to be economically and politically attractive.

Pyroprocessing has a number of methods including various chemical systems. But for this project, which is the part of Department of Energy (DOE) R&D for pyroprocessing, molten salt reprocessing using LiCl-KCl eutectic bath for metallic fuels was the only system considered.

Specifically this work is divided into two parts. The first part will evaluate the temperature variations of eutectic LiCl-KCl with the accumulation of lanthanide elements after the separations of U, Pu and other actinides. And the second part is the electrochemical studies of lanthanide elements in LiCl-KCl eutectic molten salt.

## Chapter 3: Project Description

### 3.1. Melting Point Variation

In this project, the temperature variation of LiCl-KCl eutectic was studied on addition of different lanthanide tri-chlorides species. The main objective of this work was to provide supportive information to the Department of Energy (DOE) on how the accumulation of lanthanides affects the overall reprocessing using molten salts. In Idaho National Laboratory (INL), the molten salt reprocessing research experimental reactor operates at 773 K (500°C) to reprocess SNF. They reprocess uranium, plutonium and other actinides while lanthanides in the SNF would remain in LiCl-KCl eutectic bath. During the various reprocessing runs, lots of lanthanides would accumulate in the bath which might create a problem in the future if the melting temperature exceeds the operating temperature. The accumulated lanthanides would form solid solution and affect the melting temperature of eutectic LiCl-KCl. So, it is important to study the effect of lanthanide in the melting of eutectic LiCl-KCl. The specific goal of this project was to observe the temperature variation due to lanthanides accumulation by thermal analysis. The variation in temperature was observed in the single component and multi-component mixture.

### 3.2. Electrochemistry of Lanthanides

The lanthanides are the species that are present in the spent nuclear fuels which remains in the electrolytic bath after reprocessing. The lanthanides consist of fourteen elements that are found in the periodic table with atomic numbers from 58 through 71. Those elements have similar properties. All are elements filled with 4f electron orbitals. Electrochemistry of lanthanides is the study of kinetics behavior which helps in determining the oxidation and reduction potential, activity and diffusion coefficient of lanthanides that are present in molten

salts. It is important because the properties of lanthanides are very close to actinides which make separation of actinides difficult from the lanthanides. In the reprocessing cell, lanthanide would continuously accumulate while separating out the actinides. The accumulation of lanthanide would make it difficult for further separation of actinides from the cell. According to the Nernst equation given by relation 1, when the concentration increases the reduction potential shifts to less negative and similarly when concentration decreases the reduction potential shift to more negative potential. Therefore while separating out the actinides, its concentration would be decreasing and accumulated lanthanides concentration would be more compare to actinides. That means as the potential of actinides decreases the lanthanide potential will be increasing. If this process keeps running continuously then at some point, the actinides and lanthanides would reduce at same potential. Figure 17 illustrates the increasing and decreasing of lanthanide and actinide concentration and potential in continuous reprocessing system (Table 2 shows standard potential of some actinides and lanthanides at 450 °C). So in order to maximize the processing rate of the electrorefining step, it is necessary to analyze the kinetic behavior of lanthanides presents in the electrorefiner.

$$E_{\text{cell}} = E^{\circ} + (RT/nF)\ln\{\text{Ln}^{3+}\} \quad (1)$$

Diffusion and potential data for the most actinides are already reported [55-58] but there is little data available for lanthanide elements. The reduction potential and diffusion coefficient can be obtained by using a combination of transient electrochemical techniques such as Cyclic Voltammetry and Chronopotentiometry. Some of the data were obtained by using different electrolyte medium, different temperature and different electrode with different techniques

[59-62]. In this work we will focus on a Cyclic Voltammetry study at constant temperature of 500°C in LiCl-KCl eutectic molten salt. The reduction behavior of single as well as multiple lanthanide elements present in the molten salt will be investigated.

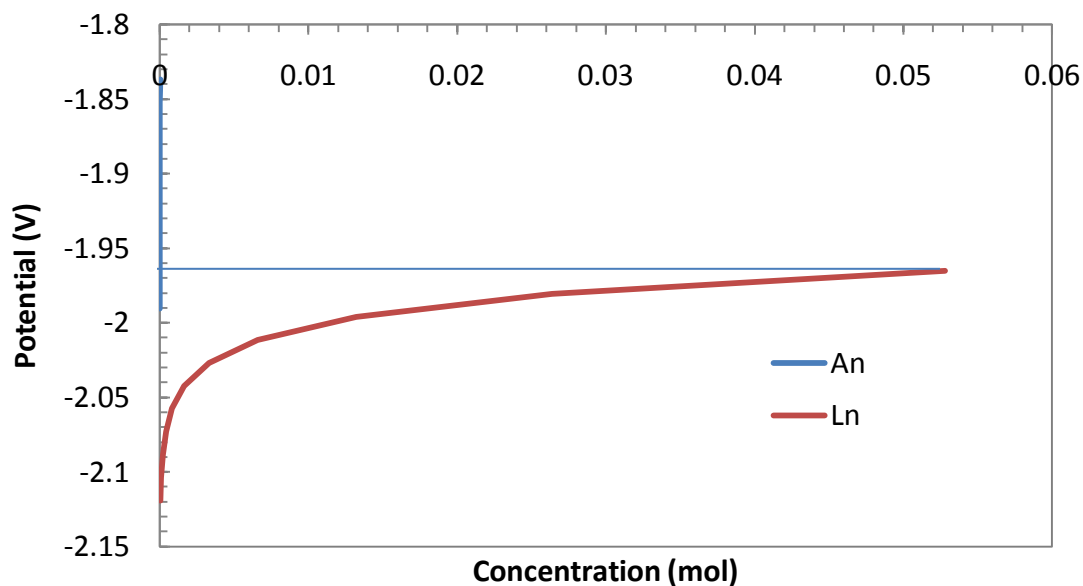


**Figure 17:** Potential vs Concentration showing actinides concentration reducing and lanthanide concentration increasing

**Table2:** Standard potential vs Ag/AgCl at 450 °C in LiCl-KCl [63]

| System                       | Potential (V) vs Ag/AgCl at 450 C |
|------------------------------|-----------------------------------|
| Uranium ( $U^{3+}/U^0$ )     | -1.28                             |
| Plutonium ( $Pu^{3+}/Pu^0$ ) | -1.59                             |
| Neptunium ( $Np^{3+}/Np^0$ ) | -1.48                             |
| Americium ( $Am^{3+}/Am^0$ ) | -1.64                             |
| Lanthanum ( $Ln^{3+}/Ln^0$ ) | -1.91                             |
| Neodymium ( $Nd^{3+}/Nd^0$ ) | -1.86                             |

# Chapter 4: Experimental Methods

---

The experimental setup designed for each separate project is described below.

## 4.1. Temperature Variations of Eutectic LiCl-KCl by Additions of Lanthanide Trichlorides

### 4.1.1. Procedure

The ultra dry anhydrous salt reagents of lanthanide trichlorides ( $\text{LnCl}_3$ :  $\text{DyCl}_3$ ,  $\text{PrCl}_3$ ,  $\text{SmCl}_3$ ,  $\text{CeCl}_3$ ,  $\text{LaCl}_3$ ,  $\text{GdCl}_3$ ,  $\text{NdCl}_3$ ), KCl, LiCl were purchased from Sigma Aldrich and Alfa/Aesar. All salt reagents were contained inside air tight ampoules and were all of 99.99% purity. The thermal analysis was performed in a furnace which was placed inside a glove box (Vacuum Atmospheres Inc., Omni Lab model) filled with ultra high purity (UHP: 99.99%) argon atmosphere. The glove box contained less than 5 parts per million (ppm) of  $\text{O}_2$  and  $\text{H}_2\text{O}$ . The furnace including the controller was supplied by Applied Test Systems (ATS) Inc. The furnace was ATS 3210 series and the controller was 900 TC16 (Allen Bradley).

The eutectic composition of LiCl-KCl and some fixed amount of salt reagents of different composition were weighed. The eutectic concentration of LiCl-KCl consists of 58.5 mol% LiCl and 41.5 mol% KCl (some of the experimental results on eutectic composition and temperature of LiCl-KCl found in the literature are presented in the Table 3). The salts were then mixed manually by using mortar and pestle and placed in a high purity alumina crucible for heating. The mixtures of salt were heated to melting and kept molten for sometime in order to make sure of complete mixing. Each experiment was repeated four times and the first result was discarded to avoid lack of mixing and the results of the remaining three experiments were

averaged. The heating rate was 2°C/min. A thermocouple (K-type, ATS Inc) was used to record the temperature. Two thermocouples were inserted into the furnace: one inside the crucible that containing the mixture of salt and one outside the crucible to observe temperature variance. Both thermocouples were connected to the thermocouple input (8-Channel, Filed Point, National Instrument) device and to the computer for the data acquisition process. The Lab View software was used for data collection. The temperatures were recorded in five second interval for each experimental run. The overall experimental setup is shown in Figures 18 and 19.

**Table 3:** Eutectic concentration and melting temperature

|                 | Aukrust [64] | Richards [65] | Basin et. al [66] |
|-----------------|--------------|---------------|-------------------|
| LiCl (mol %)    | 58.5         | 58.3          | 58.2              |
| KCl (mol %)     | 41.5         | 41.7          | 41.8              |
| Temperature (K) | 627          | 627           | 625               |

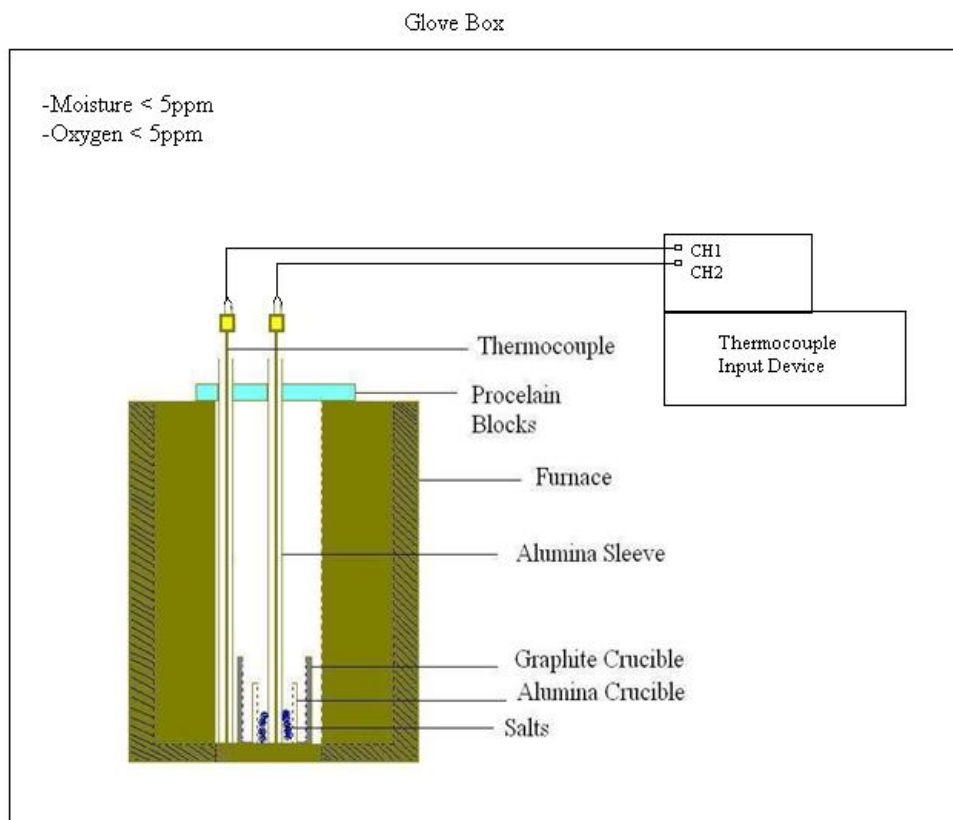


**Figure 18:** Experimental Setup for thermal analysis

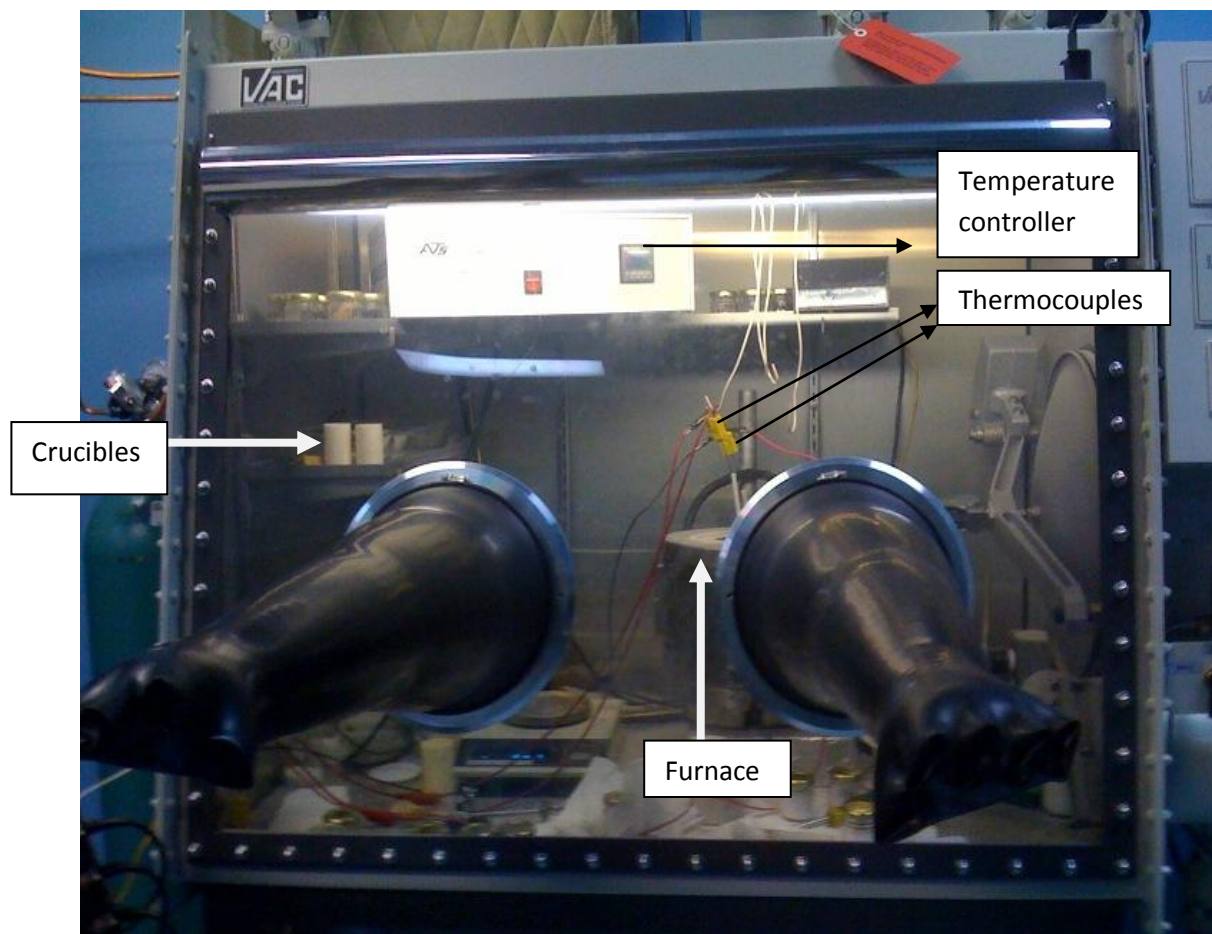


**Figure 19:** Setup inside glove box

#### 4.1.2. Data Analysis

Data analysis is needed to determine the melting point of the mixture of salt. From the experiments, the heating as well as cooling curves were obtained as shown in Figure 20. The heating curve obtained was smooth with a plateau showing the change in phase because of the good control of furnace while heating. But due to lack of control while cooling, the cooling curve shows rather super cooling. When super cooling occurs, salt starts to crystallize below the temperature at which a change of state ordinarily would take place [67]. The liquidus and solidus temperature shift lower when compared to heating. So for our investigation we

preferred heating curve to determine the melting temperature of lanthanide elements in LiCl-KCl eutectic and discard the cooling curve. In order to determine the melting point, the temperature was plotted versus time (as shown in Figure 21). The plot shows the plateau where melting occurs. These are sometimes difficult to interpret because the melting starts at one point and ends on other as shown in Figure 21. Therefore to obtain the fixed melting point where the bulk of the mixtures melt we applied different techniques. Here, numerical differentiation was applied which gives the sharp melting peak as shown in Figure 22. The first derivative approach was taken. The derivative of temperature with respect to time was taken. The first derivative of temperature with respect to time was plotted against the temperature which shows the sharp peak of melting (shown in Figure 22). The sharp peak was considered the melting temperature for the bulk of mixture. The heating curve presented in Figure 21-23 for analysis is for pure LiCl.

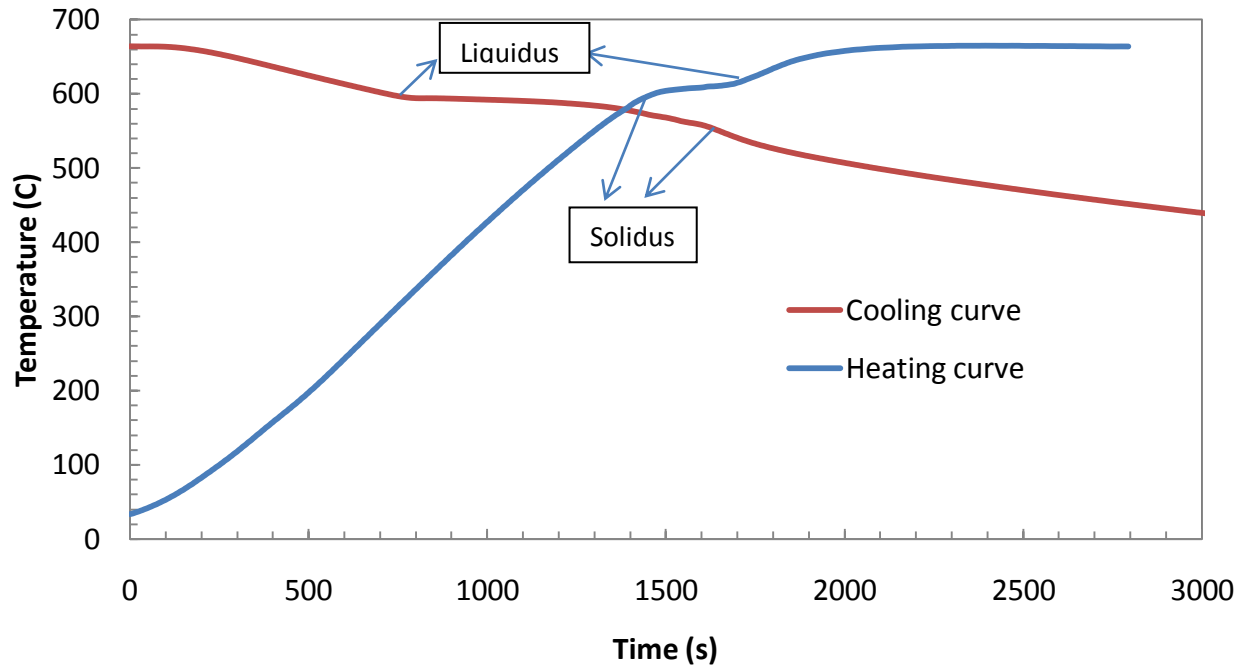


**Figure 20:** Heating and Cooling curve obtained from the experiments

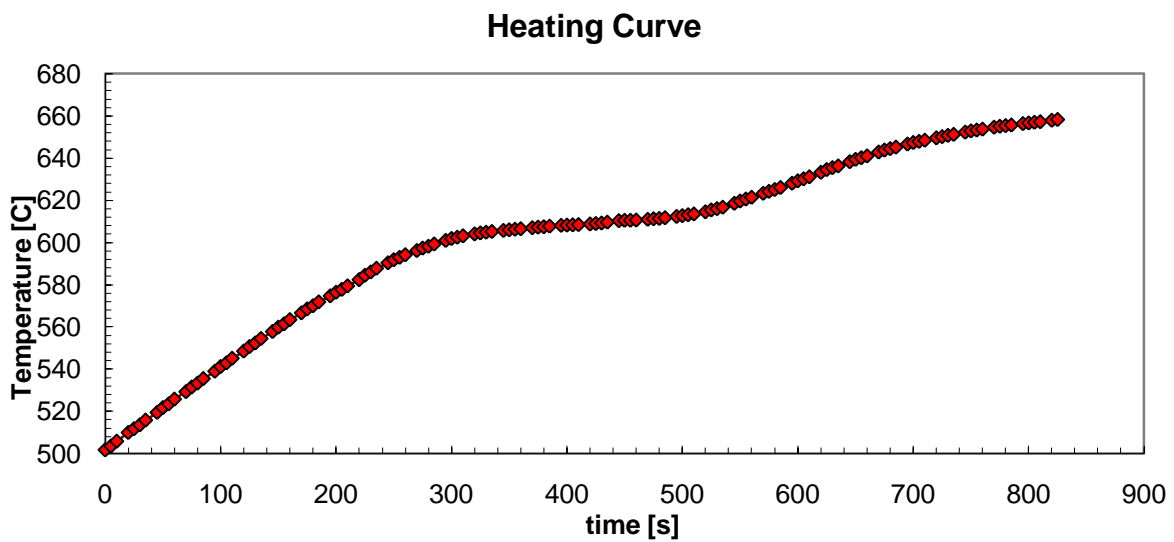


**Figure 21:** Heating curve showing halt point

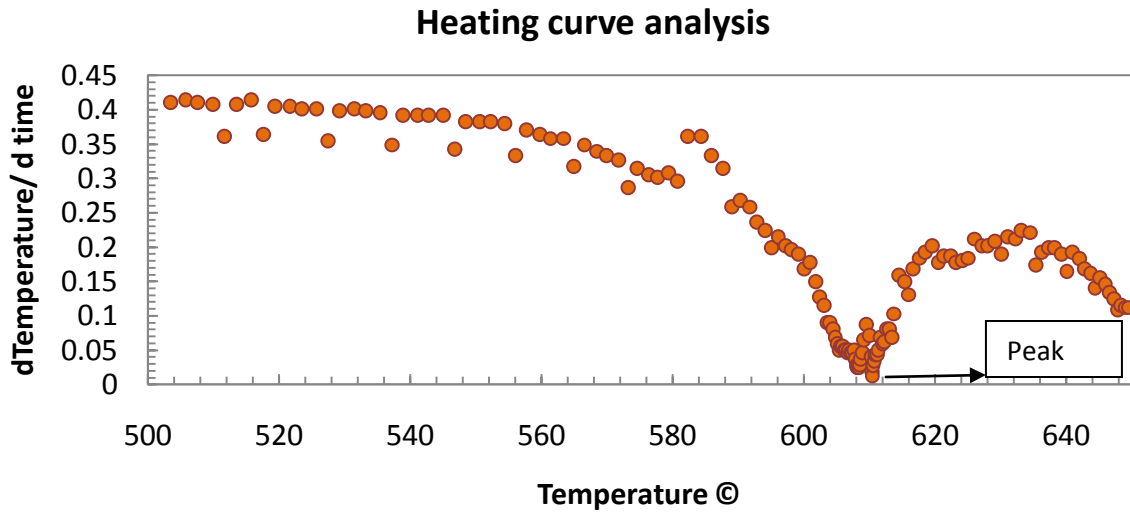


**Figure 22:** Heating Curve analysis showing peak temperature

#### 4.1.3. Mathematical Model: B-spline

In Figure 22 it was noticed that the data points are scattered in the plot which was due to the noise during experiment. The noise during heating affects the numerical differentiation so it is important to reduce the noise in the data by using different data analysis techniques. Several smoothing algorithms are suggested in the literature [68-69] including B-spline (where B stand for basis or basics) smoothing technique and moving average which were frequently used for this purpose [70]. In this work Matlab version 7.8.0 (R2009a) of B-spline was used to reduce the noise in the data.

The acquired data was smoothed using the mathematical model called B-spline. B-Spline curve is a sequence of curve segments that are connected together to form a single continuous curve. A smooth curve is fitted along a number of control points. B-spline is the mathematical function that connects the points which follows the sequence of the curve and removes all the

unwanted points. It basically smoothen the curve. The smoothened plot by using B-spline technique is provided in Figure 23. The mathematical formula for B-spline is given by the following equation [71].

$$P(u) = \sum_{k=0}^n p_k B_{k,d}(u), u_{\min} \leq u \leq u_{\max}, 2 \leq d \leq n + 1$$

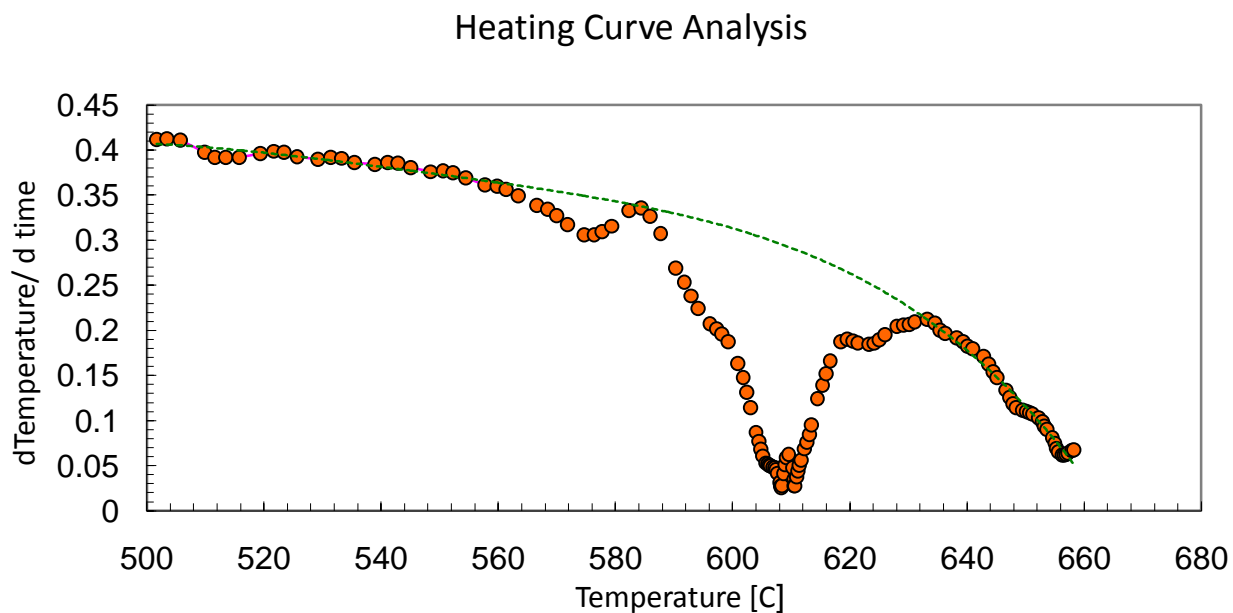
There are 'n+1' control points. The 'B<sub>k,d</sub>' basis functions are of order 'd' (degree d-1). 'd' must be at least 2 (linear), and can be no more than 'n+1' (the number of control points). The important point is that the order of the curve (linear, quadratic, cubic) is therefore not dependent on the number of control points.

The 'B<sub>k,d</sub>' depend on the value of 'd' and the values in the knot vector. 'B' is defined recursively as:

$$B_{k,d}(u) = \begin{cases} 1 & \text{if } u_k \leq u \leq u_{k+1} \\ 0 & \text{otherwise} \end{cases}$$

$$B_{k,d}(u) = \frac{u - u_k}{u_{k+d-1} - u_k} B_{k,d-1}(u) + \frac{u_{k+d} - u}{u_{k+d} - u_{k+1}} B_{k-1,d-1}(u)$$

Here each 'B<sub>k,d</sub>(u)' depends only on the 'd+1' knot values from 'u<sub>k</sub>' to 'u<sub>k+d</sub>'. B<sub>k,d</sub>(u) = 0 for u < u<sub>k</sub> or u ≥ u<sub>k+d</sub> so 'P<sub>k</sub>' only influences the curve for u<sub>k</sub> ≤ u < u<sub>k+d</sub>. Formally, 'P(u)' is a polynomial of order, d (degree d-1) on each interval u<sub>k</sub> ≤ u < u<sub>k+d</sub>. P(u) is continuous in all of its derivatives between the knots. P(u) is validly defined for u<sub>min</sub> ≤ u < u<sub>max</sub> where u<sub>min</sub> = u<sub>d</sub> and u<sub>max</sub> = u<sub>n+2</sub> [71].



## 4.2. Electrochemical Separation of Lanthanides from LiCl-KCl

The development of pyrochemical reprocessing methods requires accurate knowledge about the chemical and electrochemical behavior of lanthanides in molten salt at higher temperature. The basic electrochemical behavior of lanthanide ions in chloride media was investigated using transient electrochemical techniques, such as cyclic voltammetry and chronopotentiometry. Such techniques yield information about the oxidation/reduction mechanisms occurring and the transport behavior of the lanthanide ion in the salt melt. In this project, the electrochemical behavior of  $\text{LnCl}_3$  ( $\text{Ln} = \text{La, Ce, Nd, Dy, Pr, Gd}$  and  $\text{Sm}$ ) was studied in LiCl-KCl eutectic at 773 K (500 °C) using Cyclic Voltammetry. The main objective of this work was to observe the reduction behavior of lanthanides and see the variations in potential when different species of lanthanide elements are present in eutectic LiCl-KCl. Single lanthanide element mixtures and the combination of different mixtures were investigated.

### 4.2.1. Procedure

The electrochemical experiments, storage and handling were all carried out in a glove box (Vacuum Atmospheres Inc., Omni Lab model) filled with ultra high purity argon atmosphere ( $\text{H}_2\text{O}$  and  $\text{O}_2 < 5\text{ppm}$ ). The ultra dry anhydrous 99.99% purity salts reagents of lanthanide trichlorides ( $\text{LnCl}_3$ ), KCl, and LiCl were purchased from Sigma Aldrich and Alfa Aesar. The salts were weighed in a weighing balance and mixed together on mortar and pestle inside the glove box. Then the salt mixture was melted at 773 K ( $500\text{ }^\circ\text{C}$ ) and kept melted it few hours to ensure complete mixing before each experiment.

### 4.2.2. Experimental arrangement and apparatus

The experimental arrangement is shown in Figure 24. The system contains a small furnace with a PID controller which is capable of handling a 20 ml crucible. The small volume of molten salt is advantageous because of shallow temperature gradient within the crucible, ease of handling and cheaper. The system has adjustable electrode holders that make it more efficient to move the electrode and control the placement of electrodes inside the crucible without shorting. It is also equipped with a micro-positioner to control the movement of the working electrode holder and provides the immersion depth of the electrode in the molten salts with accuracy of 0.1 mm. So using this experimental arrangement the exposed area can be determined with a reasonable level of accuracy.

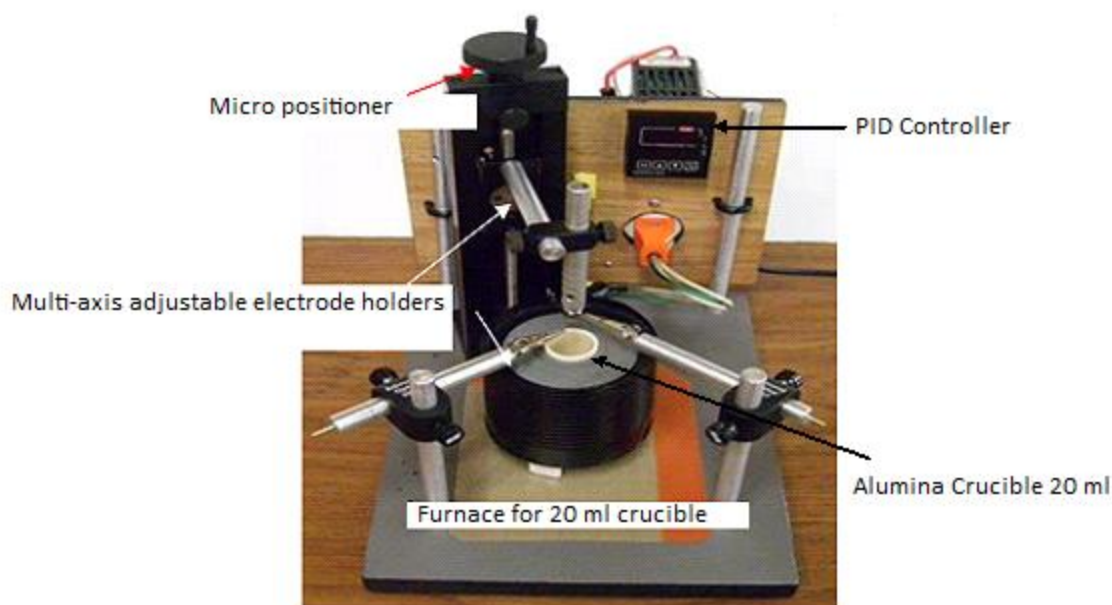


Figure 24: Experimental arrangement for electrochemical studies in molten salt

### 4.2.3. Electrolytes

The electrolytic bath consists of molten LiCl-KCl eutectic mixture. The eutectic mixture used a concentration of 58.5 mol% LiCl + 41.5 mol% KCl (from table 2) which melts at 625 K (352°C). The lanthanide chloride salts of 5 wt % and 3 wt% were added to the eutectic mixture before melting. Then the mixtures contained in alumina crucible (20 ml) were heated. The lanthanide chloride salt consisted of LaCl<sub>3</sub>, CeCl<sub>3</sub>, GdCl<sub>3</sub>, NdCl<sub>3</sub>, PrCl<sub>3</sub>, SmCl<sub>3</sub> and DyCl<sub>3</sub>. Different combinations of binary, ternary and quaternary system were investigated. The combination of (LiCl+KCl)<sub>Eutectic</sub> is one system and addition of one lanthanide salt makes it binary, two makes it ternary, three makes it quaternary and so forth. The salts were used as obtained with no further drying and the moisture level of salt was not determined. Also it should be noted that no effort was taken to remove the trace amount of moisture that was present in the salt.

#### 4.2.4. Cyclic Voltammetry

The cyclic voltammetry (CV) was carried out using a three electrode configuration. Tungsten metal wire 1 mm diameter was used as the working and counter electrode; whereas a Silver (Ag) wire was used as the reference electrode. Potential was measured against the Ag electrode. The electrode was inserted approximately 4 mm into the bath. The immersion depth and diameter were used to determine the surface area required to find out current density. The measurements were carried out by using an Autolab potentiostat (Corr Ware, Instrument #1, Solartron 1286 {0, 6}). The cyclic Voltammetry tests were carried out at different scan rates such as 10, 20, 50, 100, 200, 500 and 1000 mV/s. After the experiments, the reduction and oxidation behaviors of single as well as multi-component lanthanides were analyzed.

#### 4.2.5. Electrodeposition

The electrodepositions of the mixture of lanthanides in LiCl-KCl were carried out using an Autolab potentiostat (Corr Ware, Instrument #1, Solartron 1286 {0, 6}). The experimental arrangement was shown in Figure 24. A constant potential was applied for 10 mins and the deposited metal was stripped from the working electrode for characterization. The deposit was characterized using Scanning Electron Microscope (SEM) and X-ray Diffraction (XRD).

### 4.3. Characterization Technique

#### 4.3.1. Scanning Electron Microscope (SEM)

The deposited lanthanide elements were studied by using a cold field emission scanning electron microscope which “uses the focused beam of high-energy electrons to generate a variety of signals at the surface of the specimens” [72]. The SEM images showed the deposited luster of metals and by using energy dispersive X-ray analysis (EDX) determined the elemental

contents of the lanthanides. “EDX is the technique that is used in conjunction with SEM. An electron beam strikes the surface of a sample which causes X-rays to be emitted from that point of sample and by moving the electron beam across the material an image of each elements in the sample can be acquired” [72].

### **4.3.2. X-ray Diffraction**

X-ray diffraction was used to determine the structural information of lanthanides present in the deposit. It was done by using a Philips-12045 B/3 diffractometer with a copper target at a step scan rate of 5deg/min. In general x-ray diffraction occurs when the monochromatic beam of x-rays (wavelength of 5-25 nm) hit the surface of a crystal. Diffracted waves of different atoms in a crystal can interfere each other and form a pattern by satisfying the Bragg’s law ( $n\lambda = 2d \sin \theta$ ). The diffraction pattern of pure substances looks like a fingerprint and records the intensity with respect to  $2\theta$  [73].

# Chapter 5: Results and Discussions

---

## **5.1. Temperature Variations of Eutectic LiCl-KCl by Additions of Lanthanide Trichlorides**

The experimental results for the sample containing single and multi-component mixtures are presented in this section. Initially, the melting temperature of eutectic LiCl-KCl was calculated using our experimental setup. The eutectic temperature was found close to 625 K which is comparable to the one obtained by different researchers as shown in Table 3. The plot was shown in Figure 25. So, that temperature was used as reference melting temperature of LiCl-KCl eutectic. Further experiments were conducted for single component and multi-component mixing of lanthanide elements in eutectic LiCl-KCl and the results are presented.

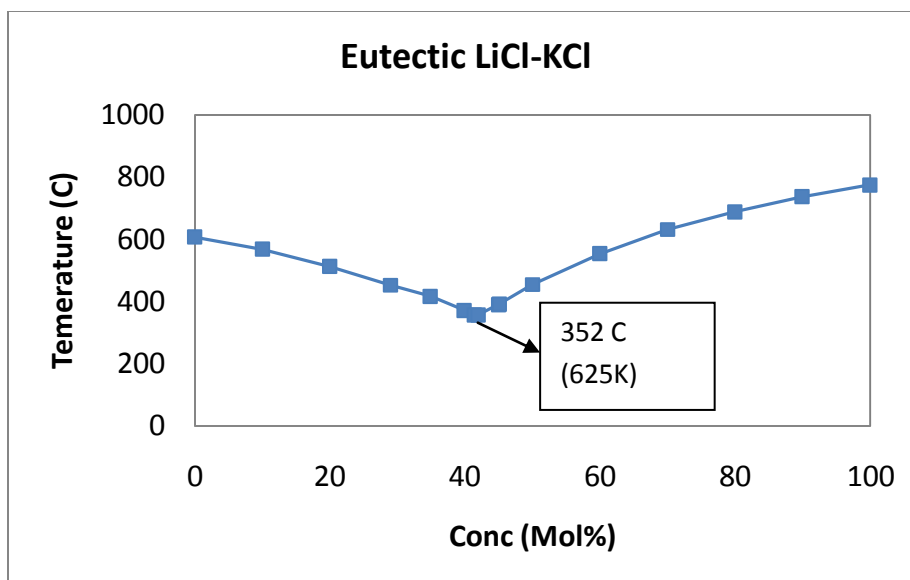


**Figure 25:** Eutectic curve obtained

### 5.1.1. Single Component

Thermal analysis was carried out at different compositions of salt. The mixture composition varies from 0.1 mol% to 5 mol%. Each individual lanthanides salt was mixed with eutectic LiCl-KCl.

The results for the each experiment containing  $\text{LaCl}_3$ ,  $\text{CeCl}_3$ ,  $\text{PrCl}_3$ ,  $\text{GdCl}_3$ ,  $\text{DyCl}_3$ ,  $\text{NdCl}_3$  in LiCl-KCl obtained by heating are shown in Tables 4-9 and plots are provided in Figures 26-31, respectively. The melting temperatures presented in the Tables are the melting temperature of the bulk of the mixtures which are obtained by first derivative approach from the experimental data as discussed in the data analysis technique in experimental methods. Melting temperature for each mixture ranging from 0.1 mol % to 5 mol% of each lanthanide salt is presented. The melting temperature above 5 mol% was already determined by Nakamura and Kurata [74] in a LiCl-KCl- $\text{LnCl}_3$  system where they presented the temperature variations and phase existence. Data in the table shows that the experiments were conducted well below 5 mol%. Most of the

melting temperatures are below the eutectic LiCl-KCl melting as predicted because all the mixtures obtained lower melting point than the pure components [75]. Also, the difference between the eutectic melting and the melting temperature obtained from the mixture of salt presented in Table 4 to 9 and in Figure 32 (3-D area plot for the temperature difference and mol%  $\text{LnCl}_3$ ) shows that melting temperature of LiCl-KCl eutectic doesn't vary significantly with addition of  $\text{LnCl}_3$  up to 5mol%. So, these results prove that there is very little effect on melting temperature of LiCl-KCl eutectic due to the accumulation of lanthanides up to 5 mol%.

**Table 4:** Change in Melting Temperature after  $\text{LaCl}_3$  addition in (LiCl-KCl)<sub>Eutectic</sub>

| LiCl-KCl-<br>$\text{LaCl}_3$ |                |  |                                      |                              |  |
|------------------------------|----------------|--|--------------------------------------|------------------------------|--|
| <b>Mol%LiCl</b>              | <b>Mol%KCl</b> | <b>Mol%<br/><math>\text{LaCl}_3</math></b> | <b>Eut LiCl-<br/>KCl<br/>Temp(K)</b> | <b>Exp. Melt<br/>Temp(K)</b> | <b>Exp. Temp -<br/>Eut. Temp =<br/><math>\Delta T</math> (K)</b> |
| 57.93875%                    | 41.94725%      | 0.11400%                                   | 625                                  | 622.60                       | -2.4   |
| 56.71043%                    | 41.05795%      | 2.23161%                                   | 625                                  | 616.83                       | -8.17  |
| 56.09350%                    | 40.61129%      | 3.29521%                                   | 625                                  | 615.2                        | -9.8   |
| 55.47254%                    | 40.16173%      | 4.36573%                                   | 625                                  | 619.66                       | -5.34  |
| 55.48967%                    | 39.744486%     | 5.35839%                                   | 625                                  | 620.5                        | -4.5   |

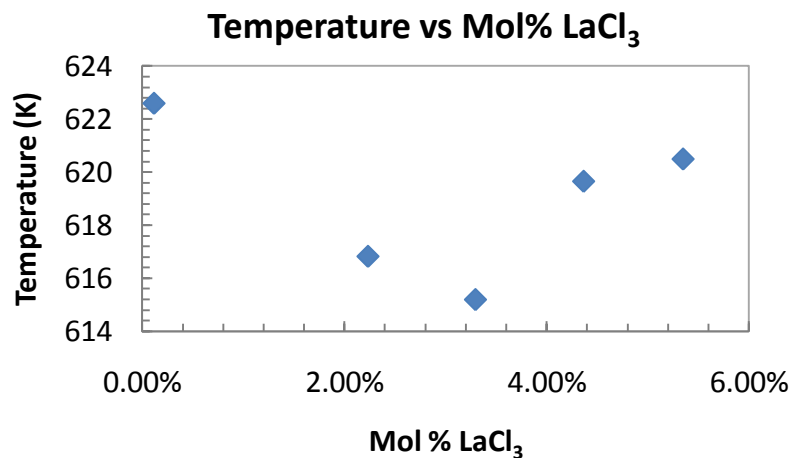


**Figure 26:** Melting temperature distribution after adding various mol % of LaCl<sub>3</sub> in (LiCl-KCl)<sub>Eutectic</sub>

**Table 5:** Change in Melting Temperature after CeCl<sub>3</sub> addition in (LiCl-KCl)<sub>Eutectic</sub>

| LiCl-KCl-CeCl <sub>3</sub> |           |                        |                      |             |                                |
|----------------------------|-----------|------------------------|----------------------|-------------|--------------------------------|
| Mol%LiCl                   | Mol%KCl   | Mol% CeCl <sub>3</sub> | Eut LiCl-KCl Temp(K) | Temp(K)     | Exp. Temp - Eut. Temp = ΔT (K) |
| 57.93858%                  | 41.94800% | 0.11343%               | 625                  | 617.04      | -7.96                          |
| 56.71670%                  | 41.06249% | 2.22081%               | 625                  | 620.8166667 | -4.18333                       |
| 56.10265%                  | 40.61792% | 3.27944%               | 625                  | 618.3666667 | -6.63333                       |
| 55.48453%                  | 40.17041% | 4.34506%               | 625                  | 621.0575    | -3.9425                        |
| 54.89675%                  | 39.74486% | 5.35839%               | 625                  | 622.0075    | -2.9925                        |

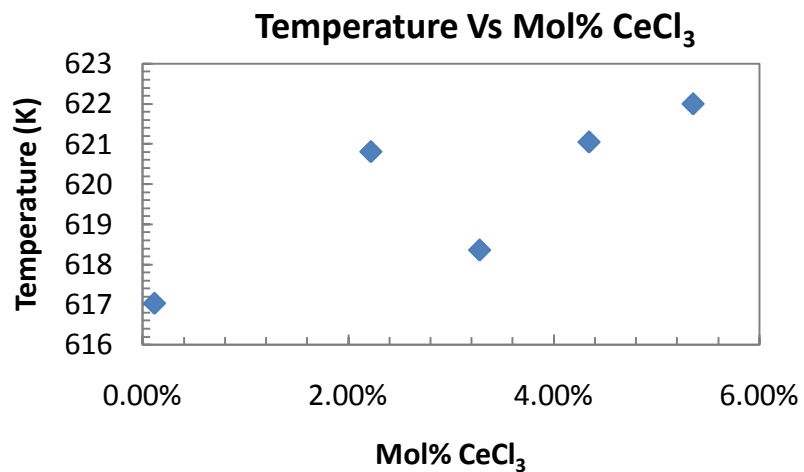


**Figure 27:** Melting temperature distribution after adding various mol % of CeCl<sub>3</sub> in (LiCl-KCl)

Eutectic

**Table 6:** Change in Melting Temperature after PrCl<sub>3</sub> addition in (LiCl-KCl) <sub>Eutectic</sub>

| LiCl-KCl-PrCl <sub>3</sub> |           |                        |                      |                   |                                |
|----------------------------|-----------|------------------------|----------------------|-------------------|--------------------------------|
| Mol%LiCl                   | Mol%KCl   | Mol% PrCl <sub>3</sub> | Eut LiCl-KCl Temp(K) | Exp. Melt Temp(K) | Exp. Temp - Eut. Temp = ΔT (K) |
| 57.93928%                  | 41.94763% | 0.11309%               | 625                  | 627.16            | 2.16                           |
| 56.72016%                  | 41.06585% | 2.21399%               | 625                  | 625.92            | 0.92                           |
| 56.10830%                  | 40.62201% | 3.26968%               | 625                  | 625.4             | 0.4                            |
| 55.49194%                  | 40.17577% | 4.33228%               | 625                  | 617.71            | -7.29                          |
| 54.90580%                  | 39.75141% | 5.34280%               | 625                  | 621.61            | -3.38                          |

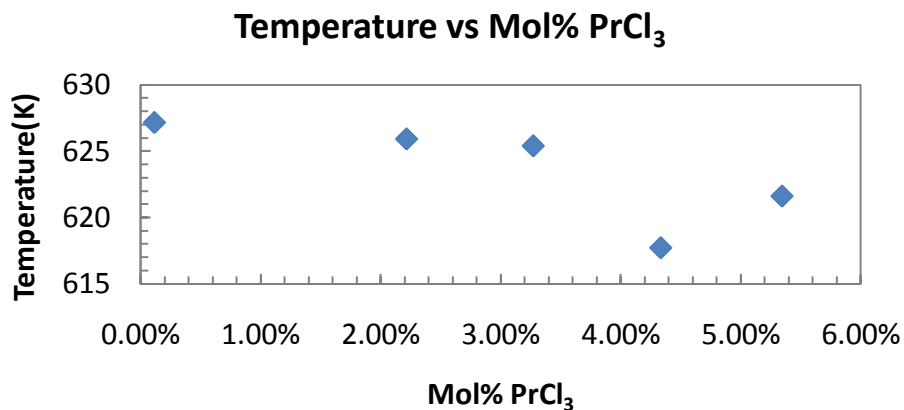


**Figure 28:** Melting temperature distribution after adding various mol % of PrCl<sub>3</sub> in (LiCl-KCl)

Eutectic

**Table 7:** Change in Melting Temperature after GdCl<sub>3</sub> addition in (LiCl-KCl)<sub>Eutectic</sub>

| LiCl-KCl-GdCl <sub>3</sub> |           |                        |                      |                   |                                |
|----------------------------|-----------|------------------------|----------------------|-------------------|--------------------------------|
| Mol%LiCl                   | Mol%KCl   | Mol% GdCl <sub>3</sub> | Eut LiCl-KCl Temp(K) | Exp. Melt Temp(K) | Exp. Temp - Eut. Temp = ΔT (K) |
| 57.94335%                  | 41.95058% | 0.10607%               | 625                  | 620.17            | -4.82                          |
| 56.79867%                  | 41.12183% | 2.07950%               | 625                  | 626.51            | 1.51                           |
| 56.22246%                  | 40.70466% | 3.07288%               | 625                  | 622.15            | -2.85                          |
| 55.64164%                  | 40.28415% | 4.07421%               | 625                  | 622.01            | -2.99                          |

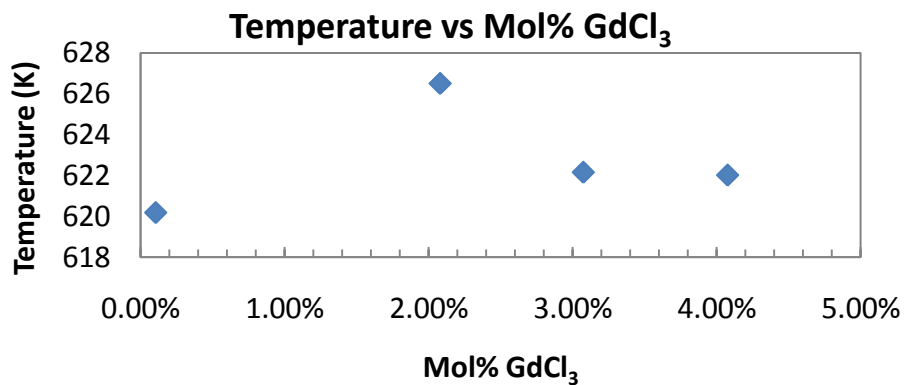


**Figure 29:** Melting temperature distribution after adding various mol % of GdCl<sub>3</sub> in (LiCl-KCl)

Eutectic

**Table 8:** Change in Melting Temperature after DyCl<sub>3</sub> addition in (LiCl-KCl) <sub>Eutectic</sub>

| LiCl-KCl-DyCl <sub>3</sub> |           |                        |                      |                   |                                |
|----------------------------|-----------|------------------------|----------------------|-------------------|--------------------------------|
| Mol%LiCl                   | Mol%KCl   | Mol% DyCl <sub>3</sub> | Eut LiCl-KCl Temp(K) | Exp. Melt Temp(K) | Exp. Temp - Eut. Temp = ΔT (K) |
| 57.94455%                  | 41.95144% | 0.10400%               | 625                  | 617.74            | -7.26                          |
| 56.82174%                  | 41.13854% | 2.03972%               | 625                  | 621.27            | -3.73                          |
| 56.25621%                  | 40.72910% | 3.01468%               | 625                  | 619.23            | -5.77                          |
| 55.68594%                  | 40.31623% | 3.99783%               | 625                  | 622.42            | -2.58                          |
| 55.14271%                  | 39.92293% | 4.93436%               | 625                  | 626.92            | 1.92                           |

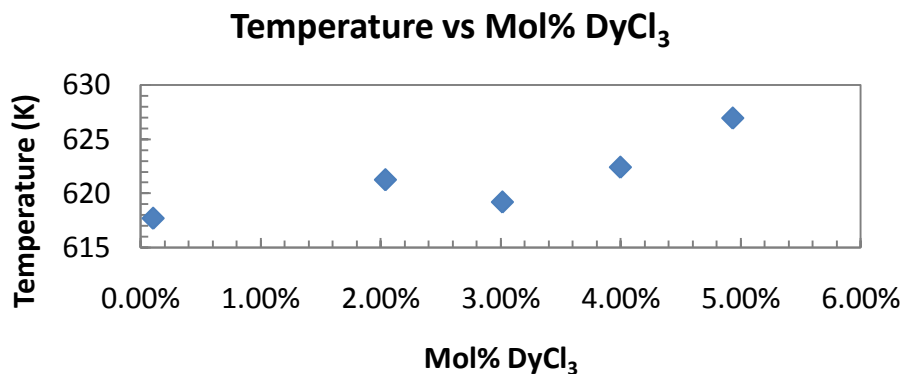


**Figure 30:** Melting temperature distribution after adding various mol % of DyCl<sub>3</sub> in (LiCl-KCl)

Eutectic

**Table 9:** Change in Melting Temperature after NdCl<sub>3</sub> addition in (LiCl-KCl)<sub>Eutectic</sub>

| LiCl-KCl-<br>NdCl <sub>3</sub> |           |                           |                         |                      |                                      |
|--------------------------------|-----------|---------------------------|-------------------------|----------------------|--------------------------------------|
| Mol%LiCl                       | Mol%KCl   | Mol%<br>NdCl <sub>3</sub> | Eut LiCl-KCl<br>Temp(K) | Exp. Melt<br>Temp(K) | Exp. Temp<br>- Eut. Temp<br>= ΔT (K) |
| 57.94016%                      | 41.94827% | 0.11157%                  | 625                     | 615.87               | -9.12                                |
| 56.73740%                      | 41.07748% | 2.18512%                  | 625                     | 627.04               | 2.04                                 |
| 56.13290%                      | 40.63982% | 3.22729%                  | 625                     | 617.98               | -7.02                                |
| 55.52418%                      | 40.19911% | 4.27671%                  | 625                     | 628.05               | 3.05                                 |

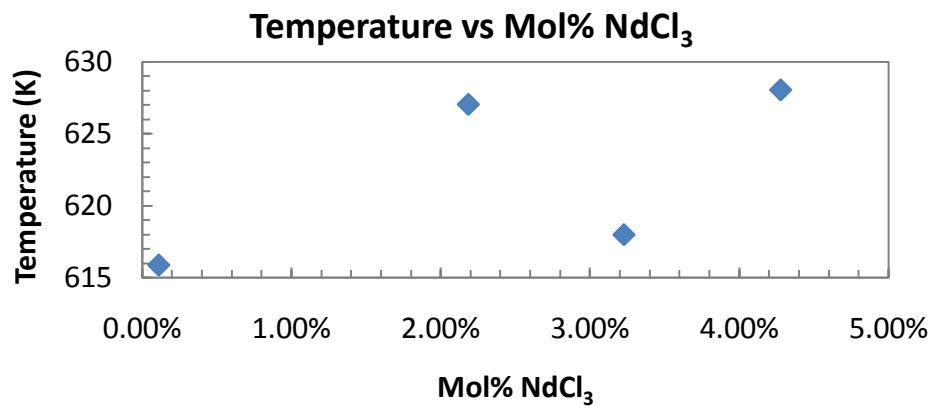


**Figure 31:** Melting temperature distribution after adding various mol % of NdCl<sub>3</sub> in (LiCl-KCl)

Eutectic

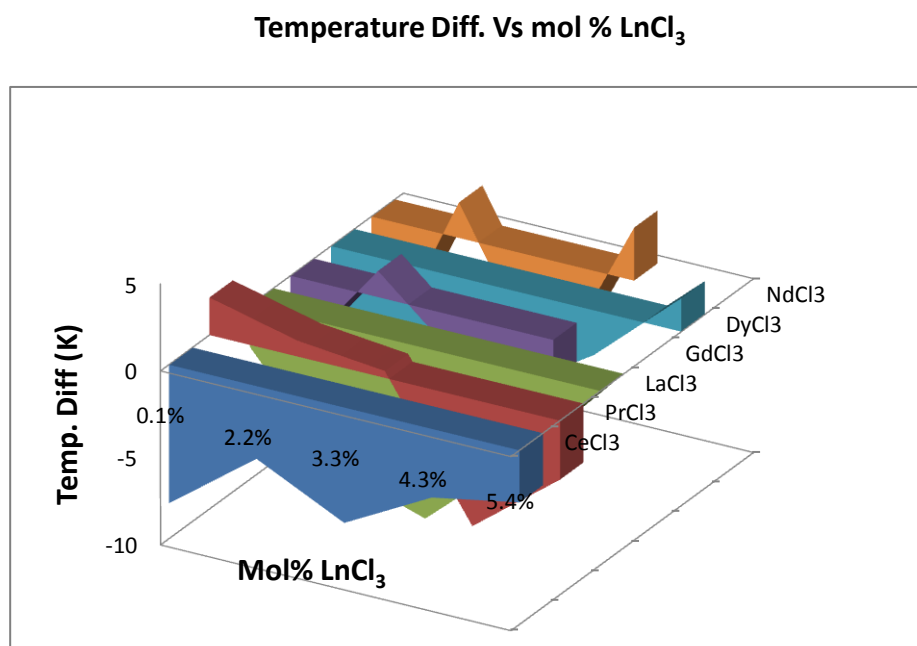


**Figure 32:** 3-D area plot of temperature difference vs mol % LnCl<sub>3</sub>

### 5.1.2. Multi-component System

The thermal analysis was conducted on different combination mixture of salt in eutectic LiCl-KCl. The mixture of salt was random to see how the accumulations of different salts affect the eutectic temperature of LiCl-KCl.

The multi-component results obtained are shown in the Tables 10 to 17. The tables list the composition of the mixtures, obtained temperature and difference between the eutectic LiCl-KCl and obtained temperature. The temperature differences of most of the mixtures tested are below the eutectic temperature of LiCl-KCl eutectic. These mixtures shown in the Tables 10 to 17 does not have any significant temperature variance. So the accumulation of salt would not affect the reprocessing plant which is already running at 773 K (500°C). The weight percentage has been converted into mol%, as presented in the tables.

**Table 10:** Change in temperature 5 wt% lanthanides in ternary system (LiCl+KCl)Eutectic+5%CeCl<sub>3</sub>+5%LaCl<sub>3</sub>

| LiCl-KCl-5%CeCl <sub>3</sub> -5%LaCl <sub>3</sub> |          |                       |                       |                          |                      |  |
|---|----------|-----------------------|-----------------------|--------------------------|----------------------|--|
| Mol%LiCl  | Mol%KCl  | Mol%CeCl <sub>3</sub> | Mol%LaCl <sub>3</sub> | Eut LiCl-KCl<br>Temp (K) | Obtained<br>Temp (K) | Exp. Temp -<br>Eut. Temp =<br>$\Delta T$ (K) |
| 57.8730%  | 41.8990% | 0.1133%               | 0.1138%               | 625                      | 617.19               | -7.81  |

**Table 11:** Change in temperature of 5 wt% lanthanides in quaternary system (LiCl+KCl)Eutectic+5%CeCl<sub>3</sub>+5%LaCl<sub>3</sub>+5%GdCl<sub>3</sub>

| LiCl-KCl-5%CeCl <sub>3</sub> -5%LaCl <sub>3</sub> -<br>5%GdCl <sub>3</sub> |         |                       |                       |                       |                              |                      |  |
|--|---------|-----------------------|-----------------------|-----------------------|------------------------------|----------------------|--|
| Mol%LiCl   | Mol%KCl | Mol%CeCl <sub>3</sub> | Mol%LaCl <sub>3</sub> | Mol%GdCl <sub>3</sub> | Eut LiCl-<br>KCl Temp<br>(K) | Obtained<br>Temp (K) | Exp. Temp -<br>Eut. Temp =<br>$\Delta T$ (K) |
| 57.812%  | 41.855% | 0.11319%              | 0.1137%               | 0.10583%              | 625                          | 617.19               | -7.81  |

**Table 12:** Change in temperature of 5 wt% lanthanides in quinary system (LiCl+KCl)Eutectic+5%CeCl<sub>3</sub>+5%LaCl<sub>3</sub>+5%GdCl<sub>3</sub>+5%PrCl<sub>3</sub>-5%DyCl<sub>3</sub>

| LiCl-KCl-5%CeCl <sub>3</sub> -5%LaCl <sub>3</sub> -5%GdCl <sub>3</sub> -5%PrCl <sub>3</sub> -5%DyCl <sub>3</sub> |          |                       |                       |                       |                       |                       |                                    |                      |  |
|--|----------|-----------------------|-----------------------|-----------------------|-----------------------|-----------------------|------------------------------------|----------------------|--|
| Mol%LiCl   | Mol%KCl  | Mol%CeCl <sub>3</sub> | Mol%LaCl <sub>3</sub> | Mol%GdCl <sub>3</sub> | Mol%PrCl <sub>3</sub> | Mol%DyCl <sub>3</sub> | Eut<br>LiCl-<br>KCl<br>Temp<br>(K) | Obtained<br>Temp (K) | Exp.<br>Temp -<br>Eut.<br>Temp =<br>$\Delta T$ (K) |
| 57.6869%   | 41.7649% | 0.11294%              | 0.11350%              | 0.10560%              | 0.11259%              | 0.10354%              | 616.1                              | 616.1                | -8.9   |

**Table 13:** Change in temperature of 10 wt% lanthanides in ternary system (LiCl+KCl)Eutectic+10%CeCl<sub>3</sub>+10%DyCl<sub>3</sub>

| LiCl-KCl-10%CeCl <sub>3</sub> -10%DyCl <sub>3</sub> |          |                       |                       |                          |                      |  |
|---|----------|-----------------------|-----------------------|--------------------------|----------------------|--|
| Mol%LiCl  | Mol%KCl  | Mol%CeCl <sub>3</sub> | Mol%DyCl <sub>3</sub> | Eut LiCl-KCl<br>Temp (K) | Obtained<br>Temp (K) | Exp. Temp -<br>Eut. Temp =<br>$\Delta T$ (K) |
| 55.5850%  | 40.2431% | 2.1765%               | 1.9953%               | 625                      | 625.7                | 0.7  |

**Table 14:** Change in temperature of 10 wt% lanthanides in ternary system (LiCl+KCl)  
Eutectic+10%CeCl<sub>3</sub>+10%GdCl<sub>3</sub>

| LiCl-KCl-10%CeCl <sub>3</sub> -10%GdCl <sub>3</sub> |          |                       |                       |                          |                      |  |
|---|----------|-----------------------|-----------------------|--------------------------|----------------------|--|
| Mol%LiCl  | Mol%KCl  | Mol%CeCl <sub>3</sub> | Mol%GdCl <sub>3</sub> | Eut LiCl-KCl<br>Temp (K) | Obtained<br>Temp (K) | Exp. Temp -<br>Eut. Temp =<br>$\Delta T$ (K) |
| 55.5629%  | 40.2271% | 2.17564%              | 2.03426%              | 625                      | 614.71               | -10.29                                       |

**Table 15:** Change in temperature of 10 wt% lanthanides in ternary system (LiCl+KCl)  
Eutectic+10%CeCl<sub>3</sub>+10%PrCl<sub>3</sub>

| LiCl-KCl-10%CeCl <sub>3</sub> -10%PrCl <sub>3</sub> |          |                       |                       |                          |                      |  |
|---|----------|-----------------------|-----------------------|--------------------------|----------------------|--|
| Mol%LiCl  | Mol%KCl  | Mol%CeCl <sub>3</sub> | Mol%PrCl <sub>3</sub> | Eut LiCl-KCl<br>Temp (K) | Obtained<br>Temp (K) | Exp. Temp -<br>Eut. Temp =<br>$\Delta T$ (K) |
| 55.4882%  | 40.1730% | 2.1727%               | 2.1660%               | 625                      | 617.57               | -7.43  |

**Table 16:** Change in temperature of in ternary system with (LiCl+KCl) Eutectic+10%CeCl<sub>3</sub>+20%PrCl<sub>3</sub>

| LiCl-KCl-10%CeCl <sub>3</sub> -20%PrCl <sub>3</sub> |          |                       |                       |                          |                      |  |
|---|----------|-----------------------|-----------------------|--------------------------|----------------------|--|
| Mol%LiCl  | Mol%KCl  | Mol%CeCl <sub>3</sub> | Mol%PrCl <sub>3</sub> | Eut LiCl-KCl<br>Temp (K) | Obtained<br>Temp (K) | Exp. Temp -<br>Eut. Temp =<br>$\Delta T$ (K) |
| 54.3118%  | 39.3213% | 2.1266%               | 4.2401%               | 625                      | 618.59               | -6.41  |

**Table 17:** Change in temperature of 20 wt% lanthanides in ternary system with LiCl-KCl-  
20%CeCl<sub>3</sub>-20%PrCl<sub>3</sub>

| LiCl-KCl-20%CeCl <sub>3</sub> -20%PrCl <sub>3</sub> |          |                       |                       |                          |                      |  |
|---|----------|-----------------------|-----------------------|--------------------------|----------------------|--|
| Mol%LiCl  | Mol%KCl  | Mol%CeCl <sub>3</sub> | Mol%PrCl <sub>3</sub> | Eut LiCl-KCl<br>Temp (K) | Obtained<br>Temp (K) | Exp. Temp -<br>Eut. Temp =<br>$\Delta T$ (K) |
| 53.1808%  | 38.5025% | 4.1646%               | 4.1518%               | 625                      | 617.97               | -7.03  |

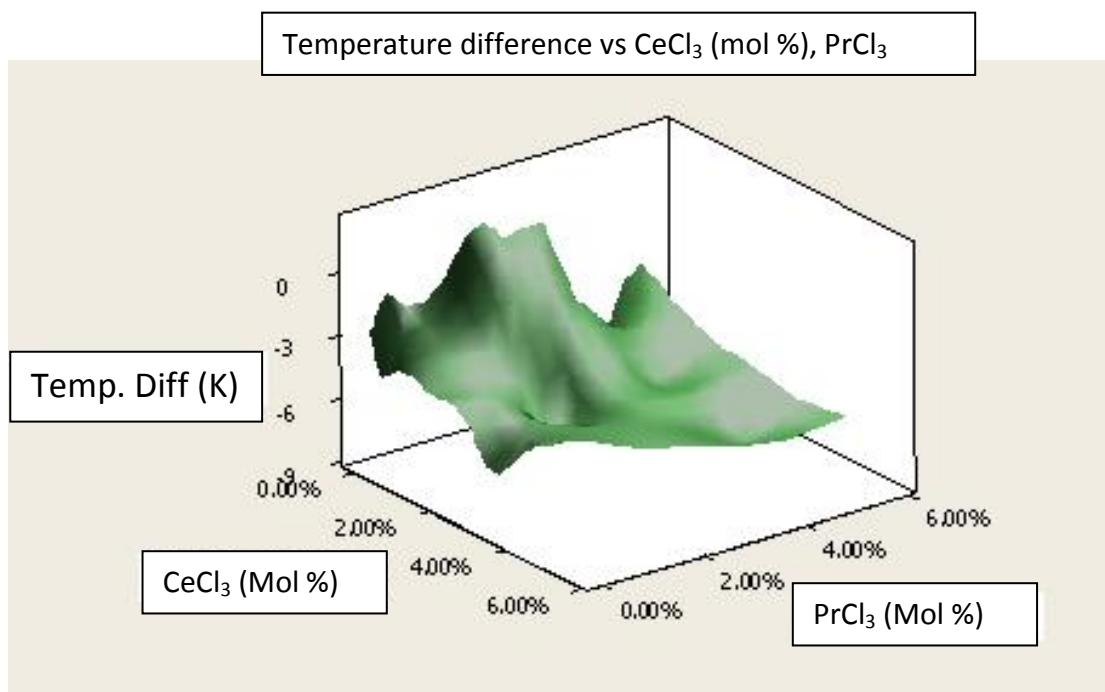


**Figure 33:** 3-D surface plot for Temperature difference vs  $\text{CeCl}_3$ ,  $\text{PrCl}_3$

## 5.2. Electrochemical Separation of Lanthanides from LiCl-KCl

Potential curve analysis of the single components as well as multi-components mixtures of lanthanide elements on LiCl-KCl eutectic is presented in the following results.

### 5.2.1. Single components: LiCl-KCl-LnCl<sub>3</sub>

Various techniques have been applied on determining the reduction potential of various lanthanide elements. Researchers have used different system against different electrode at different temperatures [59-62, 76-82]. In this work we are showing reduction potential of lanthanide elements at 773 K (500°C) in LiCl-KCl eutectic against Ag electrode. But to ensure the experimental setup, one experiment of CeCl<sub>3</sub> was performed at 450 °C against Ag electrode. The reduction potential found (shown in Figure 34) was close to the value reported by Y. Castrillejo, et al [83]. This gives us an idea that our system is working properly. The reduction potential obtained was -2.08 V from our experiment and -2.11 V from Y. Castrillejo. The little lower negative potential obtained from our experiment might be the difference in reference electrode as they used Ag/AgCl instead of Ag and also they used cerium oxide instead of cerium chloride.

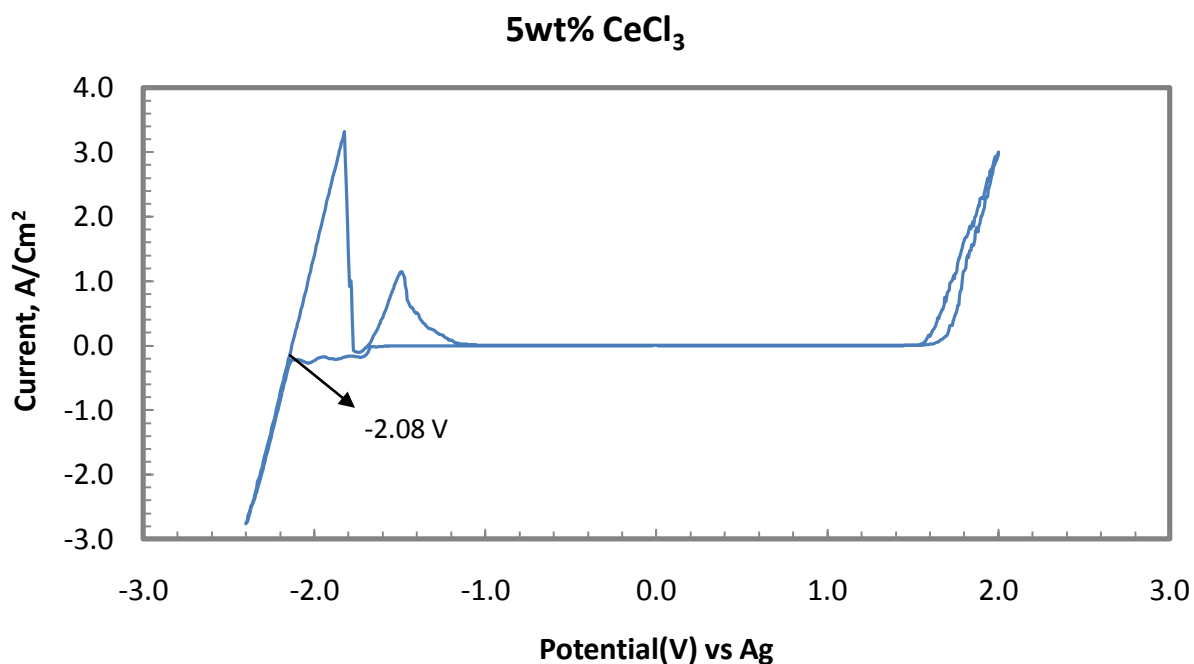


**Figure 34:** Cyclic voltammograms of  $(\text{LiCl} + \text{KCl})_{\text{Eutectic}} + 5 \text{ wt } \% \text{ CeCl}_3$  binary system at 723 K (450 °C) using tungsten as substrate at 20 mV/s scan rate

The results of Cyclic Voltammetry on mixture with  $\text{CeCl}_3$ ,  $\text{LaCl}_3$ ,  $\text{GdCl}_3$ ,  $\text{NdCl}_3$ ,  $\text{DyCl}_3$ ,  $\text{PrCl}_3$  and  $\text{SmCl}_3$  are shown in Figures 36-42, respectively. The electroreduction potential for Ln found here at 773 K (500°C) was within the same range to the ones found by other researchers for the temperature at 723 K (450°C). The reduction potential obtained at 773 K (500°C) is tabulated in Table 18 in comparison with previously published results.

A negative current density peak indicates the reduction of elements while a positive current density peak indicates the dissolution of elements which is also called stripping. In this work the reduction potential was obtained by observing the cathodic wave. The potential where large cathodic wave starts was considered to be the reduction potential of the lanthanide elements. The potentials obtained here are slightly less negative which is the consequence of using quasi

reference electrode and according to Nernst equation given by relation 1, potential shifts negative with increase in temperature.

$$E_{\text{cell}} = E^{\circ} + (RT/nF)\ln\{\text{Ln}^{3+}\} \quad (1)$$

The redox potential found in the literature for  $\text{Ln}^{3+}/\text{Ln}^0$  was obtained from the cathodic ( $E_p^c$ ) and anodic ( $E_p^a$ ) peak potentials of the cyclic voltammograms using the following relation [84]

$$E^{\circ} = (E_p^c + E_p^a)/2 \quad (2)$$

However, in this work the cathodic peak increases extensively (as observed from the figure) due to the high concentration of  $\text{LnCl}_3$  (0.14 mol/kg) so we were unable to use relation 2. The current density increases with increasing concentration of  $\text{LnCl}_3$  [82]. Alternatively the redox potential can also be obtained using relation 3 [84] by assuming the diffusivities of reducing and oxidizing species are equal and half wave potential closely represents the  $E^{\circ}$ .

$$E^{\circ} = E_p + 1.109 (RT/nF) \quad (3)$$

The cathodic and anodic peak current densities increases as the potential scan rate increases as shown in Figure 43 but the incipient potential didn't change [79]. Also it was noted that the Ln potentials are more positive than the potential of LiCl [85] which shows LiCl-KCl salt is stable enough to use for electrolysis except for samarium which cannot be reduced to Sm using LiCl-KCl bath where lithium reduction occurs prior to  $\text{Sm}^{2+}/\text{Sm}^0$  reduction [86] which obstruct the bulk extraction of samarium. Figure 35 shows the cyclic voltammograms of LiCl-KCl in which Li reduction is more negative than the Ln's reduction potential.

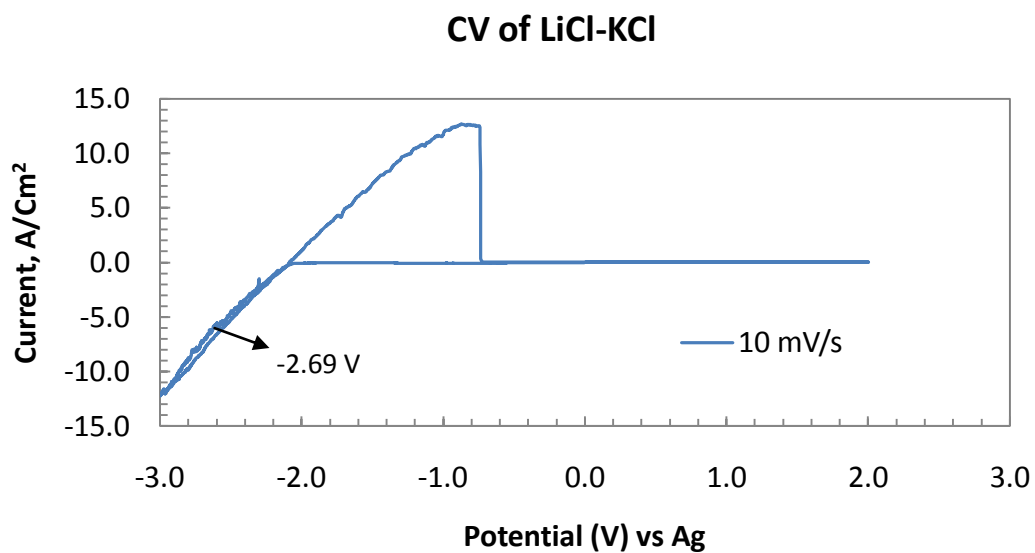


**Figure 35:** Cyclic voltammograms of  $(\text{LiCl} + \text{KCl})_{\text{Eutectic}}$  at 773 K (500 °C) using tungsten as substrate at 10 mV/s scan rate.

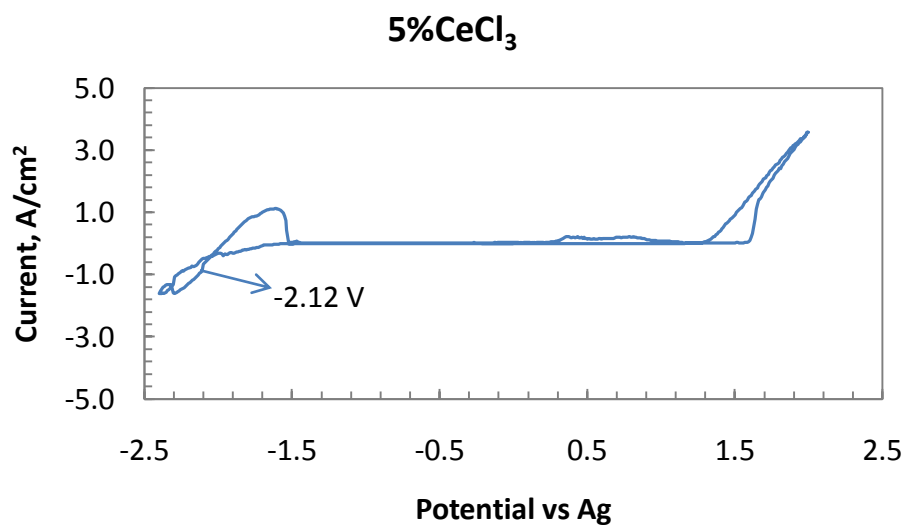


**Figure 36:** Cyclic voltammograms of  $(\text{LiCl} + \text{KCl})_{\text{Eutectic}} + 5 \text{ wt } \% \text{ CeCl}_3$  binary system at 773 K (500 °C) using tungsten as substrate at 20 mV/s scan rate.

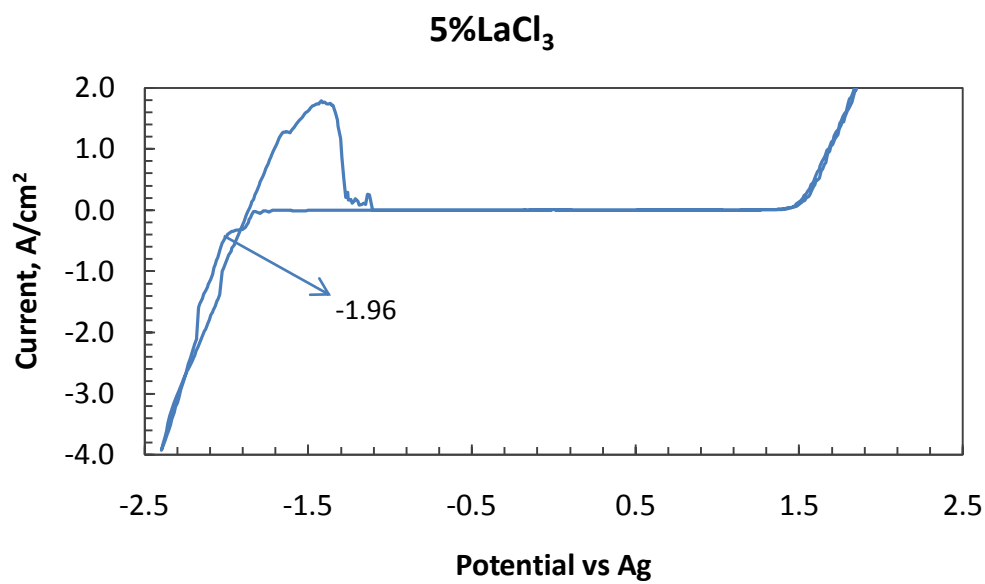


**Figure 37:** Cyclic voltammograms of  $(\text{LiCl} + \text{KCl})_{\text{Eutectic}} + 5 \text{ wt } \% \text{ LaCl}_3$  binary system at 773 K (500 °C) using tungsten as substrate at 20 mV/s scan rate.

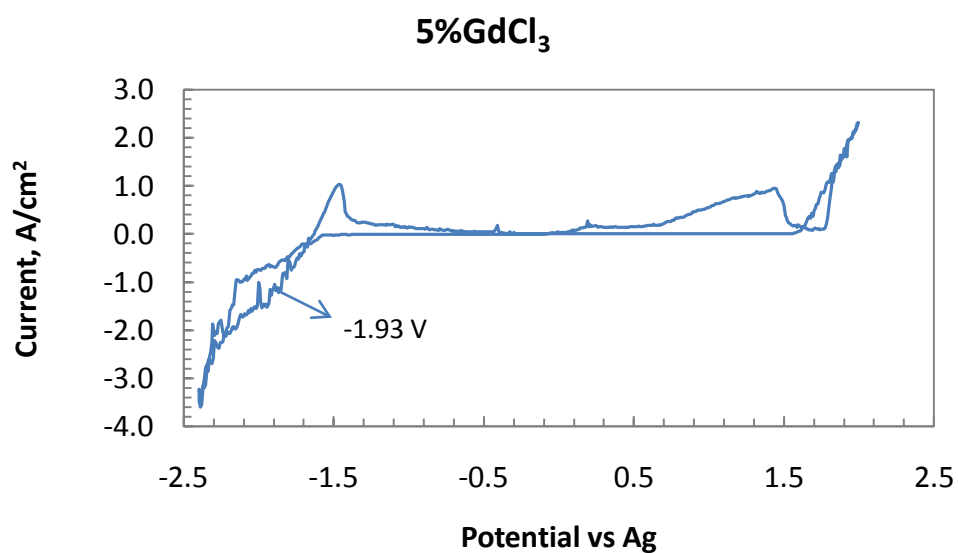


**Figure 38:** Cyclic voltammograms of  $(\text{LiCl} + \text{KCl})_{\text{Eutectic}} + 5 \text{ wt } \% \text{ GdCl}_3$  binary system at 773 K (500 °C) using tungsten as substrate at 20 mV/s scan rate.

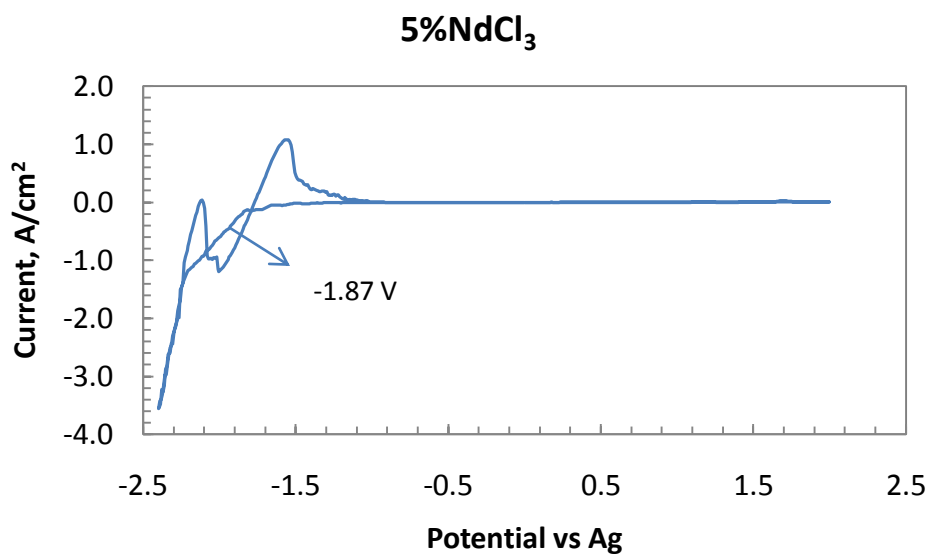


**Figure 39:** Cyclic voltammograms of  $(\text{LiCl} + \text{KCl})_{\text{Eutectic}} + 5 \text{ wt } \% \text{ NdCl}_3$  binary system at 773 K (500 °C) using tungsten as substrate at 20 mV/s scan rate.

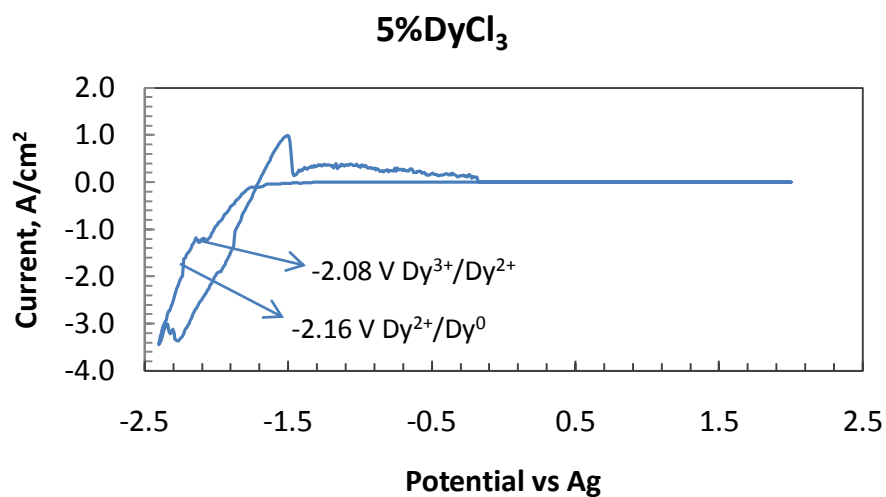


**Figure 40:** Cyclic voltammograms of  $(\text{LiCl} + \text{KCl})_{\text{Eutectic}} + 5 \text{ wt } \% \text{ DyCl}_3$  binary system at 773 K (500 °C) using tungsten as substrate at 20 mV/s scan rate.

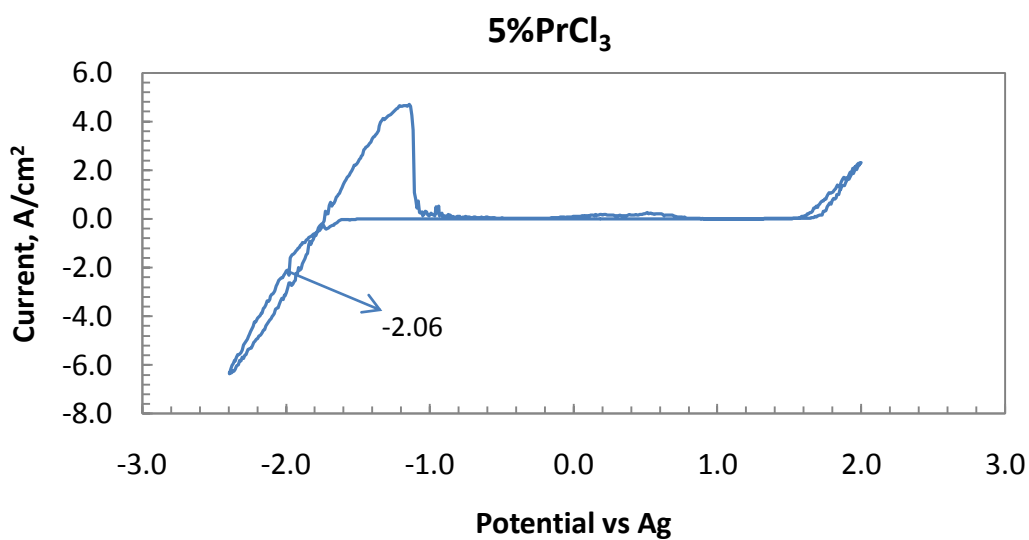


**Figure 41:** Cyclic voltammograms of  $(\text{LiCl} + \text{KCl})_{\text{Eutectic}} + 5 \text{ wt } \% \text{ PrCl}_3$  binary system at 773 K (500 °C) using tungsten as substrate at 20 mV/s scan rate.

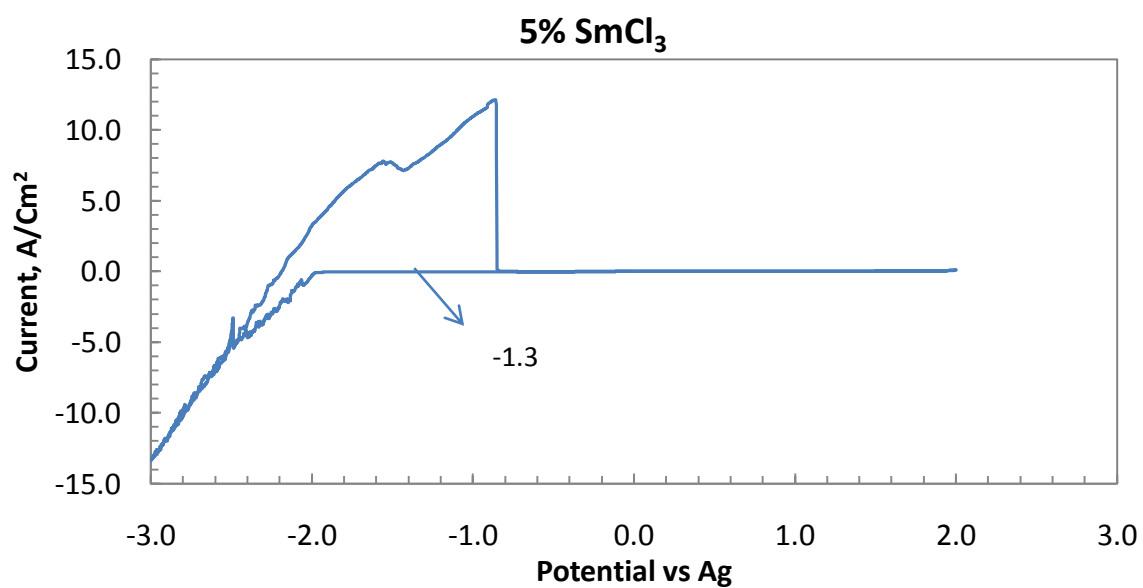


**Figure 42:** Cyclic voltammograms of  $(\text{LiCl} + \text{KCl})_{\text{Eutectic}} + 5 \text{ wt } \% \text{ SmCl}_3$  binary system at 773 K (500 °C) using tungsten as substrate at 20 mV/s scan rate.

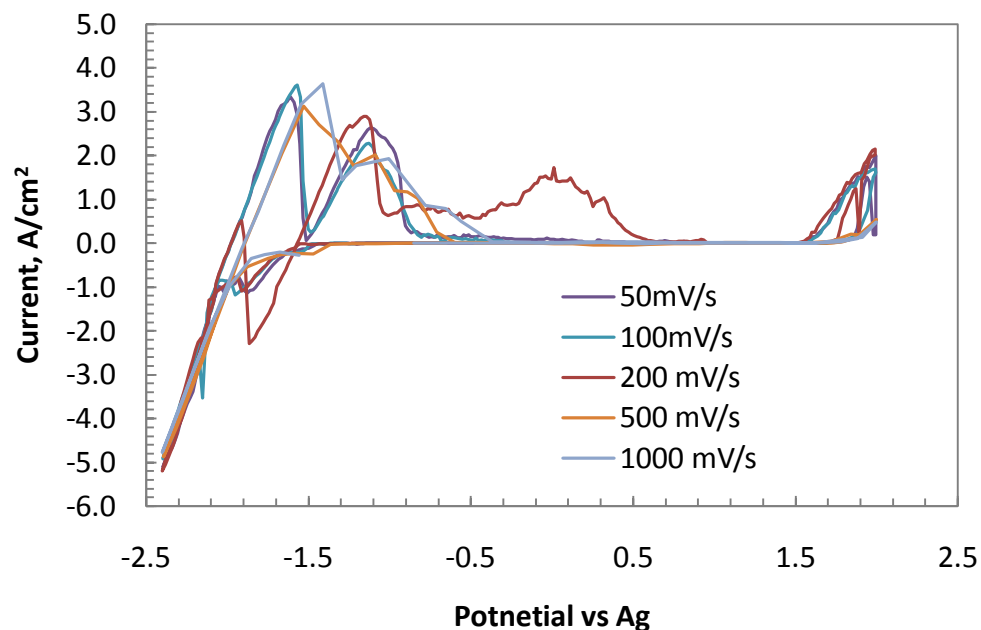


**Figure 43:** Cyclic voltammograms of  $(\text{LiCl} + \text{KCl})_{\text{Eutectic}} + 5 \text{ wt } \% \text{ GdCl}_3$  binary system at 773 K (500 °C) using tungsten as substrate at different scan rate.

**Table 18:** Obtained reduction potential in comparison with literature values

| System  | Reduction Potential (V) at 773 K (500 °C) vs Ag | Reduction potential (V) found on literature at 723 K (450 °C) vs Ag/AgCl |
|---|---|--|
| LiCl-KCl+CeCl <sub>3</sub><br>Ce <sup>3+</sup> /Ce <sup>0</sup>                                       | -2.12 (Fig. 35)                                 | -2.11 [83]   |
| LiCl-KCl+LaCl <sub>3</sub><br>La <sup>3+</sup> /La <sup>0</sup>                                       | -1.96 (Fig. 36)                                 | -1.91 [87]   |
| LiCl-KCl+GdCl <sub>3</sub><br>Gd <sup>3+</sup> /Gd <sup>0</sup>                                       | -1.93 (Fig. 37)                                 | -1.95 [61]   |
| LiCl-KCl+NdCl <sub>3</sub><br>Nd <sup>3+</sup> /Nd <sup>0</sup>                                       | -1.87 (Fig. 38)                                 | -1.86 [88]   |
| LiCl-KCl+DyCl <sub>3</sub><br>Dy <sup>3+</sup> /Dy <sup>2+</sup><br>Dy <sup>2+</sup> /Dy <sup>0</sup> | -2.08 (Fig. 39)<br>-2.23 (Fig. 40)              | -2.15 [80]<br>-2.16 [80]   |
| LiCl-KCl+PrCl <sub>3</sub><br>Pr <sup>3+</sup> /Pr <sup>0</sup>                                       | -2.06 (Fig. 41)                                 | -2.21 [79]   |
| LiCl-KCl+SmCl <sub>3</sub><br>Sm <sup>3+</sup> /Sm <sup>2+</sup>                                      | -1.3 (Fig. 42)                                  | -1.1 [86]  |

### 5.2.2. Multi-components

The experimental results with multi-component mixtures of lanthanides in LiCl-KCl eutectic are presented in this section and the reduction potential of different system are shown in Table 19. Figure 44 shows CV for ternary system mixed with  $\text{CeCl}_3 + \text{LaCl}_3$  in LiCl-KCl eutectic at 773 K ( $500^\circ\text{C}$ ) along with the individual CV of  $\text{CeCl}_3$  and  $\text{LaCl}_3$ . They show that if  $\text{CeCl}_3$  and  $\text{LaCl}_3$  mixed in LiCl-KCl eutectic the reduction potential shifts towards more positive than the individual reduction potential of Ce and La. It was observed that,  $\text{CeCl}_3 + \text{LaCl}_3$  system has only one anodic peak which means dissolution occurs as a solid solution of Ce+La at one single peak. In order to verify the solid solution formation, the potentiostatic electrodeposition was carried out at -1.8 V. The deposit was stripped and SEM/EDX and XRD were performed. Figure 45 shows the XRD pattern of the deposit which confirmed the solid solution showing only dominant cerium peak pattern assuming lanthanum peak was overlapped. Figure 46a shows luster of deposit of Ce+La as solid solution and Figure 46b shows elements contents.

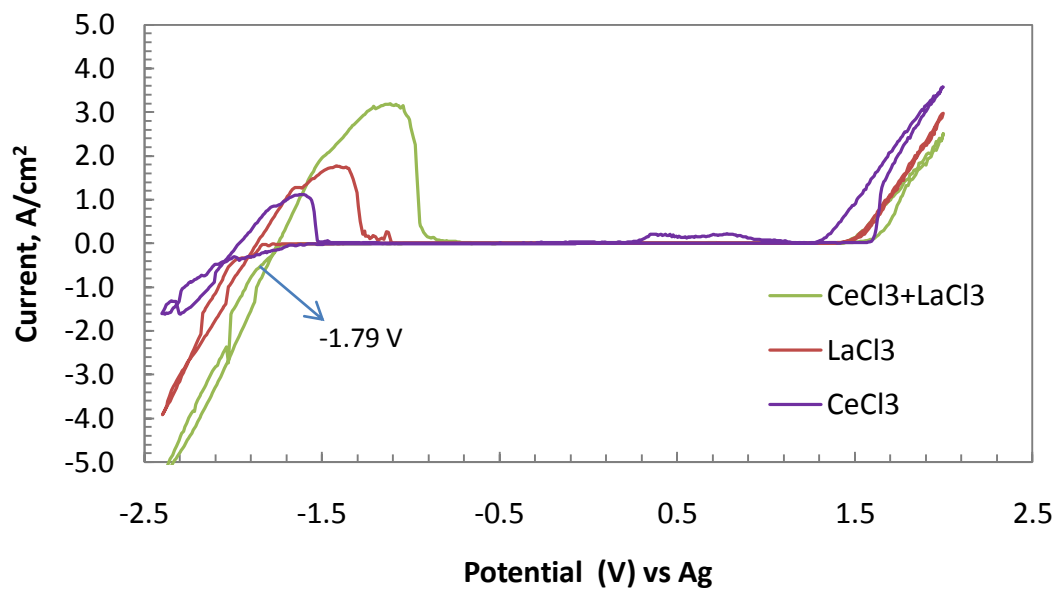


**Figure 44:** CV of  $(\text{LiCl-KCl})_{\text{Eutectic}} + 5\text{wt}\% \text{CeCl}_3$  and  $(\text{LiCl-KCl})_{\text{Eutectic}} + 5\text{wt}\% \text{LaCl}_3$  binary systems in comparison with ternary  $(\text{LiCl-KCl})_{\text{Eutectic}} + 5\text{wt}\% \text{CeCl}_3 + 5\text{wt}\% \text{LaCl}_3$  system at 773 K (500 °C) at 20 mV/s

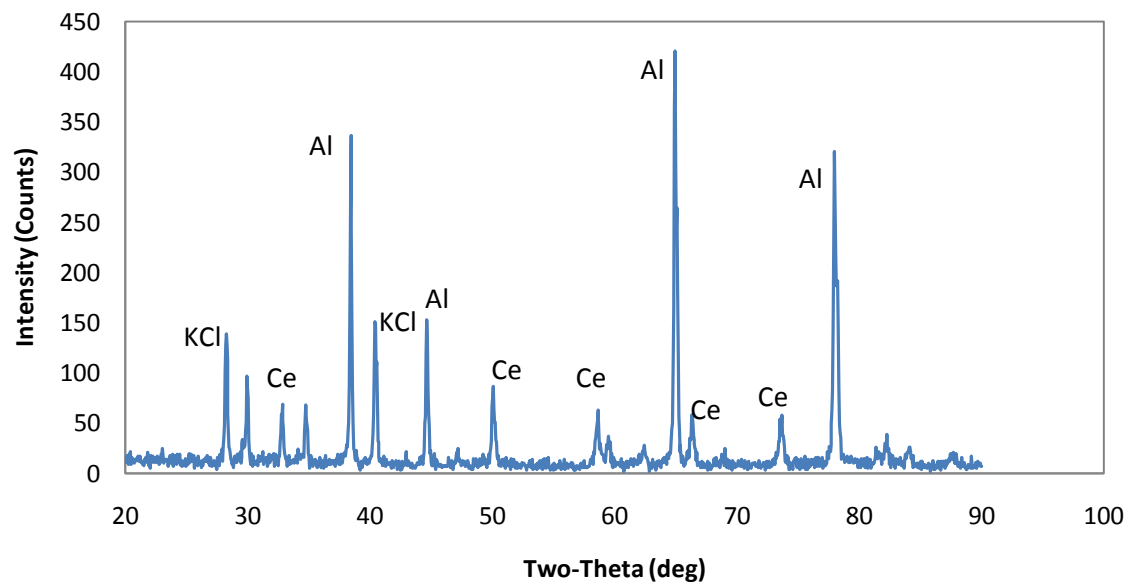


**Figure 45:** XRD pattern of the deposit of  $(\text{LiCl} + \text{KCl})_{\text{Eutectic}} + 5 \text{ wt } \% \text{ CeCl}_3 + 5 \text{ wt } \% \text{ LaCl}_3$  ternary system at 773 K (500 °C) using tungsten as substrate at -1.8 V.

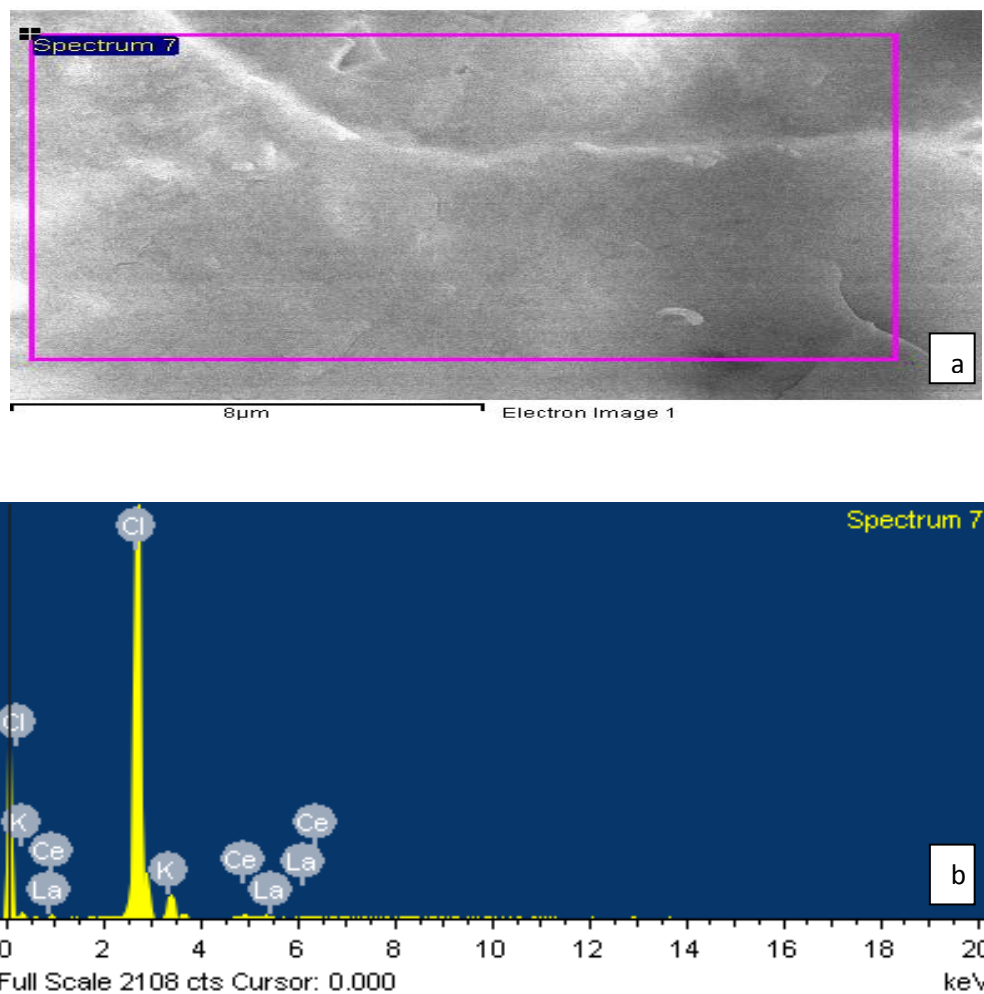


**Figure 46:** (a) SEM image of deposit obtained at -1.8 V of the ternary  $(\text{LiCl}+\text{KCl})_{\text{Eutectic}}+5 \text{ wt}\%$   $\text{CeCl}_3 + 5 \text{ wt}\%$   $\text{LaCl}_3$  system at 773 K (500 °C) at 20 mV/s scan rate; and (b) EDX analysis of the deposit.

The ternary system with  $\text{NdCl}_3$  and  $\text{CeCl}_3$  is shown in Figure 47. The system also shows that the cathodic wave indicating the reduction shift to a less negative potential. In this system the dissolution occurs at one anodic peak of about -1.6 V indicating the solid solution formation between Ce and Nd which is the reason for the stripping of metals from tungsten electrode

occurring at same potential. In order to prove the solid solution formation and incipient shifting more positive, the potentiostatic electrodeposition was carried out at potential -1.8 V. This potential is a more positive potential than the individual reduction of Ce and Nd. The deposit was stripped to carry out SEM and EDX analysis. According to the SEM image shown in Figure 48a and EDX analysis in Figure 48b, the formation of solid solution between Ce and Nd can be confirmed. Figure 48a shows the luster of Ce+Nd deposit while Figure 48b shows elemental contents of Ce and Nd. It was also noticed that the presence of chloride (in Figure 48b) could be the occluded salt layers in the deposit which was not washed out.

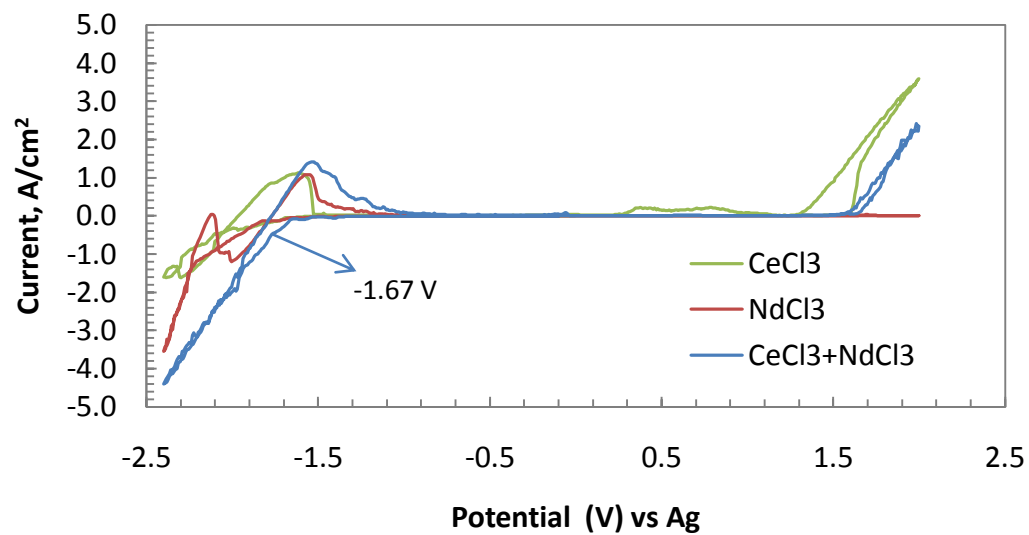


**Figure 47:** CV of  $(\text{LiCl-KCl})_{\text{Eutectic}} + 5\text{wt}\% \text{CeCl}_3$  and  $(\text{LiCl-KCl})_{\text{Eutectic}} + 5\text{wt}\% \text{NdCl}_3$  binary systems in comparison with ternary  $(\text{LiCl-KCl})_{\text{Eutectic}} + 5\text{wt}\% \text{CeCl}_3 + 5\text{wt}\% \text{NdCl}_3$  system at 773 K (500 °C) at 20 mV/s

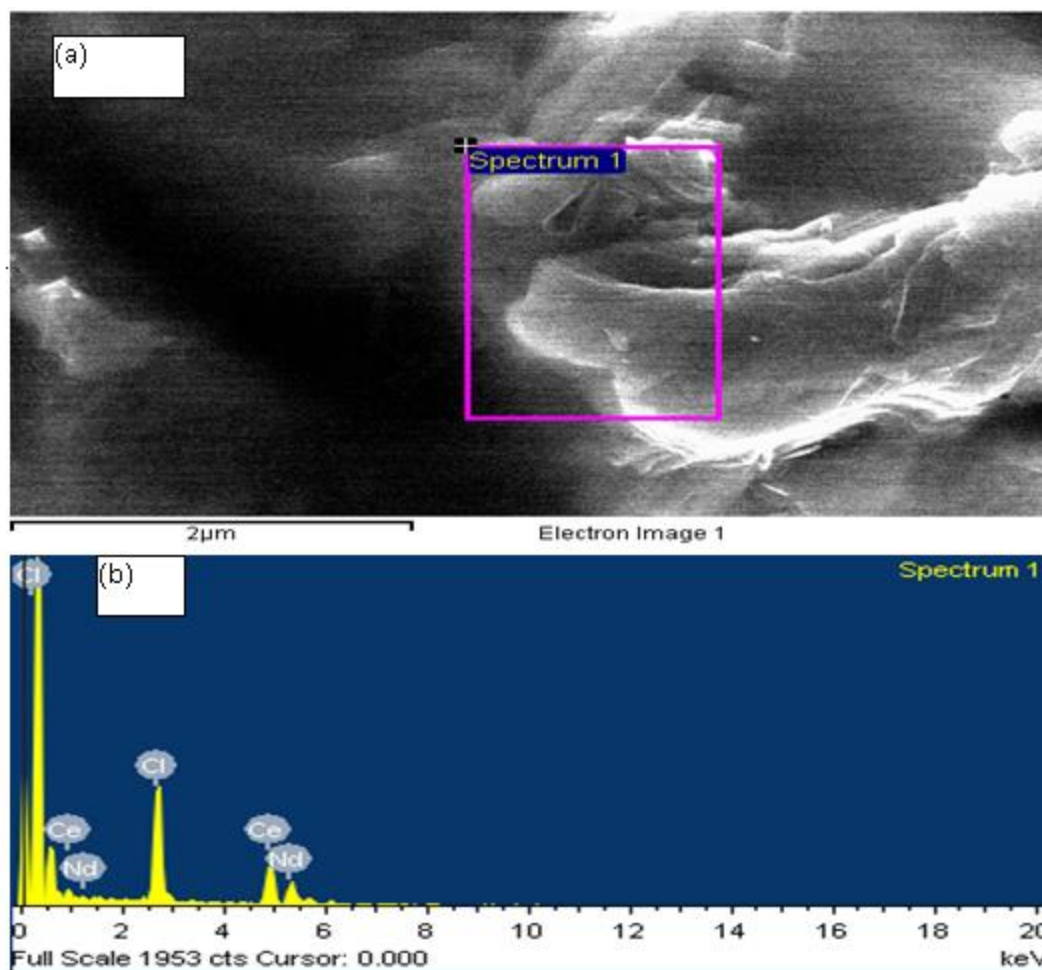


**Figure 48:** (a) SEM image of deposit obtained after cathodic scan of CV until -1.8 V of the ternary  $(\text{LiCl}+\text{KCl})_{\text{Eutectic}}+5 \text{ wt\% CeCl}_3 + 5 \text{ wt\% NdCl}_3$  system at 773 K (500 °C) at 20 mV/s scan rate; and (b) EDX analysis of the deposit.

Figure 49 shows the CV result of the  $\text{CeCl}_3 + \text{SmCl}_3$  system in comparison with CV of Ce and Sm. As it was reported, Sm reduces in two steps  $\text{Sm}^{3+}/\text{Sm}^{2+}$  and  $\text{Sm}^{2+}/\text{Sm}^0$ , but with the addition of Ce with Sm, it was clearly seen that reduction of Sm occurring at  $-1.83 \text{ V}$  along with Ce which indicates a solid solution between Ce and Sm. It was also observed that cathodic and anodic current densities increase in addition of Sm in Ce system which indicates reduction of additional species from the molten salt. The analysis of the deposit shows that the ratio of Ce and Sm deposit was 3:1.

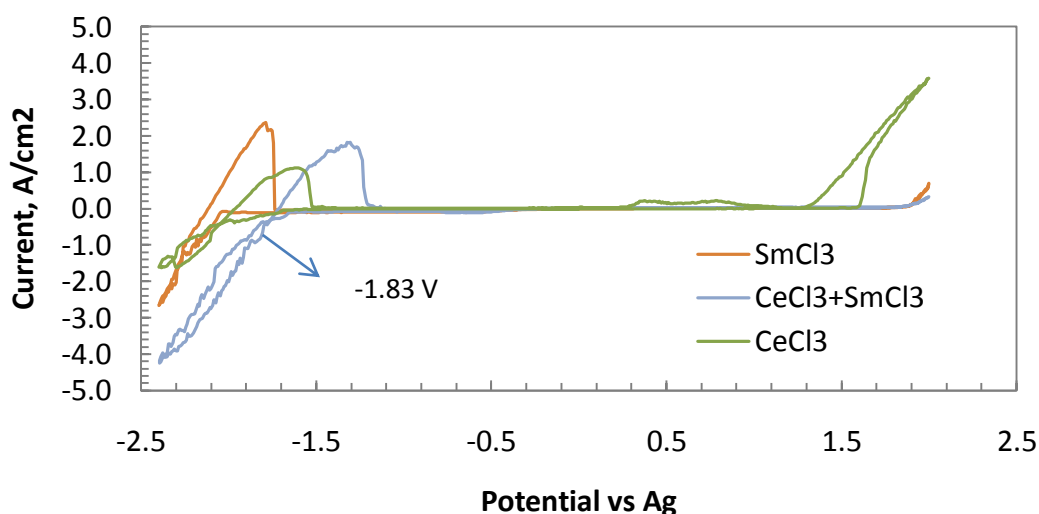


**Figure 49:** CV of  $(\text{LiCl-KCl})_{\text{Eutectic}} + 5\text{wt}\% \text{CeCl}_3$  and  $(\text{LiCl-KCl})_{\text{Eutectic}} + 5\text{wt}\% \text{SmCl}_3$  binary systems in comparison with ternary  $(\text{LiCl-KCl})_{\text{Eutectic}} + 5\text{wt}\% \text{CeCl}_3 + 5\text{wt}\% \text{SmCl}_3$  system at  $773 \text{ K}$  ( $500 \text{ }^\circ\text{C}$ ) at  $20 \text{ mV/s}$

A quaternary system of  $\text{CeCl}_3 + \text{LaCl}_3 + \text{GdCl}_3$  in comparison with ternary system is shown in Figure 50. This is yet another evident of incipient shifting more positive with addition of lanthanide elements. In the quaternary system, the anodic wave has two peaks occurring at about  $-1.34 \text{ V}$  and  $-1.13 \text{ V}$  which signifies the dissolution at two steps. As shown in figure 44, the one anodic peak might be the dissolution of solid solution of Ce + La while other is the

dissolution of Gd. The occurrence of the anodic peak at such less-negative potentials could be the indication of stripping taking place as mischmetals rather single elements. Mischmetals typically are the mixture of composition of 48.5% Ce, 24% La, 17.5% Nd and 5.2% Pr [89].

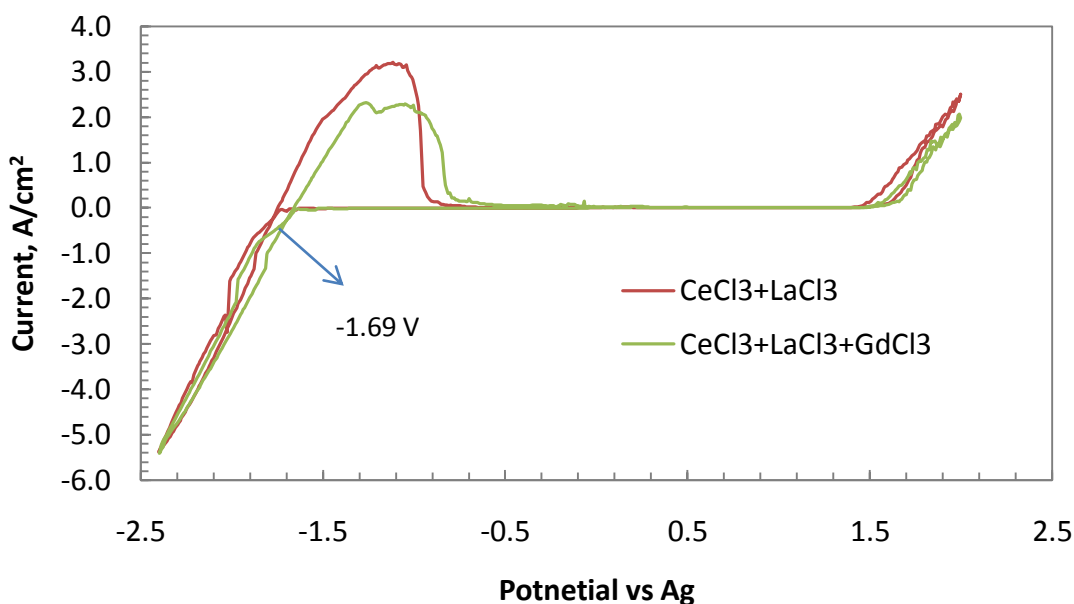


**Figure 50:** CV of  $(\text{LiCl-KCl})_{\text{Eutectic}} + 5\text{wt}\% \text{CeCl}_3 + 5\text{wt}\% \text{LaCl}_3$  ternary system in comparison with quaternary  $(\text{LiCl-KCl})_{\text{Eutectic}} + 5\text{wt}\% \text{CeCl}_3 + 5\text{wt}\% \text{NdCl}_3$  system at 773 K (500 °C) at 20 mV/s

The CV results of quaternary system of  $\text{CeCl}_3 + \text{SmCl}_3 + \text{NdCl}_3$  in comparison with ternary system of  $\text{CeCl}_3 + \text{SmCl}_3$  is shown in Figure 51. The quaternary system contained only 3 wt% compared to ternary system which contains more than 5wt%. While comparing these two systems, it was observed that the incipient potential was not shifted positively unlike the previous system where the concentration was 5 wt %. This indicates that the concentration plays an important role of potential not shifting more positive because at less concentration complete mixing of Sm to the solid solution of Ce+Nd did not take place. Also in the Figure 51 the quaternary system having lower concentration has two anodic peaks. We would assume the first anodic

peak at -1.98 V was the stripping of Sm+Li and the other peak at -1.54 V was stripping of Ce+Nd solid solution. And it is envisaged that increasing the lanthanides concentration would have resulted in complete solid solution of Ce+Nd+Sm and would pose only one anodic peak like ternary system. We performed the electrodeposition for 5wt% Ce+Nd+Sm in order to show the solid solution formation and performed SEM/EDX analysis. Figure 52 shows the SEM images and EDX analysis of deposit of 5wt% Ce+Nd+Sm where we can see the cluster of metals in 52a showing solid solution and elements present in 52b. This proves that the system with less concentration of lanthanide elements will not form solid solution and increasing the concentration increases the possibility of complete mixing of lanthanides. Several analyses indicate that the deposit of 5wt% Ce+Nd+Sm contains 54% of Ce, 26% of Nd and 4.4 % of Sm.

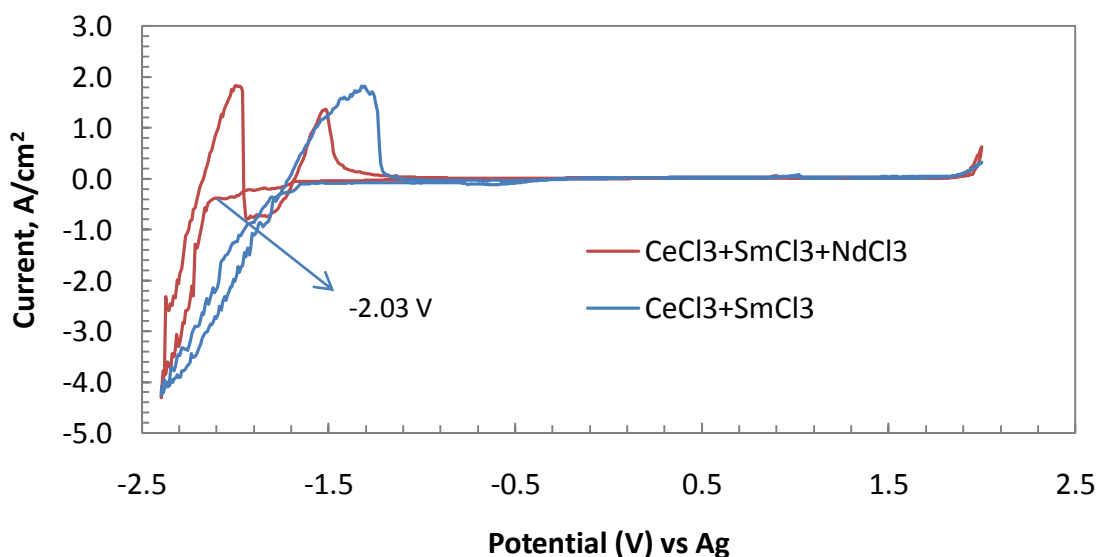


**Figure 51:** CV of  $(\text{LiCl-KCl})_{\text{Eutectic}} + 5\text{wt}\% \text{CeCl}_3 + 5\text{wt}\% \text{SmCl}_3$  binary system in comparison with ternary  $(\text{LiCl-KCl})_{\text{Eutectic}} + 3\text{wt}\% \text{CeCl}_3 + 3\text{wt}\% \text{SmCl}_3$  system at 773 K (500 °C) at 20 mV/s

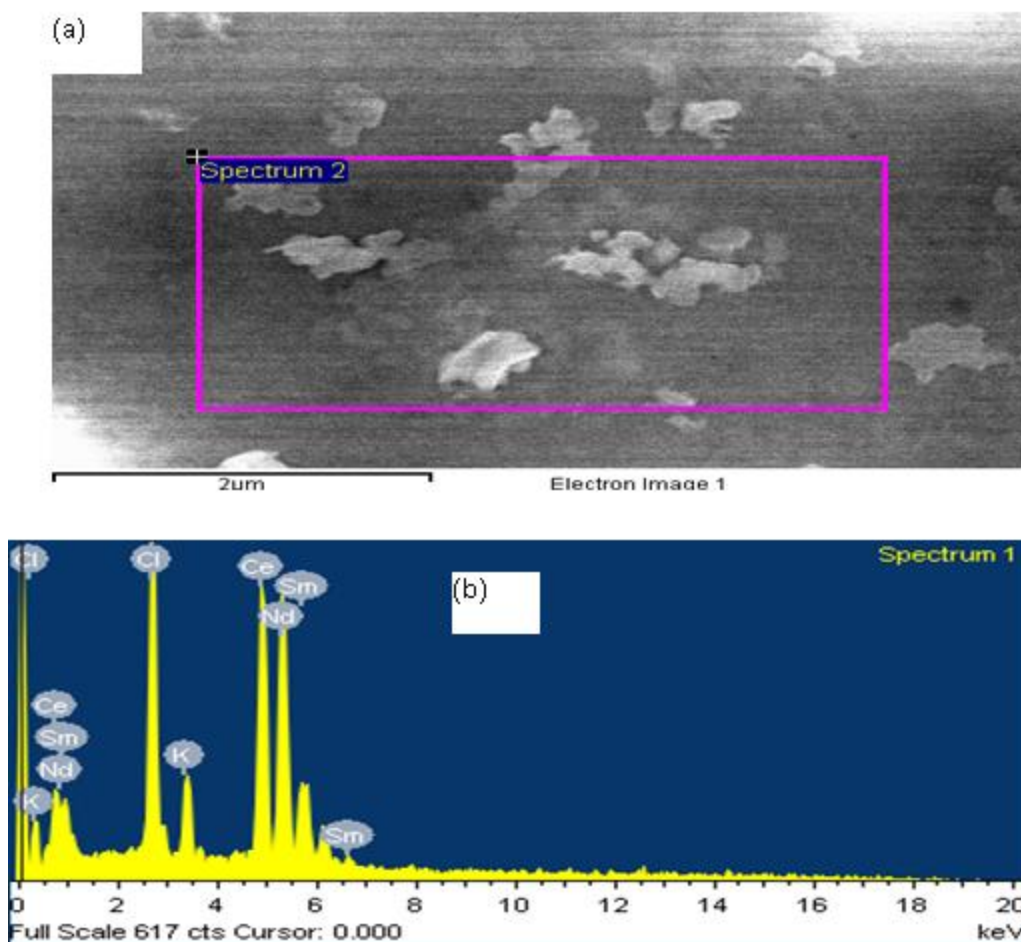


**Figure 52:** (a) SEM image of partial deposit removed from tungsten wire after deposition at -1.9 V for 60 seconds in quaternary  $(\text{LiCl}+\text{KCl})_{\text{Eutectic}}+5 \text{ wt\% CeCl}_3 + 5 \text{ wt\% NdCl}_3 + 5 \text{ wt\% SmCl}_3$  system at 773 K (500 °C); and (b) EDX analysis of the deposit.

The CV result for  $3\% \text{CeCl}_3 + 3\% \text{LaCl}_3$  mixed with LiCl-KCl eutectic in comparison with the individual Ce and La is shown in Figure 53. In this system also the incipient potential did not shift more positive unlike Figure 44 where the concentration was 5 wt% and showed the shifting to a more positive potential. It is also noticed the anodic dissolution occurs in two steps. The first peak represents the dissolution of Ce and the second represents the dissolution

of La. Thus, further proves that solid solution does not occur at low concentration. Similarly it is true for Ce and Nd system when the concentration is less as shown in Figure 54.

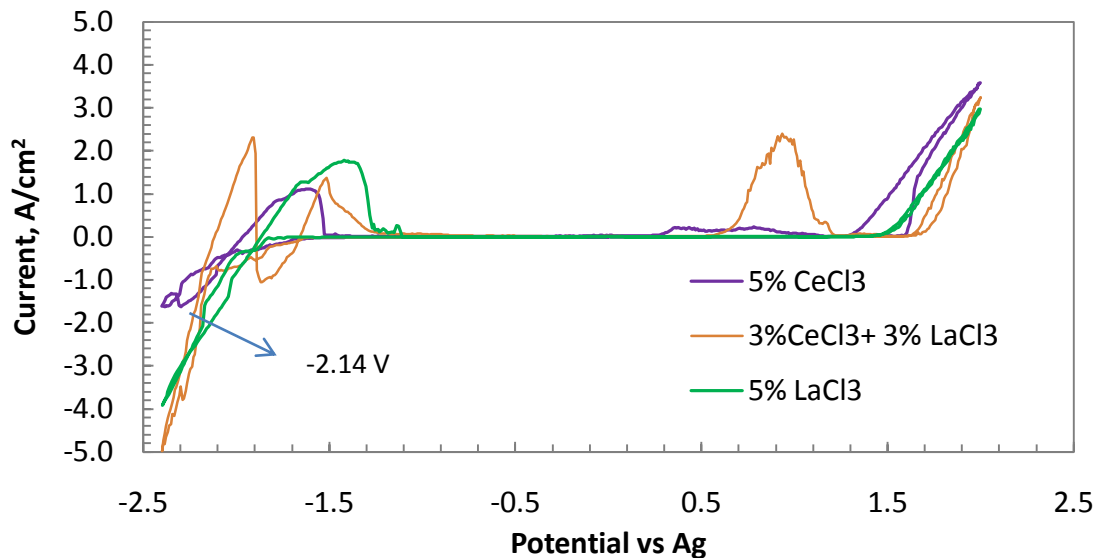


**Figure 53:** CV of  $(\text{LiCl-KCl})_{\text{Eutectic}} + 5\text{wt}\% \text{CeCl}_3$  and  $(\text{LiCl-KCl})_{\text{Eutectic}} + 5\text{wt}\% \text{LaCl}_3$  binary systems in comparison with ternary  $(\text{LiCl-KCl})_{\text{Eutectic}} + 3\text{wt}\% \text{CeCl}_3 + 3\text{wt}\% \text{LaCl}_3$  system at 773 K (500 °C) at 20 mV/s.

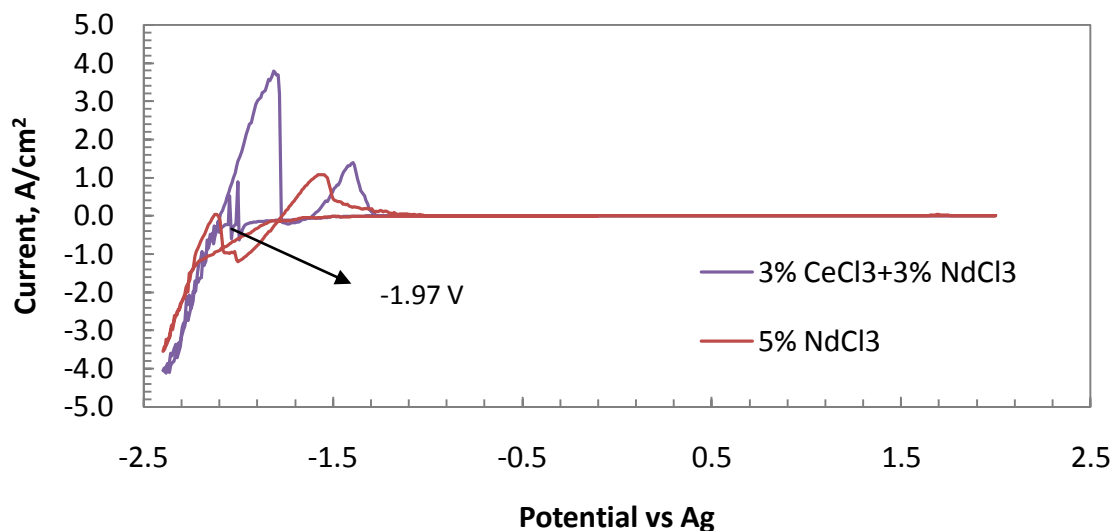


**Figure 54:** CV of  $(\text{LiCl-KCl})_{\text{Eutectic}} + 5\text{wt}\% \text{CeCl}_3$  and  $(\text{LiCl-KCl})_{\text{Eutectic}} + 5\text{wt}\% \text{NdCl}_3$  binary systems in comparison with ternary  $(\text{LiCl-KCl})_{\text{Eutectic}} + 3\text{wt}\% \text{CeCl}_3 + 3\text{wt}\% \text{NdCl}_3$  system at 773 K (500 °C) at 20 mV/s

**Table 19:** Obtained reduction potential for multicomponent system

| Multi-Components System  | Reduction Potential (V) at 773 K (500 °C) vs Ag |
|--|---|
| LiCl-KCl+ 5wt% CeCl <sub>3</sub> + 5wt% LaCl <sub>3</sub>                          | -1.79 (Fig. 44)                                 |
| LiCl-KCl+5wt% CeCl <sub>3</sub> + 5wt% NdCl <sub>3</sub>                           | -1.67 (Fig. 47)                                 |
| LiCl-KCl+5wt% CeCl <sub>3</sub> + 5wt%SmCl <sub>3</sub>                            | -1.83 (Fig.49)                                  |
| LiCl-KCl+5wt% CeCl <sub>3</sub> + 5wt% LaCl <sub>3</sub> + 5wt% GdCl <sub>3</sub>  | -1.69 (Fig. 50)                                 |
| LiCl-KCl+ 3wt% CeCl <sub>3</sub> + 3wt% SmCl <sub>3</sub> + 3wt% NdCl <sub>3</sub> | -2.03 (Fig. 51)                                 |
| LiCl-KCl+3wt% CeCl <sub>3</sub> + 3wt% LaCl <sub>3</sub>                           | -2.14 (Fig. 53)                                 |
| LiCl-KCl+3wt% CeCl <sub>3</sub> + 3wt% NdCl <sub>3</sub>                           | -1.97 (Fig. 54)                                 |

In all the figures listed above for multi-component system, it was observed that every system consist of Cerium. This tells us that any system mixed with Cerium would shift the potential towards less negative when the concentration is more than 5 wt%.

In summary, we observed the binary, ternary and quaternary system and discovered that 5 wt% mixture of lanthanides in LiCl-KCl eutectic shift the incipient potential towards more positive as indicated by the potential wave in each figure. An explanation of this is associated with two phenomena: one is under potential deposition where the interaction of reducing species (R) with the substrate (S) is more favorable than the species-species (R-R) interaction [90]; and other is when the two species A and B formed compound ( $A_nB_m$ ) is more favorable by having a negative free energy ( $-\Delta G$ ) and the deposition potential is positively shifted from the redox potential of the more negative species by an amount ( $-\Delta G/nF$ ) [91-92]. These assumptions were not valid for the binary system where only one lanthanide element was added to (LiCl-KCl)<sub>eutectic</sub> system because they did not show any under potential deposition. However, this is true in case of multi-component where we saw the shift in potentials. But the second assumption might not be valid for multi-component elements. According to the Hume Rothery rule, atoms will form solid solution if the atoms having similar diameter (diameter less than 15 %), similar crystal structures, same valency and atoms having similar electronegativity [93]. So the lanthanide elements follow the Hume Rothery principles because they have similar properties and would not form compound, but rather would form solid solutions. The mischmetals are the extended solid solution of lanthanide elements which are separated from the naturally occurring minerals called monazite. In all but a few ternary and quaternary systems of the lanthanide elements form solid solution easily which signify that solid solution is a thermodynamically more

favorable process in those systems. Thus, shifting of cathodic wave of quaternary and ternary system with respect to individual elements reduction potential is the result of change in the free energy of formation of solid solution.

Other possible reasons for the positive shift in the reduction potential of multi-component lanthanide system could be lowered stability of the lanthanide clusters in the molten alkali salt. In general mixture of lanthanides in LiCl-KCl eutectic mixture forms clusters of  $\{\text{Ln}(\text{KCl})_n\}^{3+}$  and  $\{\text{Ln}(\text{LiCl})_n\}^{3+}$ , with the coordination number  $n$  varying from 4 to 9 whereas the coordination number is 6-9 in the presence of single lanthanide elements. The coordination numbers for lighter ions like  $\text{La}^{3+}$  and  $\text{Nd}^{3+}$  is 8 while 9 for heavier ions like  $\text{Tb}^{3+}$  and  $\text{Eu}^{3+}$  [94]. Further Hazebroucq et al [95] shows that the stable coordination number of Gd (III) was 6 and for La (III) it was 7-8. This proves that when multiple lanthanide components were present, the coordination of the solvated clusters would be affected significantly and their stability would be reduced which change the free energy and this in results attributed the positive shift in the reduction potential for multi-component system.

# Chapter 6: Conclusion

---

## 5.1. Melting Temperature Variations

Thermal analysis on melting temperature variations of eutectic LiCl-KCl (58.5 mol % LiCl+ 41.5 mol% KCl) by addition of lanthanide elements up to 5 mol% in case of single component and multicomponent has shown little variations. The maximum temperature variation was 8 K below the eutectic and 4 K above the eutectic temperature. Those variations can be easily neglected noting that the reprocessing is being conducted at 773K (500°C) which is well above the eutectic temperature of 625K (352°C). Therefore few degrees variation in temperature with lanthanide accumulation up to 5 mol% would not affect the overall reprocessing of spent nuclear fuels. This suggests that the fuels can be reprocessed many times as long as the accumulation of lanthanide is less than 5 mol %. The results of these observations provide the supporting data for future reprocessing of spent fuels.

## 5.2. Electrochemical Studies

The result for the cyclic voltammetry of binary, ternary and quaternary system of  $\text{LnCl}_3$ - $(\text{LiCl}+\text{KCl})_{\text{Eutectic}}$  at 773 K (500°C) was obtained. It shows that the incipient potential of cathodic reduction waves shifted to lower negative values in multisystem (ternary and quaternary) with the increased amount of lanthanide concentrations. The concentration was more than 5 wt %. The shift in potential to less negative could be attributed to the free energy change due to formation of solid solutions and lower stability of the solvated clusters of lanthanide in molten salt. The results also showed that when the concentration of lanthanide was low (less than 3 wt %), the potential didn't shift. This could be attributed to a lack of formation of solid solution and

this indicates that the lanthanide elements do not form solid solutions at lower concentration.

But the positive shift in the potentials of the multi-component lanthanide system with the increasing concentration clearly indicates that the enrichment of lanthanide in reprocessing cell could detrimentally affect the separation of actinides from the lanthanides.

## Chapter 7: References

---

- [1] DOE, "Advanced fuel cycle initiative: The future path for advanced spent fuel treatment and transmutation research," Department of Energy. 2003.
- [2] NERAC, "A technology roadmap for generation IV Nuclear Energy Systems," vol. 03-GA50034, ed: U.S DOE Nuclear Energy Research Advisory Committee and Generation IV International Forum, 2002, pp. 1-2.
- [3] M. D. Schmitz. (02-10-2010). Nuclear Power as an Alternative to Coal. [Thesis]. Available: <http://www.schmitztech.com/nostalgia/documents/files/high/nuclear.pdf>
- [4] WNA. (2009, 02-20-2010). The Biosphere at Risk. 2. Available: <http://www.world-nuclear.org/why/biosphere.html>
- [5] D. Y. Goswami and F. Krieth. (2007). *Energy conversion*.
- [6] L. O'Sullivan. (2008, 30th April). *Alternative Sources of Energy*. Available: [http://energy-conservation.suite101.com/article.cfm/alternative\\_sources\\_of\\_energy](http://energy-conservation.suite101.com/article.cfm/alternative_sources_of_energy)
- [7] ICJT, "Nuclear power plants in the world," Nuclear training centre 2008.
- [8] DOE, "National Energy Education development project."
- [9] J. Kenneth Shultis and R. E. Faw. (2002). *Fundamentals of nuclear science and engineering [electronic resource]*.
- [10] *Nuclear Fission Reactor*. Available: [www.resourcefulphysics.org](http://www.resourcefulphysics.org)
- [11] NERAC, "A Technology Roadmap for Generation IV Nuclear Energy Systems," vol. 03-GA50034, ed: U.S. DOE Nuclear Energy Research Advisory Committee and International Generation IV forum, 2002, pp. 5-7.
- [12] NERAC, "A technology roadmap for generation IV nuclear energy system," vol. 03-GA50034, ed: U.S DOE Nuclear Energy Research Advisory Committee and Generation IV International Forum, 2002, p. 5.
- [13] W. N. Association. (2009, (2-11-2010). Nuclear Power Reactors. 3. Available: <http://www.world-nuclear.org/info/inf32.html>
- [14] J. S. Wiley, "Boiling and Pressurized Light-Water Reactors," *Power Reactor Technology*, vol. 8, pp. 3-8, 1965.
- [15] U. S. N. R. Commission. (2008, 2-20-2010). Pressurized Water Reactors. Available: <http://www.nrc.gov/reactors/pwrs.html>
- [16] U. S. N. R. Commission., "Nuclear Reactors," U.S. Nuclear Regulatory Commission 2007.
- [17] W. N. Association, "Nuclear Power Reactors," ed: World Nuclear Association, 2009, p. 4.
- [18] I. E. Engineers. 05-01-2010). Nuclear Reactors Type. 3. Available: [http://www.carnegieendowment.org/static/npp/reports/nuclear\\_reactors.pdf](http://www.carnegieendowment.org/static/npp/reports/nuclear_reactors.pdf)
- [19] WNA. (2009, Nuclear Power Reactor. Available: <http://www.world-nuclear.org/info/inf32.html>
- [20] WNA. (2009, 2-15-2010). Nuclear Power Reactors. 5. Available: <http://www.world-nuclear.org/info/inf32.html>
- [21] W. N. Association. (2009, 2-15-2010). Nuclear Power Reactors. 5. Available: <http://www.world-nuclear.org/info/inf32.html>
- [22] W. N. Association. (2009, 2-11-2010). Nuclear Power Reactors. 6. Available: <http://www.world-nuclear.org/info/inf32.html>
- [23] Hore-Lacy. (2009, *Nuclear power reactor*.
- [24] N. E. Association. *GIF membership*. Available: <http://www.gen-4.org/GIF/About/membership.htm>

- [25] W. N. Association. (2009, 2-11-2010). Generation IV reactors. Available: <http://www.world-nuclear.org/info/inf77.html>
- [26] NERACA, "A technology roadmap for generation IV Nuclear Energy Systems," vol. 03-GA50034, U. S. D. N. E. R. A. Committee, Ed., ed, (2002), p. 11.
- [27] M. Benedict, *et al.* ((1981)). *Nuclear Chemical Engineering*.
- [28] F. V. Hippel, "Spent fuel reprocessing," ed: Princeton University, 2009.
- [29] INL, "Global Nuclear Energy Partnership Technology Development Plan," ed, (2007), p. 102.
- [30] INL, "Global Nuclear Energy Partnership Technology Development Plan," I. N. Laboratory, Ed., ed, (2007), p. 103.
- [31] N. E. R. A. Committee, "A technology roadmap for generation IV nuclear energy systems," vol. GIF-002-00, ed: U.S DOE Nuclear Energy Research Advisory Committee and Generation IV International Forum, 2002, p. 16.
- [32] D. o. Energy. *Legacy story, chapter 2. nuclear weapons production processes and history*. Available: [http://www.em.doe.gov/pdfs/pubpdfs/linklegacy\\_011\\_030.pdf](http://www.em.doe.gov/pdfs/pubpdfs/linklegacy_011_030.pdf)
- [33] BRWM, "Research needs for high level waste stored at tanks and bins at U.S. department of energy sites," N. R. Council, Ed., ed: Board on Radioactive Waste Management (BRWM), (2001).
- [34] M. Benedict, *et al.*, *Nuclear Chemical Engineering* vol. second ed: McGraw-Hill Book Company, (1981).
- [35] C. E. Stevens, "The EBR-II fuel cycle story," *American Nuclear Society*, (1987).
- [36] J. J. Laidler, *et al.*, "Development of pyroprocessing technology," *Progress in Nuclear Energy*, vol. 31, pp. 131-140, (1997).
- [37] W. N. Association. (2010, Processing of Used Nuclear Fuel. Available: <http://www.world-nuclear.org/info/inf69.html>
- [38] R. G. Wymer. (2009), Spent Nuclear Reactor Fuel Reprocessing: Past, Present, and Future.
- [39] A.G. Croff, *et al.*, "Background, Status, and Issues Related to the Regulation of Advanced Spent Nuclear Fuel Recycle Facilities," vol. NUREG-1909, A. C. o. N. W. a. Materials, Ed., ed: United States Nuclear Regulatory Commission, 2008.
- [40] I. A. E. Agency, "Spent Fuel Reprocessing Options," N. F. C. a. M. Section, Ed., ed. Vienna, Austria: International Atomic Energy Agency, 2008.
- [41] W. N. Association. ((2009), Processing of used Nuclear Fuel. 4. Available: <http://www.world-nuclear.org/info/inf69.htm>
- [42] ENS. 2010-05-03). *Purex Process*. Available: <http://www.euronuclear.org/info/encyclopedia/p/purex-process.htm>
- [43] A. A. Clifford, *et al.*, "Modelling of the extraction of uranium with supercritical carbon dioxide," *Journal of Nuclear Science and Technology*, vol. 38, pp. 433-438, Jun 2001.
- [44] T. Koyama, "Present status of the advanced aqueous separation process technology development," in *International Symposium NUCEF2005*, (2005).
- [45] T. S. Rudisill, *et al.* ((2003), Demonstration of the urex solvent extraction process with dresden reactor fuel. *Tech. Rep. WSRC-MS-2003-00089, Rev. 1 Westinghouse Savannah River Company*.
- [46] IAEA. Development of Advanced Reprocessing Technologies. Available: [http://www.iaea.org/About/Policy/GC/GC52/GC52InfDocuments/English/gc52inf-3-att4\\_en.pdf](http://www.iaea.org/About/Policy/GC/GC52/GC52InfDocuments/English/gc52inf-3-att4_en.pdf)
- [47] NEA, "Pyrochemical Separations in Nuclear Applications," Paris, Status Report2004.
- [48] M. C. C., *et al.*, "Application of the pyrochemical process to recycle of actinides from LWR spent fuel," *Progress in Nuclear Energy*, vol. 31, pp. 175-186, (1997).

- [49] W. N. Association. ((2009), Processing of used Nuclear Fuel. 7. Available: <http://www.world-nuclear.org/info/inf69.html>
- [50] N. R. Council. (1996)). *Nuclear wastes: Technologies for separations and transmutation*. Available: [http://books.nap.edu/openbook.php?record\\_id=4912&page=153](http://books.nap.edu/openbook.php?record_id=4912&page=153)
- [51] J. D. Briscoe, *et al.*, "Anode Invention For Lithium/Transition Metal Fluorides Molten Salt Cells and Batteries," France Patent, 2002.
- [52] N. E. Agency, "Pyrochemical Separations in Nuclear Applications," Paris, Status Report 2004.
- [53] T. Koyama, *et al.*, "An experimental study of molten salt electrorefining of uranium using solid iron cathode and liquid cadmium cathode for development of pyrometallurgical reprocessing," *Journal of Nuclear Science and Technology*, vol. 34, pp. 384-393, Apr 1997.
- [54] NEA, "Actinide separation chemistry in nuclear waste streams and materials," 1997).
- [55] Y. Sakamura, *et al.*, "Separation of actinides from rare earth elements by electrorefining in LiCl-KCl eutectic salt," *Journal of Nuclear Science and Technology*, vol. 35, pp. 49-59, Jan 1998.
- [56] S. P. Fusselman, *et al.*, "Thermodynamic properties for rare earths and americium in pyropartitioning process solvents," *Journal of the Electrochemical Society*, vol. 146, pp. 2573-2580, Jul 1999.
- [57] R. J. M. Konings and D. Haas, "Fuels and targets for transmutation," *Comptes Rendus Physique*, vol. 3, pp. 1013-1022, Sep-Oct 2002.
- [58] J. Serp, *et al.*, "Electrochemical behaviour of plutonium ion in LiCl-KCl eutectic melts," *Journal of Electroanalytical Chemistry*, vol. 561, pp. 143-148, Jan 1 2004.
- [59] F. Lantelme and Y. Berghoute, "Electrochemical studies of LaCl<sub>3</sub> and GdCl<sub>3</sub> dissolved in fused LiCl-KCl," *Journal of the Electrochemical Society*, vol. 146, pp. 4137-4144, Nov 1999.
- [60] Y. Castrillejo, *et al.*, "Solubilization of rare earth oxides in the eutectic LiCl-KCl mixture at 450 degrees C and in the equimolar CaCl<sub>2</sub>-NaCl melt at 550 degrees C," *Journal of Electroanalytical Chemistry*, vol. 545, pp. 141-157, Mar 27 2003.
- [61] C. Caravaca, *et al.*, "Electrochemical behaviour of gadolinium ion in molten LiCl-KCl eutectic," *Journal of Nuclear Materials*, vol. 360, pp. 25-31, Jan 15 2007.
- [62] C. Nourry, *et al.*, "Data acquisition in thermodynamic and electrochemical reduction in a Gd(III)/Gd system in LiF-CaF<sub>2</sub> media," *Electrochimica Acta*, vol. 53, pp. 2650-2655, Jan 1 2008.
- [63] Y. Sakamura, *et al.*, "Measurement of standard potentials of actinides (U, Np, Pu, Am) in LiCl-KCl eutectic salt and separation of actinides from rare earths by electrorefining," *Journal of Alloys and Compounds*, vol. 271, pp. 592-596, Jun 12 1998.
- [64] E. Aukrust, *et al.*, "Activities in Molten Salt mixtures of Potassium Lithium-Halide Mixtures: A Preliminary Report," *Ann. N.Y. Acad. Sci.*, vol. 79, p. 830, 1960.
- [65] T. W. Richards and W. B. Meldrum, "The melting points of the chlorides of lithium, rubidium and caesium and the freezing points of binary and ternary mixtures of these salts including potassium and sodium chloride," *Journal of American Chemical Society*, vol. 39, p. 1816, 1917.
- [66] A. S. Basin, *et al.*, "The LiCl-KCl binary system," *Russian Journal of Inorganic Chemistry*, vol. 53, pp. 1509-1511, Sep 2008.
- [67] O. KIYOSHI, *et al.*, "Supercooling Behavior of Aqueous Sodium Salt Solutions," *Scientific and Engineering Reports of the National Defense Academy*, vol. 39, pp. 85-88, 2001.
- [68] S. Robert E, Jr., Joseph M, Price, Lonu M. Howser. (1974, A SMOOTHING ALGORITHM USING CUBIC SPLINE FUNCTIONS. NASA TECHNICAL NOTE (NASA TN 0-7397). Available: <http://www.pdas.com/refs/tnd7397.pdf>
- [69] R. Annino and R. D. Driver, "Scientific and Engineering Applications with personal computers," *John Wiley and Sons*, 1986.
- [70] I. Felde, *et al.* Effect of smoothing methods on the results of different inverse modeling technique.

- [71] M. Capps. *Splines*. Available: <http://www.cs.nps.navy.mil/people/faculty/capps/iap/class2/splines/>
- [72] J. Goldstein, *Scanning electron microscopy and x-ray microanalysis*: Kluwer Academic/Plenum Publishers, 2003.
- [73] B. D. Cullity and S. R. Stock, *Elements of X-Ray Diffraction*, 3rd Edition ed., 2001.
- [74] K. Nakamura and M. Kurata, "Thermal analysis of pseudo-binary system: LiCl-KCl eutectic and lanthanide trichloride," *Journal of Nuclear Materials*, vol. 247, pp. 309-314, Aug 1997.
- [75] K. E. Harding, "Melting point range and phase diagrams - Confusing laboratory textbook descriptions," *Journal of Chemical Education*, vol. 76, pp. 224-226, Feb 1999.
- [76] P. Masset, *et al.*, "Thermochemical properties of lanthanides (Ln = La, Nd) and actinides (An = U, Np, Pu, Am) in the molten LiCl-KCl eutectic," *Journal of Nuclear Materials*, vol. 344, pp. 173-179, Sep 1 2005.
- [77] Y. Castrillejo, *et al.*, "Electrode reaction of cerium into liquid bismuth in the eutectic LiCl-KCl," *Electrochemistry*, vol. 73, pp. 636-643, Aug 2005.
- [78] Y. Castrillejo, *et al.*, "The electrochemical behaviour of the Pr(III)/Pr redox system at Bi and Cd liquid electrodes in molten eutectic LiCl-KCl," *Journal of Electroanalytical Chemistry*, vol. 579, pp. 343-358, Jun 1 2005.
- [79] Y. Castrillejo, *et al.*, "Electrochemical behaviour of praseodymium (III) in molten chlorides," *Journal of Electroanalytical Chemistry*, vol. 575, pp. 61-74, Jan 15 2005.
- [80] Y. Castrillejo, *et al.*, "Electrochemical behaviour of dysprosium in the eutectic LiCl-KCl at W and Al electrodes," *Electrochimica Acta*, vol. 50, pp. 2047-2057, Mar 15 2005.
- [81] J. Serp, *et al.*, "Electrochemical separation of actinides from lanthanides on solid aluminum electrode in LiCl-KCl eutectic melts," *Journal of the Electrochemical Society*, vol. 152, pp. C167-C172, 2005.
- [82] E. Steeman, *et al.*, "Electrochemical Reduction of Lanthanide Ions .2. 2nd Reduction Step of Europium(III), Ytterbium(III) and Samarium(III) in Acidic Tetramethylammonium Perchlorate Solution," *Journal of Electroanalytical Chemistry*, vol. 89, pp. 113-122, 1978.
- [83] Y. Castrillejo, *et al.*, "Use of electrochemical techniques for the study of solubilization processes of cerium-oxide compounds and recovery of the metal from molten chlorides," *Journal of Electroanalytical Chemistry*, vol. 522, pp. 124-140, Apr 5 2002.
- [84] A. J. Bard and L. R. FAULKNER, *Electrochemical Methods Fundamentals and Applications*: Wiley, New York, 1980.
- [85] S. W. Kwon, *et al.*, "A study on the recovery of actinide elements from molten LiCl-KCl eutectic salt by an electrochemical separation," *Journal of Industrial and Engineering Chemistry*, vol. 15, pp. 86-91, Jan 2009.
- [86] G. Cordoba and C. Caravaca, "An electrochemical study of samarium ions in the molten eutectic LiCl plus KCl," *Journal of Electroanalytical Chemistry*, vol. 572, pp. 145-151, Oct 15 2004.
- [87] S. A. Kuznetsov, *et al.*, "Determination of uranium and rare-earth metals separation coefficients in LiCl-KCl melt by electrochemical transient techniques," *Journal of Nuclear Materials*, vol. 344, pp. 169-172, Sep 1 2005.
- [88] C. Hamel, *et al.*, "Neodymium(III) cathodic processes in molten fluorides," *Electrochimica Acta*, vol. 49, pp. 4467-4476, Oct 1 2004.
- [89] E. Morrice and M. M. Wong, "Fused-Salt Electrowinning and Electrorefining of Rare-Earth and Yttrium Metals," *Minerals Science and Engineering*, vol. 11, pp. 125-136, 1979.
- [90] H. Hummrich and J. V. Kratz. "The phenomenon of under potential deposition - Comparison of radiochemical and electrochemical experiments in case of the deposition of Pb on Ag". Available: <http://www.gsi.de/informationen/wti/library/scientificreport2003/files/177.pdf>
- [91] Budevski E, *et al.*, "An introduction of initial stage of metal deposition", *Electrochemical phase formation and growth*, 1996.

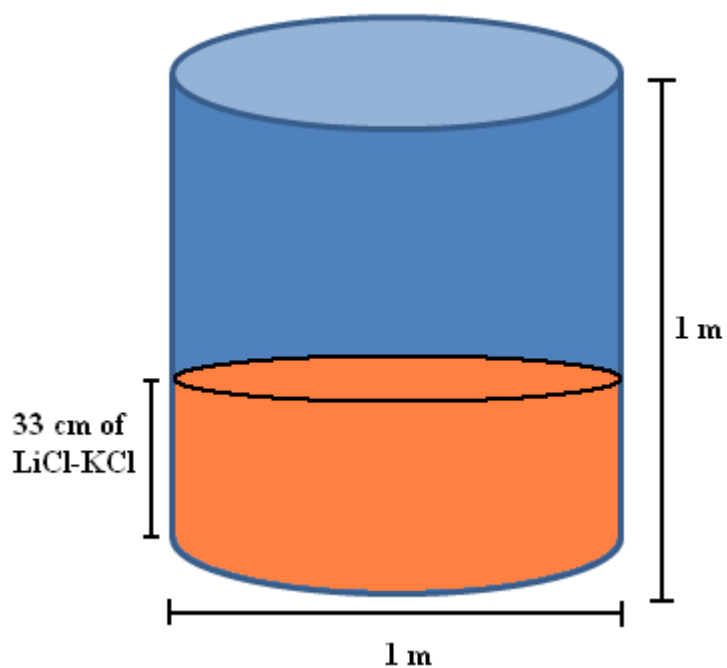
- [92] U. Cohen, "Electrodeposition of Niobium-Germanium Alloys from Molten Fluorides," *Journal of the Electrochemical Society*, vol. 130, pp. 1480-1485, 1983.
- [93] R. Abbaschian, *et al.*, *Physical Metallurgy Principles*, 4th Edition ed.
- [94] O. Schafer and C. Daul, "Modeling of the hydration sphere of gadolinium(III) ion using density functional theory," *International Journal of Quantum Chemistry*, vol. 61, pp. 541-546, Jan 20 1997.
- [95] S. Hazebroucq, *et al.*, "A theoretical investigation of gadolinium (III) solvation in molten salts," *Journal of Chemical Physics*, vol. 122, pp. -, Jun 8 2005.

## Appendix-1

Calculation to determine number of times the reprocessing has to run to get 5 mol% of Cerium

Typical Feed stock of spent fuels

|   | Feed Stock        | gm    |
|---|-------------------|-------|
| Electrorefiner of 1m depth and 1m diameter<br>33 cm depth of LiCl-KCl | La                | 29.5  |
|   | Ce                | 56.8  |
|   | Pr                | 28    |
|   | Nd                | 96.1  |
|   | Pm                | 2.67  |
|   | Sm                | 16.9  |
|   | Eu                | 1.1   |
|   | Gd                | 0.4   |
|   | U                 | 8280  |
|   | Np                | 4.34  |
|   | Pu                | 44.6  |
|   | Am                | 0.001 |
|   | Total Spent Fuels |       |



The typical electrorefiner container in Idaho National Laboratory (INL) has 100 cm depth and 100 cm diameter to start with and filled with LiCl-KCl molten salt upto 33 cm of the container then the volume of container after it is filled is given by the following relation

$$\text{Volume} = h \cdot (d/2)^2 \cdot \pi$$

$$V := 33 \cdot \left(\frac{100}{2}\right)^2 \cdot \pi$$

$$V = 2.592 \times 10^5 \text{ cm}^3$$

Density of LiCl-KCl = 1.6766 g/cm<sup>3</sup>

Mass of LiCl-KCl (M) presents in the electrorefiner

$$M := V \cdot 1.6766$$

$$M = 4.345 \times 10^5 \text{ gm of LiCl-KCl}$$

Molar weight of LiCl-KCl

$$\text{Mol}_{\text{wt}} := 0.575 \cdot 42.394 + 0.415 \cdot 74.55$$

$$\text{Mol}_{\text{wt}} = 55.315 \text{ gm/mol}$$

Now Number of moles of LiCl-KCl in a container is

$$M_{\text{LiCl.KCl}} = \frac{M}{\text{Mol}_{\text{wt}}}$$

$$M_{\text{LiCl.KCl}} = 7.856 \times 10^3 \text{ moles of LiCl-KCl in a container}$$

We Know, total Lanthanide in feed stock = 231.7 gm

Total Cerium presents= 56.8 gm

Mole of Ce

$$C_{e,mol} := \frac{56.8}{140.116}$$

$$C_{e,mol} = 0.405 \text{ mol}$$

Now mole % of Ce in LiCl-KCl

$$C_{e,mol,LiCl,KCl} = \frac{C_{e,mol}}{(M_{LiCl,KCl} + C_{e,mol})} \cdot 100$$

$$C_{e,mol,LiCl,KCl} = 5.16 \times 10^{-3} \text{ \% of Ce in LiCl-KCl}$$

Now

To get 5 mol % of Ce, Lets x be the number of moles present in total LiCl-KCl

$$x := 0.05 \cdot \frac{M_{LiCl,KCl}}{0.95} \cdot 100$$

$$x = 4.135 \times 10^4 \text{ be the number of actual mole \% for 5 mol \% in LiCl-KCl}$$

Now to get number of times the reprocessing has to recycle to get 5 mol % would be

$$N := \frac{x}{C_{e,mol,LiCl,KCl}}$$

$$N = 8.013 \times 10^6 \text{ times has to reprocessed to get 5 mol\% of Ce.}$$

## Appendix II

Table 1: Calculated potential by using Nernst Equation and obtained potential from the experiment at 500 °C

| $E_{\text{cell}} = E^{\circ} + (RT/nF)\ln\{\text{Ln}^{3+}\}$ |               |                              |                     |                  |
|--|---------------|------------------------------|---------------------|------------------|
| LiCl-<br>KCl+LnCl <sub>3</sub>                               | Conc<br>(Mol) | $E^{\circ}$ (V)<br>(Aqueous) | E (V)<br>calculated | E(V)<br>obtained |
| Ce <sup>3+</sup> /Ce <sup>0</sup>                            | 0.00284       | -2.336                       | -2.466              | -2.120           |
| La <sup>3+</sup> /La <sup>0</sup>                            | 0.002854      | -2.379                       | -2.509              | -1.960           |
| Gd <sup>3+</sup> /Gd <sup>0</sup>                            | 0.002655      | -2.279                       | -2.410              | -1.930           |
| Nd <sup>3+</sup> /Nd <sup>0</sup>                            | 0.002793      | -2.323                       | -2.453              | -1.870           |
| Dy <sup>3+</sup> /Dy <sup>2+</sup>                           | 0.002604      | -2.600                       | -2.732              | -2.080           |
| Dy <sup>2+</sup> /Dy <sup>0</sup>                            | 0.002604      | -2.230                       | -2.362              | -2.230           |
| Pr <sup>3+</sup> /Pr <sup>0</sup>                            | 0.002016      | -2.353                       | -2.490              | -2.060           |
| Sm <sup>3+</sup> /Sm <sup>2+</sup>                           | 0.002726      | -1.550                       | -1.681              | -1.300           |

## 3-D surface plots

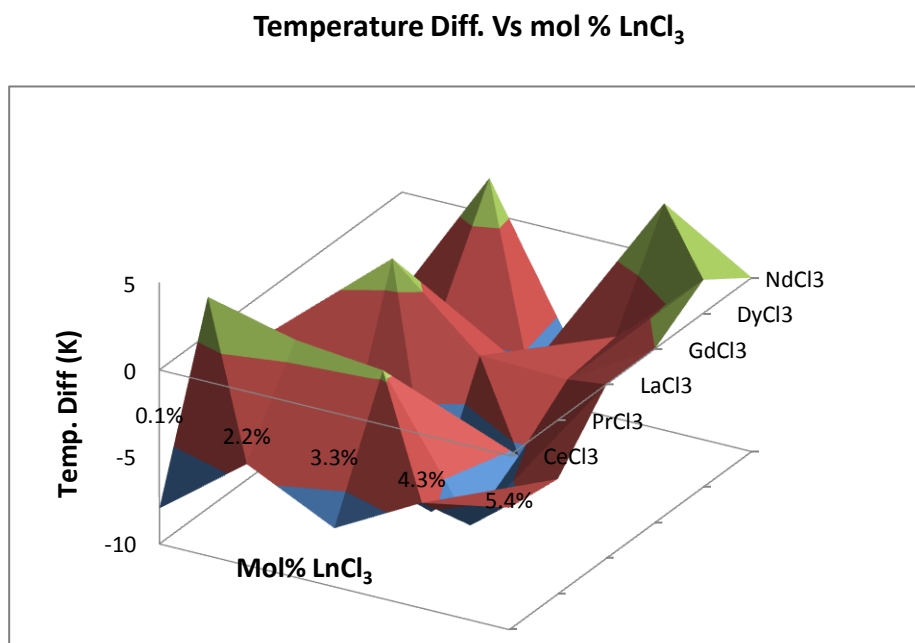


**Figure:** 3-D surface plot for single component Temperature Diff. Vs Mol%  $\text{LnCl}_3$